

HIGHLIGHTS FROM SuperKEKB PHASE 2 COMMISSIONING

Y. Ohnishi*, KEK, 1-1 OHO, Tsukuba, Ibaraki 305-0801, Japan

on behalf of the SuperKEKB Commissioning Group and the Belle II Commissioning Group

Abstract

SuperKEKB is an electron-positron asymmetric-energy collider to search new physics phenomena appeared in B-meson decays. In order to accomplish this purpose, 40 times the luminosity as high as the KEKB collider is demanded. The strategy is that the vertical beta function at the IP is squeezed down to 1/20 and the beam currents double those of KEKB while keeping the same beam-beam parameter. The vertical beta function at the interaction point(IP) will be much smaller than the bunch length, however, the hour-glass effect which degrades the luminosity will be reduced by adopting a novel “nano-beam” scheme. First of all, the Phase 2 commissioning was focused on the verification of nano-beam scheme. Secondary, beam related background at the Belle II detector was also studied for the preparation of the pixel vertex detector installed before the Phase 3 operation. The preliminary results and accomplishments of the commissioning in Phase 2 will be reported in this article.

INTRODUCTION

SuperKEKB is an electron-positron collider [1] and the Belle II detector [2] built to explore new phenomena in particle physics. The physics program of the next B-factory delivering ultra high statistics is almost independent of, and complementary to, the high energy experiments at the LHC. The target luminosity is $8 \times 10^{35} \text{ cm}^{-2}\text{s}^{-1}$, which is 40 times the performance of the predecessor, KEKB [3], which has been operated for 11 years until 2010. The strategy for the luminosity upgrade is a nano-beam scheme. The nano-beam scheme was first proposed by P. Raimondi in Italy [4]. The collision of low emittance beams under a large crossing angle allows squeezing the beta functions at the IP much smaller than the bunch length. Consequently, extremely higher luminosity can be expected with only twice the beam current of KEKB.

The SuperKEKB operation is divided by 3 stages, Phase 1, Phase 2, and Phase 3. The upgrade work was started after the shutdown of KEKB, and it took 6 years to make the Phase 1 commissioning ready. The final focus system(QCS) [5] and Belle II detector were not installed in Phase 1 [6]. The subjects were vacuum scrubbing for new vacuum system replaced with ante-chambers, low emittance tuning for new arc lattice to realize low emittance, and beam background study prepare for the installation of Belle II detector before Phase 2. The final focus system and Belle II detector were installed during a long shutdown between Phase 1 and Phase 2. Prior to the main ring operation, the commissioning of the positron damping ring [7] started on 8th February 2018 almost in 2 years after the Phase 1 commissioning. The

* yukiyoshi.ohnishi@kek.jp

Phase 2 commissioning started on 19th March 2018. The commissioning in Phase 2 was finished on 17th July 2018 and the duration was about 4 months in total. The common machine parameters during Phase 2 are shown in Table 1.

The Phase 3 operation will start in the early 2019, which is a full-scale collider experiment after installation of the pixel vertex detector(PXD) to Belle II.

Table 1: Machine Parameters related to the RF system in Phase 2. The intra-beam scattering and other collective effects are not included.

	LER	HER	Unit
Beam Energy	4	7	GeV
Circumference	3016.3		m
Harmonic no.	5120		
Total RF voltage	8.4	12.8	MV
α_p	2.88×10^{-4}	4.50×10^{-4}	
σ_z	4.8	5.4	mm
σ_δ	7.53×10^{-4}	6.3×10^{-4}	
U_0	1.76	2.43	MV
ν_s	-0.0220	-0.0258	

TARGET OF THE PHASE 2 COMMISSIONING

The overlap region for the narrow colliding beams with a large crossing angle can be small along the beam axis which implies a head-on collision of effective beams having the very short bunch length. A picture of the effective beams is a projection of the real beams to the x -axis which is an isovolumetric deformation. The effective beam is considered in the nano-beam scheme which is written by

$$\sigma_{z,eff} = \frac{\sigma_x^*}{\phi_x} \quad (1)$$

$$\sigma_{x,eff}^* = \sigma_z \phi_x, \quad (2)$$

where σ_x^* is the horizontal beam size at the IP, σ_z is the bunch length, and ϕ_x is the half crossing angle. Then, the luminosity and beam-beam parameters are calculated by using the effective beam. In order to avoid an hourglass effect, the following condition is necessary.

$$\beta_y^* \geq \sigma_{z,eff} = \frac{\sigma_z}{\Phi}, \quad (3)$$

where the Piwinski angle is defined by

$$\Phi = \frac{\sigma_{x,eff}^*}{\sigma_x^*}. \quad (4)$$

CHALLENGES FOR CIRCULAR e^+e^- COLLIDERS*

Frank Zimmermann[†], CERN, Geneva, Switzerland

Abstract

This paper sketches the glorious past and the tantalizing future of circular e^+e^- colliders, highlighting some of the key issues.

HISTORY

Circular e^+e^- Colliders can look back at a 50-year success story, illustrated in Fig. 1. The collider with the highest energy so far was LEP/LEP2. LEP had a circumference of about 27 km, and was in operation from 1989 to 2000. During this time it delivered an integrated luminosity of 1000 pb^{-1} . LEP2 reached a maximum c.m. energy of 209 GeV, a maximum synchrotron radiation power of 23 MW, and a critical photon energy close to 1 MeV. A further important step forward was made by the two B factories, PEP-II and KEKB; see Fig. 2. They established collider operation at very high beam current (well above 1 Ampere per beam), world record luminosities, and top-up injection as a routine mode of operation. Another machine, DAΦNE, demonstrated the merits of crab-waist collisions, with a small β_y^* and large vertical beam-beam tune shift (Fig. 3).

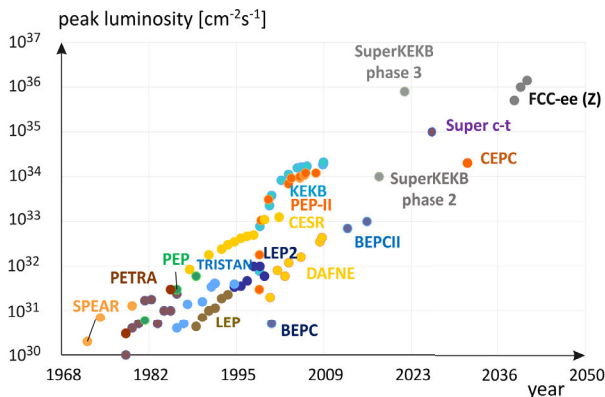


Figure 1: Peak luminosity of circular e^+e^- colliders as a function of year — for past, operating, and proposed facilities including the Future Circular Collider (Historical data courtesy of Y. Funakoshi).

NEXT STEPS

The next big step will be the SuperKEKB (Fig. 4), whose beam commissioning started in 2016. SuperKEKB will operate with a “nanobeam collision scheme” (similar to the crab waist, but without any crab-waist sextupoles). It features a design beam lifetime of no more than 5 minutes, and a vertical IP beta function β_y^* of only 0.3 mm.

* This work was supported by the European Commission under the HORIZON 2020 project ARIES no. 730871.

[†] frank.zimmermann@cern.ch

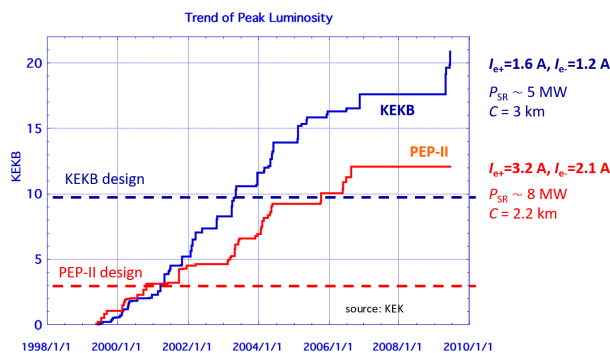


Figure 2: Peak luminosity of PEP-II and KEKB as a function of year along with the design luminosity, and a few key parameters.

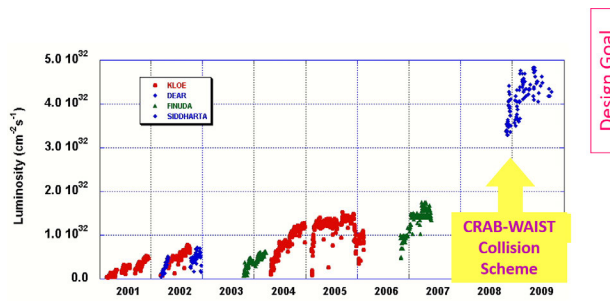


Figure 3: DAΦNE peak luminosity versus time, and the step increase in 2008/9 thanks to the introduction of crab-waist collisions (P. Raimondi, M. Zobov).

The proposed future highest-energy highest-luminosity e^+e^- colliders build on past successes and lessons. LEP has pushed high-energy beam operation and experienced synchrotron-radiation effects like those expected for FCC-ee $t\bar{t}$ running. The B-factories KEKB and PEP-II have operated with high beam currents, as needed for the FCC-ee Z pole operation. They have also established the top-up injection mode. DAΦNE has demonstrated the crab waist collision scheme. The Super B factory SuperKEKB will explore the operation with extremely low β_y^* . The SLC, KEKB and SuperKEKB have demonstrated the positron source operation at high intensity. Finally, HERA, LEP, and RHIC have delivered important lessons on spin gymnastics, spin-orbit matching and operating storage rings with polarized beams.

The next machines are combining all the recently established concepts, as indicated in Fig. 5. Figure 6 compares the resulting tantalizing performance reach of FCC-ee with other proposed future colliders.

SEVERAL TOPICS ON BEAM DYNAMICS IN FCC-ee*

K. Oide[†], KEK, Tsukuba, Japan

D. Shatilov, BINP SB RAS, Novosibirsk, Russia

S. Aumon, T. K. Charles, D. El Khechen, T. Tydecks, CERN, Geneva, Switzerland

Abstract

The FCC-ee is a double-ring e^+e^- collider to be installed in a common tunnel of ~ 100 km circumference, as a potential first step before the FCC-hh hadron collider. Several studies on the beam dynamics at FCC-ee: low emittance tuning, dynamic aperture, beam blowup with/without beam beam, are introduced in the paper.

INTRODUCTION

The beam energy of FCC-ee covers at least from the Z-pole (45.6 GeV) to $t\bar{t}$ (182.5 GeV). The design luminosity is the highest ever at each energy, under the constraint that the synchrotron radiation (SR) power is less than 100 MW for the total of two beams. The design is based on existing technologies verified in e^+e^- colliders in the world, including VEPP-IV, LEP, PEP-II, KEKB, DAΦNE, BEPC II, SuperKEKB. The main characteristics of the optics design [1] have been double ring, with ~ 100 km circumference, two interaction points (IPs) per ring, horizontal crossing angle of 30 mrad at the IP, and the crab-waist scheme with local chromaticity correction system. A so-called "tapering" of the magnets is applied, which scales all fields of magnets with the local beam energy determined by the SR. An asymmetric layout near the interaction region suppresses the critical energy of SR incoming to the detector at the IP below 100 keV. Sufficient transverse/longitudinal dynamic apertures (DAs) have been obtained to assure adequate beam lifetime with beamstrahlung and top-up injection. Table 1 lists the basic parameters of FCC-ee. For the estimation of the running plan at each energy, luminosities less than numbers in this table by 10–20% are used at each energy to have a margin for operation.

LOW EMITTANCE TUNING WITH DYNAMIC APERTURE

Due to the low emittance budget and the small β^* at the interaction point, the FCC-ee is a challenging accelerator to correct when misalignments are introduced in the simulations. These errors produce a large vertical dispersion (several hundred meters without any correction applied) and coupling, which compromise the target emittances, in particular at high energy. Several correction methods and algorithms were developed in order to preserve the emittances as close as possible to their design values.

Horizontal correctors were installed at every focusing quadrupole and vertical correctors at every defocusing quadrupole. Beam Position Monitors (BPM) were placed at each quadrupole, including at the doublet of the IPs. Skew quadrupole correctors with a trim quadrupole are placed at the sextupoles to correct the beta-beat and rematch the horizontal dispersion. Special skew quadrupoles were installed in the interaction region to compensate the tilt of the doublet quadrupoles at the IPs. The effect of the tilt of dipoles and field errors will be included in the next phase of the study. The vertical dispersion distortion was corrected with orbit correctors via the dispersion free steering method [2] first and with skew quadrupoles with the help of response matrices. The linear coupling was corrected by adjusting the linear coupling resonance driving term parameters, as tested at the ESRF [3]. Trim quadrupoles were used to rematch the phase advances between the BPMs, again using response matrices. Satisfactory results for the misalignment tolerance were found when the magnets were misaligned as defined in Table 2.

1000 seeds were tested with the correction algorithm using the input misalignments listed in Table 2 and 70% of them converged, as shown in Fig. 1, with the following results for the emittances:

$$\epsilon_y = 0.10 \pm 0.013 \text{ pm}$$

$$\epsilon_x = 1.52 \pm 0.01 \text{ nm}$$

$$\epsilon_y/\epsilon_x = 0.0065\%$$

More studies are going on with less number of orbit correctors using trim windings on the arc sextupoles, with more machine errors including the roll of dipoles, misalignments taking the scheme of girders into account, and BPM errors [4].

The resulting dynamic aperture (DA) at $t\bar{t}$ has been evaluated as shown in Fig. 2. The average of them are just on the design DA. The variation is within the margin for the plan of the integrated luminosity.

DYNAMIC AND MOMENTUM APERTURE OPTIMIZATION USING PSO

Applying particle swarm optimization (PSO) in accelerator physics to improve machine parameters is a worthwhile method to cope with the increasingly large number of degrees of freedom to optimize. With an existing machine it is possible to optimize the sextupole setting by improving dynamic aperture through lifetime optimization using PSO [5].

* Work supported by the European Commission under Capacities 7th Framework Programme project EuCARD-2, grant agreement 312453, and under the Horizon 2020 Programme project CREMLIN, grant agreement 654166.

[†] katsunobu.oide@cern.ch

STATUS OF DAΦNE: FROM KLOE-2 TO SIDDHARTA-2, EXPERIMENTS WITH CRAB-WAIST

C. Milardi[†], D. Alesini, S. Bini, O. R. Blanco-García, M. Boscolo, B. Buonomo, S. Cantarella, S. Caschera, A. De Santis, G. Delle Monache, C. Di Giulio, G. Di Pirro, A. Drago, A. D'Uffizi, L. G. Foggetta, A. Gallo, R. Gargana, A. Ghigo, S. Guiducci, S. Incremona, F. Iungo, C. Ligi, M. Maestri, A. Michelotti, L. Pellegrino, R. Ricci, U. Rotundo, L. Sabbatini, C. Sanelli, G. Sensolini, A. Stecchi, A. Stella, A. Vannozzi, M. Zobov, LNF-INFN, Frascati, Italy
 J. Chavanne, G. Le Bec, P. Raimondi, ESRF, Grenoble, France
 G. Castorina, INFN-Roma1, Roma, Italy

Abstract

DAΦNE, the Italian lepton collider, is running since more than a decade thanks to a radical revision of the approach used to deal with the beam-beam interaction: the *Crab-Waist* Collision Scheme. In this context, the collider has recently completed a long term activity program aimed at providing an unprecedented sample of data to the KLOE-2 detector, a large experimental apparatus including a high intensity axial field strongly perturbing ring optics and beam dynamics. The KLOE-2 run has been undertaken with the twofold intent of collecting data for rare decay and flavor physics studies, and testing the effectiveness of the new collision scheme in presence of a strongly perturbing experimental apparatus. The performances of the collider are reviewed and the limiting factors discussed along with the preparatory phase activities planned to secure a new collider run to the SIDDHARTA-2 experiment.

INTRODUCTION

The DAΦNE [1] accelerator complex consists of a double ring lepton collider working at the c.m. energy of the Φ -resonance (1.02 GeV) and an injection system. The collider includes two independent rings, each 97 m long. The two rings share an interaction region (IR), where the detector taking data, one at the time, is installed. Beam injection is performed on energy, also in topping-up mode during collisions as well, by a system including an S-band LINAC, 180 m long transfer lines and an accumulator damping ring. DAΦNE became operational in 2001, and it still is an attractive collider to perform relevant experiments aimed at understanding flavour physics. This has been possible thanks to a continuous effort finalized at increasing the collider performances, which culminated in 2009 with the realization of a new approach to the beam-beam interaction: the *Crab-Waist* (CW) Collision Scheme. The new approach to collisions is based on large Piwinski angle (ψ) and CW compensation of the beam-beam induced instabilities [2, 3, 4]. It was, implemented during the run dedicated to a tabletop experiment, SIDDHARTA, and allowed to increase the instantaneous luminosity by a factor three, paving the way to a new run dedicated to a revised KLOE detector: KLOE-2 [5], that, in view of a higher luminosity, extended its

physics search programs. In fact, the upgraded KLOE-2 setup includes calorimeter devices close to the IR, as well as a cylindrical GEM detector, the Inner Tracker (IT) installed at a distance of 15 cm from the Interaction Point (IP). However, a long-term run finalized to deliver a large statistical sample of data can only be planned if all the collider subsystems perform in a highly reliable way. For this reason, in the first six months of 2013, before starting the data-delivery phase, the DAΦNE infrastructure underwent a general consolidation program [6]; exploiting the long planned shutdown foreseen to install the new detector layers. Still some activities were not completed at that time, due to delays in the spare parts procurement, thus they have been finalized during the data taking, profiting from the seasonal shutdowns.

The DAΦNE collider parameters are listed in Table 1.

Table 1: DAΦNE Beam Parameters

	DAΦNE native (2000÷2006)	DAΦNE CW Since 2007
Energy (MeV)	510	
β_y^* (cm)	1.8	0.85
β_x^* (cm)	160	23
σ_x^* (μ m)	760	250
σ_y^* (μ m) at low current	5.4	3.1
σ_z (cm)	2.5	1.5
Bunch spacing (ns)	2.7	
Damping times τ_E, τ_x (ms)	17.8/36.0	
Cros. angle $\theta_{cross}/2$ (mrad)	12.5	25
Piwinski angle ψ (mrad)	0.6	1.5
ϵ (mm mrad)	0.34	0.28
RF frequency [MHz]	368.26	368.667
Harmonic number	120	

Presently DAFNE, after having successfully completed the KLOE-2 run [7], is facing the preparatory phase pro-paedeutical to a new operation period aimed at delivering data to the SIDDHARTA-2 detector [8], an upgraded version of the old one. The new experimental apparatus aims at performing the first kaonic deuterium measurement by improving its measurement resolution which, in turn, requires to considerably reduce the signal background ratio increasing, at the same time, the signal rate. The

[†] catia.milardi@lnf.infn.it

STATUS OF CIRCULAR ELECTRON-POSITRON COLLIDER

C. H. Yu^{†, 1}, Y. Zhang¹, Y. W. Wang, D. Wang, N. Wang, S. Bai, X. H. Cui, C. Meng, Y. S. Zhu, H. P. Geng, D. H. Ji, Y. Y. Wei, Y. D. Liu, J. Y. Zhai, D. J. Gong, H. J. Zheng, Q. Qin, J. Gao, T. J. Bian
 Key Laboratory of Particle Acceleration Physics and Technology,
 Institute of High Energy Physics, Chinese Academy of Sciences, Beijing 100049, China
¹also at University of Chinese Academy of Sciences, Beijing 100049, China

Abstract

Circular electron-positron collider (CEPC) is a dedicated project proposed by China to research the Higgs boson. The collider ring provides e^+e^- collision at two interaction points (IP). The luminosity for the Higgs mode at the beam energy of 120GeV is $3 \times 10^{34} \text{ cm}^{-2}\text{s}^{-1}$ at each IP while the synchrotron radiation (SR) power per beam is 30MW. Furthermore, CEPC is compatible with W and Z experiments, for which the beam energies are 80 GeV and 45.5 GeV respectively. The luminosity at the Z mode is higher than $1.7 \times 10^{35} \text{ cm}^{-2}\text{s}^{-1}$ per IP. Top-up operation is available during the data taking of high energy physics. The status of CEPC will be introduced in detail in this paper.

MACHINE LAYOUT

CEPC [1] which aims at researching Higgs boson is a double ring scheme optimized at the beam energy of 120 GeV. Super proton-proton collider (SPPC) will be the next project after the operation of CEPC in the future. The circumference of CEPC is 100km while matching the geometry of SPPC as much as possible. The circumference is determined by the requirements of SPPC so that the SPPC bending magnets can be designed and manufactured. The arc regions of the SPPC collider ring, the CEPC collider ring and the CEPC booster ring are in the same tunnel. The cross section of the tunnel in the arc region is shown in Fig. 1.

The interaction region of SPPC is located in the same long straight sections where the CEPC RF cavities are placed. The collimation region of SPPC with length of about 4km is located in the interaction region of CEPC. Due to the special collision orbit at the IP and the very large size of detector, bypass geometry or independent tunnel for SPPC and CEPC in the two regions is needed. The layout design of CEPC in the RF region and interaction region follows the space constraints. However, it still will be potential space conflict in the two regions during the geometry optimization of SPPC in the future. Since the operation of CEPC will be much earlier than SPPC. So SPPC and CEPC are arranged in the outside and inside respectively. SPPC team can optimize SPPC geometry with relatively lower magnetic field of bending magnet especially in the bypass region. The design of CEPC can keep fixed during the modification of SPPC. The booster ring of CEPC shown in Fig. 1 is located above collider ring with the distance of 2.4 m. The distance is sufficient to avoid the magnetic interference between the collider ring and the booster ring.

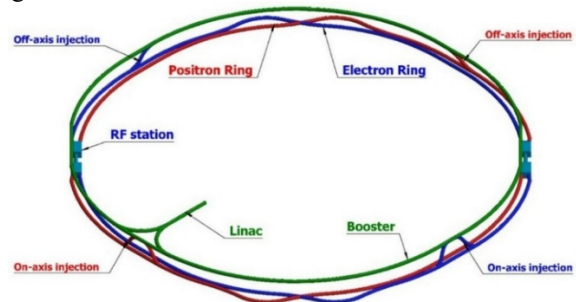


Figure 2: The layout of CEPC

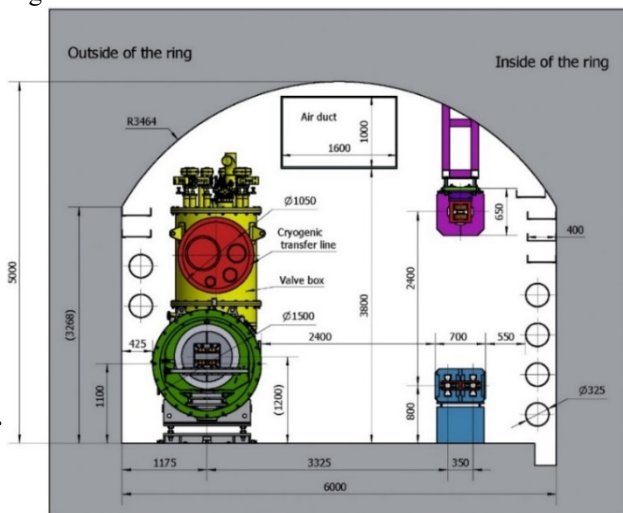


Figure 1: The cross section of the tunnel in the arc region.

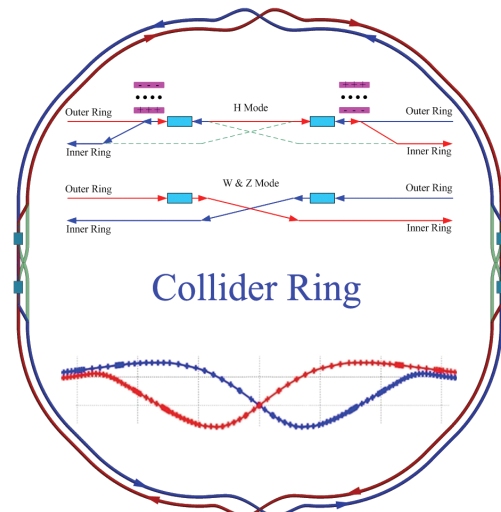


Figure 3: The layout of CEPC collider ring.

Content from this work may be used under the terms of the CC BY 3.0 licence (© 2018). Any distribution of this work must maintain attribution to the author(s), title of the work, publisher, and DOI.

[†] yuch@ihep.ac.cn

Content from this work may be used under the terms of the CC BY 3.0 licence (© 2018). Any distribution of this work must maintain attribution to the author(s), title of the work, publisher, and DOI.

ROUND COLLIDING BEAMS AT VEPP-2000 WITH EXTREME TUNESHIFTS

D. Shwartz[†], V. Anashin, O. Belikov, D. Berkaev, K. Gorchakov, A. Kasaev, A. Kirpotin,
 I. Koop¹, A. Krasnov, G. Kurkin, A. Lysenko, S. Motygin, E. Perevedentsev¹, V. Prosvetov,
 D. Rabusov, Yu. Rogovsky¹, A. Semenov, A. Senchenko¹, D. Shatilov, P. Shatunov,
 Yu. Shatunov¹, O. Shubina, M. Timoshenko, I. Zemlyansky, Yu. Zharinov

Budker Institute of Nuclear Physics, Novosibirsk, 630090, Russia
¹also at Novosibirsk State University, Novosibirsk, 630090, Russia

Abstract

VEPP-2000 is the only electron-positron collider operating with round beams that results in enhancement of beam-beam limit. VEPP-2000 with SND and CMD-3 detectors carried out two successful data-taking runs after new BINP injection complex was commissioned. The 2016/2017 run was dedicated to high energy range (640-1000 MeV per beam) while the 2017/2018 run was focused at 275-600 MeV/beam energies. With sufficient positron production rate and upgraded full-energy booster the collider luminosity was limited by beam-beam effects, namely flip-flop effect. Thorough machine tuning together with new ideas introduced to suppress flip-flop allowed to achieve high beam-beam tuneshift and bunch-by-bunch luminosity values at specific beam energies. The achieved luminosity increased 2-5 times in a whole energy range in comparison to phase-1 operation (2010-2013).

ROUND COLLIDING BEAMS

The VEPP-2000 collider [1-3] exploits the round beam concept (RBC) [4] firstly proposed for the Novosibirsk Phi-factory project [5]. This approach, in addition to the straightforward geometrical gain factor in luminosity should yield the beam-beam limit enhancement. An axial symmetry of the disruptive nonlinear counter-beam force together with the X - Y symmetry of the transfer matrix between the two IPs provide an additional integral of motion, namely, the longitudinal component of angular momentum $M_z = x'y - xy'$. Although the particles' dynamics remain strongly nonlinear due to beam-beam interaction, it becomes effectively one-dimensional. The reduction of degrees of freedom thins out the resonance grid and suppress the diffusion rate resulting finally in a beam-beam limit enhancement [6].

Thus, there are several demands upon the storage ring lattice suitable for the RBC:

1. Head-on collisions (zero crossing angle).
2. Small and equal β functions at IP ($\beta_x^* = \beta_y^*$).
3. Equal beam emittances ($\epsilon_x = \epsilon_y$).
4. Equal fractional parts of betatron tunes ($\nu_x = \nu_y$).

The first three requirements provide the axial symmetry of collisions while requirements (2) and (4) are needed for X - Y symmetry preservation between the IPs.

VEPP-2000 OVERVIEW

VEPP-2000 is a small 24 m perimeter single-ring collider operating in one-by-one bunch regime in the energy range below 1 GeV per beam. Its layout is presented in Fig. 1-2. Collider itself hosts two particle detectors [7, 8], Spherical Neutral Detector (SND) and Cryogenic Magnetic Detector (CMD-3), placed into dispersion-free low-beta straights. The final focusing (FF) is realized using superconducting 13 T solenoids. The main design collider parameters are listed in Table 1.

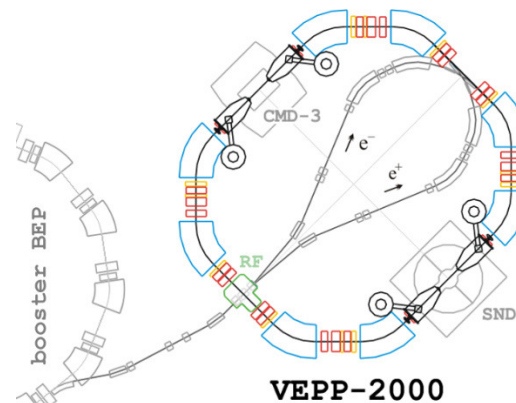


Figure 1: VEPP-2000 storage ring layout.



Figure 2: VEPP-2000 collider photo.

[†] d.b.shwartz@inp.nsk.su

REPORT FROM ARIES MUON COLLIDER WORKSHOP IN PADUA*

Marco Zanetti, INFN and University of Padua, Italy
Frank Zimmermann†, CERN, Geneva, Switzerland

Abstract

Several novel concepts could help the muon collider become a reality. These concepts include parametric ionization cooling, low-emittance muon production by positron annihilation (LEMMA scheme), production of low-emittance muon or positron beams using the Gamma Factory concept, and strategies to upgrade large accelerator complexes, like the LHC or the FCC, into a highest-energy muon collider. The muon collider workshop organized by ARIES APEC at Padua in July 2018 gathered the international community in order to review the recent progress and to formulate a common R&D strategy. Several important conclusions and recommendations were drawn.

INTRODUCTION

On 2–3 July 2018 a Muon Collider workshop at the University of Padua attracted 78 experts from Europe and the US, as illustrated in Figs. 1 and 2. This exciting and forward-looking workshop was the second event organized in the frame of the EU co-funded ARIES Work Package 6.6 (WP6.6), after the Photon Beams workshop in 2017 [1].



Figure 1: Some participants of the ARIES WP6 workshop on Muon Colliders, Padua, 2-3 July 2018.

More specifically, the muon collider workshop was organized by ARIES WP6.6 coordinators Marco Zanetti (INFN Padova) and Frank Zimmermann (CERN), together with the newly established European Muon Collider Study Group, chaired by Nadia Pastrone (INFN Torino). ARIES is an integrating activity co-funded by the European Commission in the HORIZON 2020 Research and Innovation programme under grant agreement no 730871. Work Package 6 “Accelerator Performance and Concepts” (APEC) contains a Task 6.6, which looks at far-future concepts.

* This work was supported by the European Commission under the HORIZON 2020 project ARIES no. 730871.

† frank.zimmermann@cern.ch



Figure 2: Snapshots from the ARIES WP6 workshop on Muon Colliders, including Alex Bogacz, Carlo Rubbia, Rolland Johnson, Mark Palmer, Manuela Boscolo, Marco Zanetti, Pantaleo Raimondi, and Jean-Pierre Delahaye.

ADVANCED PROTON-DRIVEN SCHEMES

Setting the stage, Carlo Rubbia, from CERN and INFN, the recipient of the 1984 Nobel Prize for Physics and a life-long Member of the Senate of the Italian Republic, called for an initial experiment to demonstrate muon cooling and the particular merits of parametric ionization cooling [2]; see Fig. 3. He pointed out that the first muon facility would comprise a ring at the scale of the PS, and hinted at the ESS as being the ideal place for a muon-beam facility in Europe.



Figure 3: Recognizing the muon collider as a project of reasonable cost and of reasonably fast construction, Nobel laureate Carlo Rubbia admonished the audience to focus on scientific work instead of PowerPoint studies.

DYNAMIC APERTURE LIMITATION IN e^+e^- COLLIDERS DUE TO SYNCHROTRON RADIATION IN QUADRUPOLES *

A. Bogomyagkov [†], E. Levichev, S. Sinyatkin, S. Glukhov,
 Budker Institute of Nuclear Physics SB RAS, 630090 Novosibirsk, Russia

Abstract

In a lepton storage ring of very high energy (e.g. in the e^+e^- Higgs factory) synchrotron radiation from quadrupoles constraints transverse dynamic aperture even in the absence of any magnetic nonlinearities. This was observed in LEP and the Future Circular e^+e^- Collider (FCC-ee). Synchrotron radiation in the quadrupoles modulates the particle energy at the double betatron frequency. Energy modulation varies transverse focusing strength at the same frequency and creates a parametric resonance of the betatron oscillations. Starting from 6d equations of motion we derive and solve the relevant differential equation describing the resonance, and show good agreement between analytical results and numerical simulation.

INTRODUCTION

Two future electron-positron colliders FCC-ee (CERN) [1] and CEPC (IHEP, China) [2] are now under development to carry experiments in the center-of-mass energy range from 90 GeV to 350 GeV. In these projects strong synchrotron radiation (power $\mathcal{P} \propto E^4$) is a source of effects negligible at low energy but essential at high energy, which influence beam dynamics and collider performance. One example is luminosity degradation caused by the particle radiation in the collective field of the opposite bunch (beamstrahlung [3]) either due to the particle loss [4] or because of the beam energy spread increase [5]. Another example is about reduction of the transverse dynamic aperture due to synchrotron radiation from quadrupole magnets. John Jowett is the first who pointed out this effect in LEP collider with maximum beam energy about 100 GeV [6]. Switching on the radiation from quadrupoles in the particle tracking decreased the stable betatron amplitude as compared to the radiation from bending magnets only. Jowett gave a description of this effect: “Here I shall briefly describe a new effect which I propose to call Radiative Beta-Synchrotron Coupling (RBSC). It is a non-resonant effect. A particle with large betatron amplitude makes an extra energy loss by radiation in quadrupoles. If you imagine that its betatron amplitude does not change much over a number of synchrotron oscillations (that is not essential to the effect), you can say that its “effective stable phase angle” will change to reflect the greater energy loss. The particle will tend to oscillate about a displaced fixed point in the synchrotron phase plane. This results in a growth of the oscillation amplitude which may eventually lead the particle outside the stable region in synchrotron

phase space.” Jowett illustrates above assertion with synchrotron phase trajectories for two stable particles (denoted by P and Q in Fig. 1) and one unstable (denoted by R) [7]. The tracking incorporates only radiation damping (quantum noise is absent) from both bending and quadrupole magnets.

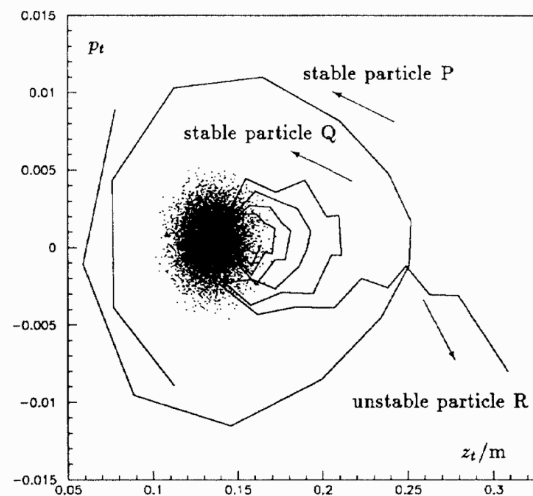


Figure 1: The vertical RBSC instability in LEP at 90 GeV projected into synchrotron phase space. Three lines show the motion of three particles P, Q and R with different initial conditions. P starts with zero betatron amplitude and large longitudinal deviation. It remains stable and damps to the equilibrium synchrotron phase. Q and R start with longitudinal coordinates corresponding to the closed orbit but with vertical amplitude 5.5 mm and 6 mm respectively. Q is stable while R’s amplitude grows in few turns until it is lost. A fourth particle has been tracked with quantum emission to give the cloud of points representing the core of the beam around the closed orbit.

In [8] Jowett has mentioned that the RBSC rarely occurs in isolation: “Most often some other effect limits the dynamic aperture before the RBSC limit is reached. In the standard (LEP) lattice the horizontal dynamic aperture is limited by a rather strong shift of the vertical tune with the horizontal action variable, bringing Q_y down onto the integer.”

Our interests to the subject was inspired by the FCC-ee lattice study. With the help of SAD accelerator design code [9] K. Oide demonstrated FCC-ee transverse dynamic aperture reduction due to radiation from quadrupoles [10], “While the radiation loss in dipoles improves the aperture, especially at $i\bar{i}$, due to the strong damping, the radiation loss in the quadrupoles for particles with large betatron amplitudes

* This work has been supported by Russian Science Foundation (project N14-50-00080).

[†] A.V.Bogomyagkov@inp.nsk.su

LOW-EMITTANCE TUNING FOR CIRCULAR COLLIDERS

T.K. Charles^{*1,2}, S. Aumon³, B. Holzer¹, K. Oide^{1,4}, T. Tydecks¹, F. Zimmermann¹,

¹ European Organization for Nuclear Research (CERN), Geneva, Switzerland

² School of Physics, University of Melbourne, 3010, Victoria, Australia

³ ADAM SA (Applications of Detector and Accelerators to Medicine), Geneva, Switzerland

⁴ KEK, Oho, Tsukuba, Ibaraki 305-0801, Japan

Abstract

The 100 km FCC-ee e^+e^- circular collider requires luminosities in the order of $10^{35} \text{ cm}^{-2} \text{ s}^{-1}$ and very low emittances of 0.27 nm-rad for the horizontal plane and 1 pm-rad in the vertical. In order to reach these requirements, extreme focusing of the beam is needed in the interaction regions, leading to a vertical beta function of 0.8 mm at the IP. These challenges make the FCC-ee design particularly susceptible to misalignment and field errors. This paper describes the tolerance of the machine to magnet alignment errors and the effectiveness of optics and orbit correction methods that were implemented in order to bring the vertical dispersion to acceptable values, which in turn limits the vertical emittance. Thousands of misalignment and error seeds were introduced in MADX simulations and a comprehensive correction strategy, which includes macros based upon Dispersion Free Steering (DFS), linear coupling correction based on Resonant Driving Terms (RDTs) and response matrices, was implemented. The results are summarized in this paper.

INTRODUCTION

Electron-positron circular colliders profit from small vertical beam size due to vertical emittances close to the quantum excitation. The light source community has propelled the drive for smaller and smaller vertical emittances [1,2]. Many of the lessons learned can be applied to circular electron-positron colliders in their strive for higher luminosity.

The Future Circular Collider (FCC) will have four energies of operation ranging from the Z-pole (45.6 GeV=beam) to the $t\bar{t}$ production threshold (182.5 GeV=beam) [3]. A summary of the key parameters can be found in Table 1 and in the upcoming Conceptual Design Report (CRD).

In order to produce a high luminosity, extreme focusing is required at the interaction regions. With this comes challenging optics parameters. For the Z resonance, a vertical β^* of 0.8 mm, and a vertical emittance of 1 pm-rad is required, for a luminosity of $230 \times 10^{34} \text{ cm}^{-2} \text{ s}^{-1}$. Within the final focusing region, the maximum values of the beta functions $\beta_{x,\text{max}} = 1587.97 \text{ m}$ and $\beta_{y,\text{max}} = 6971.55 \text{ m}$ (see Fig. 1).

These large beta values, and the strong sextupoles required for chromaticity correction, make the machine extremely sensitive to magnet misalignments and field errors.

The two main sources of vertical emittance growth are coupling between the transverse planes and residual vertical dispersion. The betatron coupling poses a large threat due

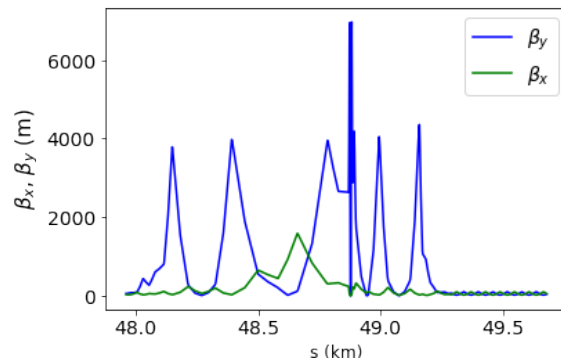


Figure 1: Beta functions near one of the IPs for the 182.5 GeV lattice. The maximum values of the beta functions $\beta_{x,\text{max}} = 1587.97 \text{ m}$ and $\beta_{y,\text{max}} = 6971.55 \text{ m}$.

Table 1: Baseline beam parameters of the four operational energies for FCCee [3].

Parameters	Z	W	H	$t\bar{t}$
Beam Energy [GeV]	45.6	80	120	182.5
ϵ_x [nm-rad]	0.27	0.28	0.63	1.45
ϵ_y [pm-rad]	1	1	1.3	2.7
Beam current [mA]	1390	147	29	5.4
\mathcal{L} [$10^{34} \text{ cm}^{-2} \text{ s}^{-1}$]	230	32	8	1.5

to the small emittance ratio (or coupling ratio) of $\epsilon_y/\epsilon_x = 0.27 \%$ (for the Z energy). The vertical dispersion grows the vertical emittance in accordance with the equilibrium emittance equation,

$$\epsilon_y = \left(\frac{dp}{p} \right)^2 (\gamma D_y^2 + 2\alpha D_y D_y' + \beta D_y'^2) \quad (1)$$

where D_y is the vertical dispersion, D_y' is the derivative of the dispersion with respect to s , dp/p is the momentum spread, and γ , α and β are the usual Twiss parameters.

Generally the smaller the value of the beta function at the IP, β_y^* , the larger the chromaticity, and the stronger the chromaticity correction required [4]. The sextupole magnets employed for this chromaticity correction introduce nonlinearities in the ring, which can lead to difficulties in performing the correction schemes that are outlined in the next section. This is because the correction techniques are inherently linear. If the beam is directed off-axis through the sextupole magnets, the effect to the beam seeing a skew quadrupole field, unaccounted for in the correction schemes.

* tessa.charles@cern.ch

OPTICS CORRECTIONS INCLUDING IP LOCAL COUPLING AT SuperKEKB*

A. Morita[†], H. Koiso, Y. Onishi, H. Sugimoto, K. Ohmi, D. Zhou,
 KEK, 1-1 Oho, Tsukuba, Ibaraki 305-0801, Japan

Abstract

SuperKEKB is an asymmetric energy electron-positron collider designed by using a novel collision scheme. The beam collision test was performed during the phase-2 commissioning. In the phase-2 commissioning, global optics corrections worked fine except for local coupling at the interaction point(IP). IP local coupling was adjusted by IP tuning knobs to maximize luminosity. After IP local coupling adjustment, the specific luminosity improvement by squeezing the vertical beta function at IP down to half of the bunch length was confirmed.

INTRODUCTION

The SuperKEKB accelerator [1] is an asymmetric energy electron-positron collider which is designed to achieve a luminosity of $8 \times 10^{35} \text{cm}^{-2}\text{s}^{-1}$ by using the “nano-beam” collision scheme. Its main rings are constructed by 7 GeV electron high energy ring (HER) and 4 GeV positron log energy ring (LER). The SuperKEKB accelerator commissioning is divided into 3 phases. At this moment, the second phase so called “phase-2 commissioning” has been completed and we are preparing the phase-3 commissioning.

The phase-1 commissioning [2] without the final focus system was performed from February 1, 2016 to June 28, 2016 for establishing the low emittance beam operation. After the phase-1 commissioning both the final focus system and the Belle II detector were installed. The phase-2 commissioning [3] was performed from March 19, 2018 to July 17, 2018 to verify “nano-beam” collision.

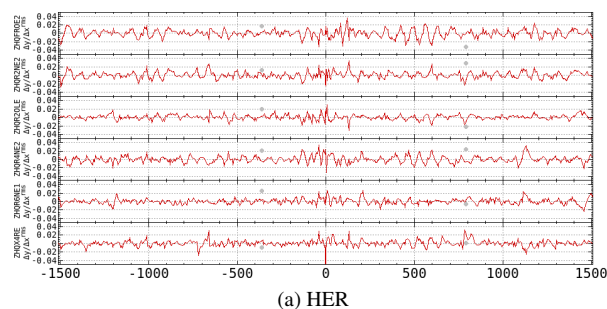
In the following sections, the global optics correction performed as a part of beam commissioning and the IP local coupling issue are reported.

GLOBAL OPTICS CORRECTION

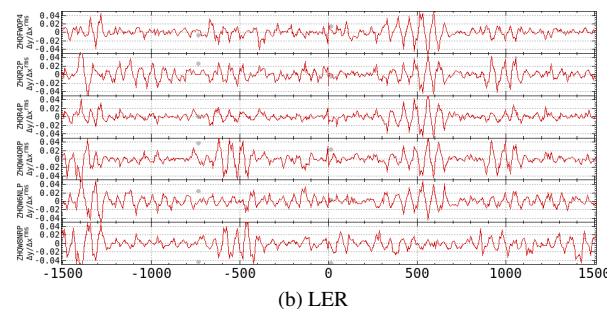
Both optical function measurement and correction algorithm for the phase-2 beam operation are same as the phase-1 commissioning [4]. The optical function measurement of the SuperKEKB standard operation is based on the closed orbit response measurement by using the multi-turn beam position monitors(BPMs). In the optics correction, the correction parameter is calculated from both the linear model response and the measured optical function error by using the singular value decomposition (SVD). The global optics correction sequence for the beam operation contains XY-coupling correction, physical dispersion correction and beta correction.

* Work supported by JSPS KAKENHI Grant Number 17K05475.

[†] akio.morita@kek.jp

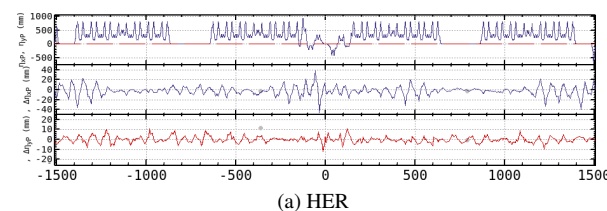


(a) HER

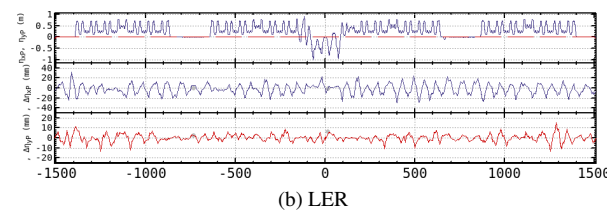


(b) LER

Figure 1: XY-Coupling measurement. Horizontal axis shows the distance from the IP in m units. Each graph columns show the discrepancy between model prediction and measurement of vertical leakage orbit of single horizontal steering kick shown in column label.



(a) HER



(b) LER

Figure 2: Physical dispersion measurement. From the top of the graph columns, graph columns correspond with model dispersion, horizontal dispersion error and vertical dispersion error, respectively.

OPTICS ABERRATION AT IP AND BEAM-BEAM EFFECTS

K. Ohmi*, K. Hirosawa, Y. Funakoshi, H. Koiso, A. Morita, Y. Ohnishi, D. Zhou,
 KEK/Soken-dai, Tsukuba, Japan

Abstract

Collision in SuperKEKB phase II commissioning has started in April 2018. Luminosity was lower than the geometrical value even in very low bunch current at the early stage. Linear x-y coupling at IP caused by skew of QCS was conjectured as error source. x-y coupling correction using skew corrector of QCS resulted in luminosity recover of 2 times. After the QCS skew correction, luminosity is still limited at relatively low bunch current. Nonlinear x-y coupling at IP is conjectured as a source of the luminosity limitation in the next stage. We discuss effects of linear and nonlinear x-y coupling at IP on the beam-beam performance.

INTRODUCTION

SuperKEKB is asymmetric e^+e^- collider, which consists of low and high energy rings (LER & HER) with the energies $E = 4$ and 7 GeV, respectively. The target luminosity is $L = 8 \times 10^{35} \text{ cm}^{-2}\text{s}^{-1}$ at beam current $I_{+,tot} = 3.6$ A and $I_{-,tot} = 2.6$ A with the number of bunches $N_b = 2,500$. Two beams collide with half crossing angle $\theta_c = 41.5$ mrad. Beta function at Interaction Point (IP) is squeezed to $\beta_x^* \sim 30$ mm and $\beta_y^* \sim 0.3$ mm. Piwinski angle is $\theta_c \sigma_z / \sigma_x$ is very large ~ 20 ; so-called, nano-beam/ superbunch/ large Piwinski angle collision is adopted. Phase-I commissioning in 2016 was focused to start the operation of the two storage ring (LER and HER) without collision. In Phase-II commissioning started from March 2018, beam-beam collision and luminosity tuning were main subjects. β^* was squeezed step-by-step during the commissioning. Table 1 summarizes the parameters. The beam-beam tune shift $\Delta\nu_{x,y}$ in Phase-II is calculated by the emittance without collision. Beam-beam parameter $\xi_y \sim \Delta\nu_y$ estimated by the achieved luminosity is lower than the value; lower value is $\xi_{L,-} = 2r_e\beta_y^*L/(N_- \gamma f_{rep}) \sim 0.02$ due to a vertical emittance increase mainly in e^+ beam at beam-beam collision..

Optics aberrations at the interaction point have affected the beam-beam performance since KEKB operation. The operation had been continued while scanning the IP optics parameters for most of the time in day-by-day. Correction of the aberrations should be also very important for SuperKEKB. We discuss correction of linear aberration done in Phase-II and nonlinear aberrations toward future commissioning, Phase-III.

LINEAR COUPLING CORRECTION AT IP IN PHASE-II OPERATION

Specific luminosity, which is bunch luminosity normalized by bunch current product, is used as a measure for

Table 1: Parameters for SuperKEKB

parameter	design		Phase-II	
	LER	HER	LER	HER
$N_{\pm} (10^{10})$	9	6.5	4.8	4.0
$\varepsilon_{x/y} \text{ (nm/pm)}$	3.2/8.64	4.6/13	2.1/21	4.6/30
$\beta_{x/y}^* \text{ (mm)}$	32/0.27	25/0.3	200/3	100/3
ν_z	0.0247	0.028	0.022	0.026
$\Delta\nu_x$	0.0028	0.0012	0.0073	0.0025
$\Delta\nu_y$	0.088	0.081	0.075	0.077
ξ_L	0.088	0.081	0.03	0.02
$\sigma_z \theta_c / \sigma_x$	24.7	19.4	12.1	11.6

the beam-beam performance. When the beam particles distribute Gaussian in the transverse plane, the specific luminosity is represented only by the rms beam size,

$$L_{sp} = \frac{L}{I_+ I_-} = \frac{1}{2\pi\sigma_{xc}\sigma_{yc}e^2 f_0}, \quad (1)$$

where the beam size is square mean of e^{\pm} beams, $\sigma_{yc} = \sqrt{\sigma_{y+}^2 + \sigma_{y-}^2}$. For collision with a large crossing angle $\theta_c \sigma_z / \sigma_x \gg 1$, the horizontal beam size is effectively projection of the bunch length into horizontal plane: i.e., $\sigma_{x,eff} = \theta_c \sigma_z$, where θ_c is the half crossing angle. σ_{xc} is square mean of the effective horizontal size of the two beams. The specific luminosity is characterized by the vertical beam size and bunch length. We expect that the specific luminosity is given by the vertical beam size determined by the vertical emittance ε_y and β_y^* , when beam-beam effect is negligible. By increasing beam current, the beam-beam effect dominates. Vertical beam size blow-up due to the beam-beam interaction results decrease of the specific luminosity.

Figure 1 presents the specific luminosity as function of beam current product at early stage of squeezing beta to $\beta_y = 4$ mm (June 10, 2018). Vertical beam size is measured by X-ray monitor for both beams. As the beta function at the monitor is well-calibrated, the beam size corresponds to the vertical emittance. The beam sizes written in the figure are calculated by the measured vertical emittance $\sigma_y^* = \sqrt{\varepsilon_y \beta_y^*}$ in each (total) current, where the number of bunches are 788. The specific luminosity calculated by Eq. (1) using the beam size is plotted by red stars. The specific luminosity disagrees at low current. This result means the beam size at IP is deviate from $\sqrt{\beta_y^* \varepsilon_y}$ geometrically. The discrepancy of the specific luminosity is small at high bunch current. Electron beam is enlarged strongly at high current. Peak luminosity was $L_{peak} = 1.2 \times 10^{33} \text{ cm}^{-2}\text{s}^{-1}$ for 285mA(e^-)x340mA(e^+) at $N_b = 788$.

There are several possibility for the disagreement of the specific luminosity. Beam collision offset is scanned in

* ohmi@post.kek.jp

OFF-MOMENTUM OPTICS AT SuperKEKB

Y. Ohnishi*, H. Koiso, A. Morita, K. Ohmi, H. Sugimoto, KEK, OHO 1-1, Tsukuba, Japan
 K. Oide, CERN, Geneva, Switzerland

Abstract

The nano-beam scheme can squeeze the vertical beta function at the IP much smaller than the bunch length. It implies that the large chromaticity is generated in the vicinity of the final focus quadrupole magnets and the strong sextupoles, for instance the local chromaticity corrections, are adopted to correct the chromaticity. While understanding of the off-momentum optics is important to optimize the dynamic aperture to make Touschek lifetime long and to reduce the luminosity degradation due to chromatic behaviors. In general, there is a discrepancy between measurements of chromaticity and those obtained from the optics model. The chromatic phase-advance is introduced to measure the off-momentum optics and correct by adjustments of sextupole magnets.

INTRODUCTION

SuperKEKB is an electron-positron double-ring collider [1] and the Belle II detector [2] built to explore new physics in the collider experiment. The physics program of the recent B-factory delivering extremely high statistics is almost independent of and complementary to the high energy experiments at the LHC. The target luminosity is $8 \times 10^{35} \text{ cm}^{-2} \text{ s}^{-1}$, which is 40 times the performance of KEKB [3] that has been operated for 11 years until 2010. The strategy for the luminosity upgrade is a nano-beam scheme. The collision of low emittance beams under a large crossing angle allows squeezing the beta functions at the IP to value much smaller than the bunch length. Consequently, extremely higher luminosity can be expected with only twice the beam current of KEKB.

The small beta functions at the IP implies that a large chromaticity is generated in the vicinity of the final focus magnets (QC1 and QC2). The natural chromaticity calculated from the lattice model in Phase 2 is shown in Table 1. Because the chromaticity generated from QC1 and QC2 is very large, we adopt local chromaticity corrections for both x and y directions. The local chromaticity correction and the arc lattice utilize non-interleaved sextupole correction scheme. Two identical sextupole magnets are connected by $-I'$ transfer matrix. A nonlinear kick from either of two sextupole magnets can be compensated by another sextupole magnets for on-momentum particles in this scheme. Therefore, a large dynamic aperture can be expected. The number of sextupole families is 54 for each ring. The field strength of the sextupole magnet is optimized to maximized the dynamic aperture or Touschek lifetime as well as adjustments of the linear chromaticity.

Figure 1 shows comparisons between typical measured chromaticity and that calculated from the model lattice. The

Table 1: Typical parameters such as the beta functions and chromaticity in Phase 2

	LER	HER	Unit
Beam Energy	4	7	GeV
β_x^*	200	100	mm
β_y^*	3	3	mm
β_x at QC2L	62.2	235.2	
β_x at QC2R	62.1	288.0	
β_y at QC1L	255.6	578.0	
β_y at QC1R	254.7	581.6	
ξ_{x0}	-69	-97	
ξ_{y0}	-146	-168	
ξ_x (QC2)	-8	-25	
ξ_y (QC1)	-67	-100	
ν_x	44.558	45.541	
ν_y	46.615	43.610	
α_p	2.88×10^{-4}	4.50×10^{-4}	

optical functions are calculated by using SAD [4] for the model lattice. There are discrepancies between the measured value and the model by $\Delta\xi_x = 1 \sim 1.5$ and $\Delta\xi_y = 2.5 \sim 3.3$ in the LER, $\Delta\xi_x = 0.5 \sim 0.7$ and $\Delta\xi_y = 3 \sim 3.3$ in the HER, which corresponds to 1~2 % deviation.

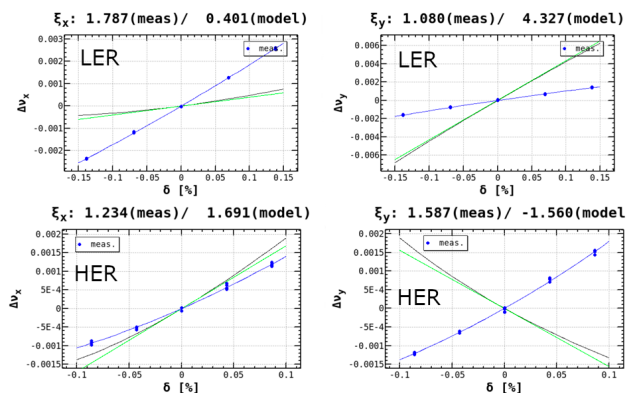


Figure 1: Chromaticity in the LER and HER, respectively. The blue plots indicate measured tune shift and black line for the model calculation. The green line show a derivative of the model tune shift at the on-momentum.

First of all, as the motivation of this article, why there is discrepancy between model and measurement? We can change the chromaticity as a relative value by using model calculations. However, the absolute value is unclear even though optics corrections have been done and worked well for corrections of beta functions and dispersions. Secondary, the off-momentum optics is necessary to understand well to

* yukiyoshi.ohnishi@kek.jp

PROGRESS OF PRELIMINARY WORK FOR THE ACCELERATORS OF A 2-7 GeV SUPER TAU CHARM FACILITY AT CHINA *

Q. Luo[†], D. Xu, National Synchrotron Radiation Laboratory,
University of Science and Technology of China, 230029 Hefei, China

Abstract

As the most successful tau-charm factory of the world, BEPC II will celebrate its 10th birthday this year and will finish its historical mission in the next decade. Because of its very important role in high energy physics study, BEPC II will certainly need a successor, a new tau-charm collider. This paper discusses the feasibility of a greenfield next generation tau-charm collider named HIEPA. The luminosity of this successor is about $5 \times 10^{34} \text{ cm}^{-2}\text{s}^{-1}$ pilot and $1 \times 10^{35} \text{ cm}^{-2}\text{s}^{-1}$ nominal, with the electron beam longitudinally polarized at the IP. The general scheme of the accelerators and the beam parameters are shown. Several key technologies such as beam polarization and beam emittance diagnostics are also discussed.

INTRODUCTIONS

The most successful tau-charm factory of the world in operation is Beijing Electron Positron Collider II (BEPC II), which reached a luminosity of higher than $1 \times 10^{33} \text{ cm}^{-2}\text{s}^{-1}$ in the year 2016. We believe that the unique collider in China would finish its historical mission in the next decade, maybe around the year 2022 or later. Although many scientists show strong interests in the very ambitious Higgs factory proposal known as CEPC-SPPC in China, it is clear that the Higgs factory will be a long-term plan that will cost a price of several orders higher than a tau charm factory and a period of study and construction of more than 20 years, and require global cooperation. As a transitional choice, a new tau charm collider facility was proposed by high energy physicists in the Collaborative Innovation Center for Particles and Interactions (CICPI, China) [1] to replace BEPC II after its retirement and before the construction of CEPC. The new tau-charm collider was named High Intensity Electron Positron Accelerator (HIEPA) due to its very high luminosity and current. It will be a next generation electron-positron collider operating in the range of center-of-mass energies from 2 to 7 GeV utilize polarized electron beam in collision. The pilot luminosity will be $5 \times 10^{34} \text{ cm}^{-2}\text{s}^{-1}$ and the nominal luminosity will be $1 \times 10^{35} \text{ cm}^{-2}\text{s}^{-1}$.

The construction of a new 2-7 GeV tau-charm factory will help to maintain China's leading advantage at tau-charm area. In addition, many common technologies which are useful for both CEPC-SPPC and tau charm factory will be developed and a strong team of scientists will be trained. At last, a tau-charm factory would be a good backup plan if the CEPC-SPPC construction cannot begin on time as

planned. We expect the new tau charm facility to be an important part of Hefei Comprehensive National Science Center. This paper discussed not only the feasibility of the next tau-charm factory, but also several related key technologies needed to be developed in the future 5~10 years. The accelerator division of the National Synchrotron Radiation Laboratory of China now organizes the preliminary study of STCF accelerators.

BEAM PARAMETERS AND LATTICE DESIGN OF THE ACCELERATOR

Last year we reported two possible routes that might lead to a successor of BEPC II [2]. Now IHEP is planning to upgrade the luminosity of the BEPC II to 2-3 times higher. This paper will only introduce the plan of a greenfield tau-charm collider.

Table 1: Main Parameters for Accelerators, Pilot

Parameters	Value
Peak Luminosity	$5 \times 10^{34} \text{ cm}^{-2}\text{s}^{-1}$
Beam Energy	2GeV, 1-3.5GeV tunable
Circumference	324.3m
Current	1.5 A
Beam Emittance ϵ_x/ϵ_y	2.4/0.03 nm-rad
β_x^*/β_y^*	66.5/0.55 mm
Crossing Angle	60 mrad
Hourglass factor H	0.8
ξ_y	0.06

Table 2: Main Parameters for Accelerators, Nominal

Parameters	Value
Peak Luminosity	$1 \times 10^{35} \text{ cm}^{-2}\text{s}^{-1}$
Beam Energy	2GeV, 1-3.5GeV tunable
Circumference	324.3m
Current	2 A
Polarization	>85% (e-)
Beam Emittance ϵ_x/ϵ_y	5/0.05 nm-rad
β_x^*/β_y^*	67/0.6 mm
Crossing Angle	60 mrad
Hourglass factor H	0.8
ξ_y	0.08

As shown in Table 1 and 2, the whole construction of the collider will be divided to two stages: the pilot and the nominal. During the pilot stage, the peak luminosity will achieve $5 \times 10^{34} \text{ cm}^{-2}\text{s}^{-1}$. During the nominal stage, the peak

* Work supported by National Natural Science Foundation of China U1832169 and the Fundamental Research Funds for the Central Universities, Grant No WK2310000046

[†] Email address: luoping@ustc.edu.cn

DIFFERNET OPTICS WITHIN LARGE ENERGY REGION AT BEPCII

C. H. Yu^{†, 1}, Y. Zhang¹, Q. Qin, J. Q. Wang, G. Xu, C. Zhang, D. H. Ji, Y.Y. Wei, J. Xing, X. H. Wang, X.M. Wen, Z. Duan, Y. Jiao, N. Wang, Y. M. Peng, Y. Y. Guo, S. K. Tian, Y. S. Sun, J. Wu, Y. Bai, S. C. Jiang, C. C. Du, Key Laboratory of Particle Acceleration Physics and Technology, Institute of High Energy Physics, Chinese Academy of Sciences, Beijing 100049, China
¹also at University of Chinese Academy of Sciences, Beijing 100049, China

Abstract

BEPCII is designed at the beam energy of 1.89 GeV. According to the requirements of high energy physics, BEPCII has been operated in the energy region from 1.0 GeV to 2.3 GeV since 2009. The energy region is quite large so that it is very important to select optics for the optimized luminosity. Different optics within different energy region at BEPCII will be introduced in detail in this paper.

INTRODUCTION

Beijing Electron-Positron Collider (BEP) has been well operated not only for high energy physics, but also for synchrotron radiation application for more than 15 years since 1989. Its upgrade scheme BEPCII is a double-ring collider which two beams have same energies. It aims at the research of τ -charm physics with a designed luminosity of $1.0 \times 10^{33} \text{ cm}^{-2}\text{s}^{-1}$, which is about two orders higher than BEPC at the beam energy of 1.89 GeV. The two new rings have been built in the existing BEPC tunnel while keeping the machine as a synchrotron radiation source. According to the requirements of high energy physics, BEPCII has been operated in a large energy region from 1.0 GeV to 2.3 GeV since 2009.

OPTICS OPTIMIZATION AT 1.89 GeV

The main parameters of designed lattice is shown in Table 1. The commissioning of BEPCII at the energy of 1.89 GeV started on June 22nd, 2008. The horizontal tune was moved from 6.530 to 6.505 on May 5th, 2009 for higher luminosity. The data taking at the energy of 1.89 GeV started from the beginning of 2010. The beam current and luminosity were improved step by step, together with the control of detector background and the luminosity optimization systematically. The maximum beam current and luminosity reached 750 mA and $6.49 \times 10^{32} \text{ cm}^{-2}\text{s}^{-1}$, respectively until April 28th, 2011. There are two limitations to restrict the luminosity further improvement. One is the beam current, and the other is beam-beam parameter. It's very hard to increase the beam current, especially above 700 mA due to heating problem, which were mainly caused by synchrotron radiation power and high order mode. Several serious hardware failures were happened during the operation, such as kicker magnet, RF coupler, SR monitor, bellows, feedback system, etc. The beam-beam parameter was limited obviously under 0.033 at any bunch current shown in Fig. 1. Bunch lengthening effect was considered to explain the phenomenon.

[†] yuch@ihep.ac.cn

Table 1: Main Design Parameters of BEPCII

Parameters	Values
Operation energy	1.0~2.1 GeV
Optimized energy	1.89 GeV
Beam current	910 mA
Bunch current	9.8 mA
Circumference	237.5 m
Number of particles	4.5×10^{12}
β function at IP β_x/β_y	1.0 m/1.5 cm
Horizontal emittance	144 nm-rad
Working point ν_x/ν_y	6.53/5.58
Harmonic number	396
Bunch number	93
Bunch spacing	2.4 m
RF voltage	1.5 MV
RF frequency	499.8 MHz
RF cavity number per ring	1
Energy loss per turn	121 keV
Synchrotron radiation power	110 kW
Damping time $\tau_x/\tau_y/\tau_E$	25/25/12.5 ms
Natural energy spread	5.16×10^{-4}
Momentum compaction	0.0235
Natural bunch length	1.35 cm
Crossing angle at IP	11×2 mrad
Beam-beam parameter	0.04
Luminosity	$1.0 \times 10^{33} \text{ cm}^{-2}\text{s}^{-1}$

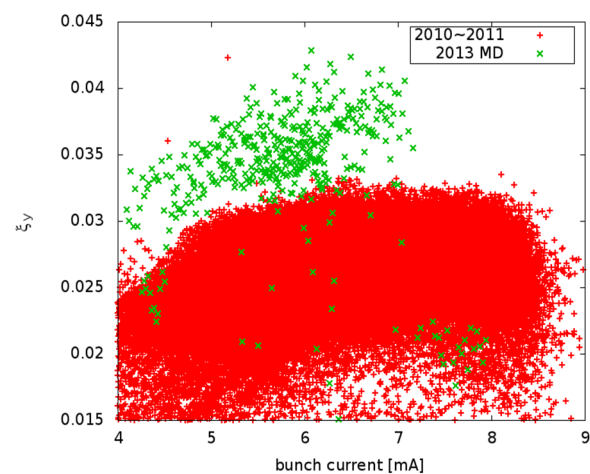


Figure 1: Comparison of beam-beam parameter with the schemes of different bunch lengths.

Content from this work may be used under the terms of the CC BY 3.0 licence (© 2018). Any distribution of this work must maintain attribution to the author(s), title of the work, publisher, and DOI.

HIGH CURRENTS EFFECTS IN DAΦNE

C. Milardi[†], D. Alesini, S. Bini, A. Drago, A. Gallo, A. Ghigo,
 S. Guiducci, M. Serio, A. Stella, M. Zobov, LNF-INFN, Frascati, Italy
 F. Marcellini, PSI, Villigen, Switzerland
 P. Raimondi, ESRF, Grenoble, France

Abstract

DAΦNE, the Italian lepton collider, operates routinely with high intensity electron and positron colliding beams. The high current multi-bunch beams are stored in two independent rings, each of them 97 m long, and are distributed into 100÷110 contiguous buckets out of the 120 available, spaced by only 2.7 ns.

Since its construction, DAΦNE has been operated in different configurations which, overall, allowed to store currents up to 1.4 A and 2.45 A in the positron and in the electron beam respectively. To this day DAΦNE holds the record for the highest electron beam current ever stored in particle factories and modern synchrotron radiation sources.

The DAΦNE experience, in terms of beam dynamics optimization aimed at achieving the high intensity beams, is presented with special emphasis on the *e-cloud* related issues which represent the dominant effect limiting the positron beam current.

INTRODUCTION

DAΦNE [1, 2] is an accelerator complex consisting of a double ring lepton collider working at the energy of the Φ -resonance, (1.02 GeV) and an injection system. The collider includes two independent rings, each ~97 m long.

The two rings share an interaction region (IR), where the detector on duty is installed. A full energy injection system, including an S-band LINAC, 180 m long transfer lines, and an accumulator/damping ring provides fast and high efficiency electron–positron injection in topping-up mode.

Since its construction DAΦNE has been mainly operated in two configurations, differing essentially for the approach to the beam-beam interaction. In fact, till 2006, the main rings shared two ≈10 m long interaction regions, although only one detector at a time was taking data. Due to the common beam pipe, the two beams collided with a rather small horizontal angle, of the order of 25 mrad, which was also compliant with the Piwinski criterion [3]. During this initial phase, the collider performances have been significantly improved by several progressive upgrades and a wide program of machine measurements and studies, aimed at pointing out the physics processes limiting the maximum achievable current and luminosity, has been undertaken. This activity largely contributed to define a proposal for an original collision scheme based on large Piwinski angle and *Crab-Waist* (*CW*) compensation of the beam-beam interaction [4, 5]. In 2006 the novel approach to collision has been implemented on DAΦNE during a six months shutdown planned to install a compact detector

without longitudinal magnetic field, offering an optimal simplified environment to test the new configuration: the SIDDHARTA experiment.

The parameter of the DAΦNE collider in the nominal and in the *CW* configurations are reported in Table 1.

Table 1: DAΦNE Beam Parameters

	DAΦNE native (2000÷2006)	DAΦNE CW Since 2007
Energy (MeV)	510	
β_y^* (cm)	1.8	0.85
β_x^* (cm)	160	23
σ_x^* (μm)	760	250
σ_y^* (μm) _{low current}	5.4	3.1
σ_z (cm)	2.5	1.5
Bunch spacing (ns)	2.7	
Damping times τ_E, τ_x (ms)	17.8/36.0	
Cros. Angle $\theta_{\text{cross}}/2$ (mrad)	12.5	25
Pwinski Angle ψ (mrad)	0.6	1.5
ϵ (mm mrad)	0.34	0.28
RF frequency [MHz]	368.26	368.667
Harmonic number	120	
$L \cdot 10^{32}$ ($\text{cm}^{-2} \text{s}^{-1}$)	1.5	4.36

HIGH CURRENT DESIGN STRATEGY

The efforts aimed at achieving high intensity beams and at optimizing beam quality have been comparable to the ones invested in the beam-beam interaction approach.

Since the design stage all the main ring vacuum components have been specified in order to store large total current in a large number of bunches, which required special emphasis on vacuum and collective effect related topics.

Each ring vacuum chamber [6] consists of 4 arcs and straight sections. The chamber of the arcs is made by a special Al-Mg alloy (Al 5083 H321), while the straight section ones use a slightly different composition Al-Si alloy (Al 6082 T6). The dipole and wiggler beam pipes in the arcs are all equipped with antechambers and synchrotron radiation absorbers in order to improve pumping efficiency.

It is well known that collective instabilities in accelerators mostly come from an intense particle beam electromagnetically interacting with its vacuum chamber environment. This interaction, which can easily drive the beam to instability, is described by the wakefield (time domain) and beam-coupling impedance (frequency domain) concepts. Hence the need for a detailed evaluation of the impedance impact on single and multibunch dynamics [7]. Since the

[†] catia.milardi@lnf.infn.it

IMPEDANCE AND COLLECTIVE EFFECTS IN JLEIC*

R. Li, K. Deitrick, F. Mauhauser, T. Michalski

Thomas Jefferson National Accelerator Facility, Newport News, VA 23693, USA

Abstract

JLEIC is the high luminosity and high polarization electron-ion collider (EIC) currently under design at Jefferson Lab. Its luminosity performance relies on the beam stability under high-intensity electron and ion beam operation. The impedance budget analysis and the estimations of beam instabilities are currently underway. In this paper, we present the update status of our back-of-envelope estimations for these collective instabilities, and identify area or parameter regimes where special attentions for instability mitigations are required.

INTRODUCTION

The JLEIC baseline parameters [1] are conceived based on the unique luminosity concept of the design, featuring small bunch emittances, relatively low bunch charge, and very high bunch repetition rate [2]. These features further determine the behaviour of collective instabilities in the collider rings during bunch collision. It implies moderate single-bunch instabilities; yet it poses strong requirements on the fast feedback systems to mitigate longitudinal and transverse coupled-bunch instabilities. For a complete design study, the collective effects need to be assessed for a wide range of beam energies and ion species, and also for the entire ion bunch formation process. In this presentation, we only focus on cases for a few selected collision energies.

Ideally, the wakefield induced beam instabilities can be analytically and numerically studied once the machine impedance budget is available. However, developing impedance budget and performing instability estimations are an iterative and gradually refining process. Presently, JLEIC design is still at its early phase and the engineering design has just begun. At this stage, a preliminary estimation of impedance thresholds, for various coherent instabilities, is necessary for the engineer design to make design choices so as to minimize machine impedances and ensure beam stability. In this paper, we discuss the current status of the JLEIC impedance studies, and present our initial back-of-envelop estimations for the single and coupled bunch instabilities using the recent JLEIC baseline design parameters. The estimated impedance threshold will be compared with the expected machine impedances for the JLEIC collider rings, as inferred from the impedance budgets of some existing machines. We will also give preliminary discussions about the two-stream instabilities, i.e., the electron cloud effects in the ion ring and the ion effects in the electron ring.

* This material is based upon work supported by the U.S. Department of Energy, Office of Science, Office of Nuclear Physics under contract DE-AC05-06OR23177.

JLEIC IMPEDANCE ESTIMATIONS

In a storage ring, the electromagnetic response of the vacuum chamber to the beam current is characterized by the broadband and narrowband impedances, which could cause respectively the single-bunch and coupled-bunch collective instabilities. The narrowband impedances for the JLEIC electron and ion rings are discussed in the section on the coupled-bunch instabilities. For broadband impedances, the estimation of the impedance budget requires engineer drawings of the vacuum chamber. Yet for JLEIC, presently the machine engineering design has just begun, hence no details are available except for the element counts for most of the impedance-generating components in both rings (see Table 1). Without the actual component designs, at present we can only use the impedance budgets for some existing machines, such as PEP-II, SUPERKEKB, or RHIC, as references [3-5]. One reason for using PEP-II for reference is that there is consideration for the JLEIC e-ring to adopt the RF cavities, as well as the components for vacuum system and diagnostics, from PEP-II HER. Another convenient feature is that the bunch length ($\sigma_z \approx 1.2$ cm) for JLEIC is comparable to that in PEP-II, given that the effective impedances are bunch-length dependent. With the PEP-II impedance budget and the JLEIC component counts in Table 1, and assuming these components are identical with those used in the PEP-II HER, we get the estimation for the JLEIC e-ring: the inductance $L \approx 99.2$ nH, the effective longitudinal impedance $|Z_{||}/n| \approx 0.09 \Omega$, the loss factor ≈ 7.7 V/pC, and the effective transverse impedance $k_{\perp} \approx 60$ k Ω /m. If components in SUPERKEKB are used as reference, the JLEIC e-ring impedance estimation becomes:

$$\approx 28.6 \text{ nH}, |Z_{||}/n| \approx 0.02 \Omega, k_{||} \approx 19 \text{ V/pC}, |Z_{\perp}| \approx 13 \text{ k}\Omega/\text{m},$$

with the note that the shorter bunch length ($\sigma_z \approx 0.5$ cm) for beams in SUPERKEKB than that in JLEIC may cause underestimation of the effective impedances.

For the JLEIC ion ring, the ion beam undergoes the bunch formation process including the injection, acceleration, bunch splitting, and finally collision. The bunch length varies through the whole process, and the short ion bunch ($\sigma_z \approx 1.2$ cm) at the collision state is made possible only by employing the envisioned high-energy electron cooling [6]. Since such short bunch length is unprecedented for the ion beams in existing ion rings, it is more appropriate [7] to use the PEP-II rings rather than the existing ion rings for reference when estimating the JLEIC

STUDY TO MITIGATE ELECTRON CLOUD EFFECT IN SuperKEKB

Y. Suetsugu[†], H. Fukuma, K. Ohmi, M. Tobiyama, K. Shibata
 High Energy Accelerator Research Organization (KEK), 305-0801, Tsukuba, Japan

Abstract

During Phase-1 commissioning of the SuperKEKB from February to June 2016, electron cloud effect (ECE) was observed in the positron ring. The electron clouds at high-beam-current region were found to be in the beam pipes in drift spaces of the ring, where antechambers and titanium nitride (TiN) film coating were prepared as countermeasures against ECE. Permanent magnets and solenoids to generate magnetic fields in the beam direction were attached to the beam pipes as additional countermeasures. Consequently, during Phase-2 commissioning from March to July 2018, experiments showed that the threshold of current linear density for exciting ECE increased by a factor of at least two when compared to that during Phase-1 commissioning. While the countermeasures were strengthened, the effectiveness of the antechambers and TiN film coating had to be re-evaluated. By performing various simulations and experiments during Phase-2 commissioning, it was found that the antechamber was less effective than anticipated with regards to reducing the number of photoelectrons in the beam channel. The TiN film coating, on the other hand, had low secondary electron yield as expected.

INTRODUCTION

The SuperKEKB is an electron-positron collider with asymmetric energies in KEK that aims for an extremely high luminosity of $8 \times 10^{35} \text{ cm}^{-2} \text{ s}^{-1}$ [1]. The main ring (MR) consists of two rings, i.e. the high-energy ring (HER) for 7-GeV electrons and the low-energy ring (LER) for 4-GeV positrons. Each ring has four arc sections and four straight sections, as shown in Fig. 1.

Electron cloud effect (ECE) is a serious problem in the SuperKEKB LER [2]. The threshold density of electrons ($n_{e,th} [\text{m}^{-3}]$) at which ECE is excited was estimated to be $\sim 3 \times 10^{11} \text{ m}^{-3}$ by various simulation studies [3]. Hence, highly effective countermeasures against ECE were required for the SuperKEKB LER [4], which are summarized in Table 1. Beam pipes with antechambers for suppressing the effect of photoelectrons and a TiN film coating for reducing the secondary electron yield (SEY) were used for in the majority of the new beam pipes, most of which were made of aluminum (Al) -alloy. A schematic of a typical beam pipe at arc sections is presented in Fig. 2. The beam pipes for bending magnets have longitudinal grooves in the beam channel along with the TiN film coating in order to further reduce the SEY. Clearing electrodes were installed in the beam pipes for wiggler magnets instead of the TiN film coating, but they also have the antechambers. The beam pipes for wiggler magnets were made of copper. Approximately 90% of the beam pipes in the ring possess the

antechambers and TiN film coating. Magnetic fields are applied in the beam direction by solenoids to the beam pipes in drift spaces between electromagnets, such as quadrupole magnets and bending magnets. With these all countermeasures, an electron density ($n_e [\text{m}^{-3}]$) of approximately $2 \times 10^{10} \text{ m}^{-3}$ was expected at the designed beam parameters, i.e. a beam current of 3.6 A at a bunch fill pattern of one train of 2500 bunches, with a bunch spacing of 2 RF-buckets (referred to 1/2500/2RF hereafter). Here, one RF-bucket corresponds to 2 ns. This value of n_e is sufficiently lower than the $n_{e,th}$, $3 \times 10^{11} \text{ m}^{-3}$. It must be noted that the magnetic fields in the beam direction ($B_z [\text{G}]$) at drift spaces were not prepared before Phase-1 commissioning, since the maximum stored beam current was not expected to be so high during the commissioning, i.e. approximately 1 A at the maximum.

The n_e around the beam orbit in an Al -alloy beam pipe with antechambers was measured via electron current monitors, which were also used in the previous KEKB experiments [5]. Two electron monitors were set up at the bottom of the beam channel of a test beam pipe. The voltage applied to the electron collector was 100 V, while that applied to the grid (repeller) varied from 0 V to -500 V. These two electron monitors were attached to the same beam pipe: one in the region with TiN film coating (as in the other typical beam pipes in the ring) and one in the region without the TiN film coating (i.e. bare Al surface). The test beam pipe was placed in an arc section of the ring. The line density of photons of the synchrotron radiation (SR) is $1 \times 10^{15} \text{ photons s}^{-1} \text{ m}^{-1} \text{ mA}^{-1}$, i.e. 0.16 photons $\text{posi.}^{-1} \text{ m}^{-1} \text{ turn}^{-1}$. This line density is almost same as the average value of arc sections.

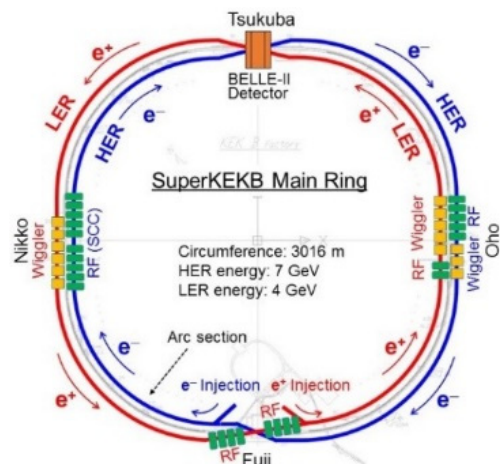


Figure 1: Layout of the SuperKEKB Main Ring (MR). One ring consists of four arc sections and four straight sections.

[†] yusuke.suetsugu@kek.jp

BENCHMARKING OF SIMULATIONS OF COHERENT BEAM-BEAM INSTABILITY WITH SUPERKEKB MEASUREMENT

K. Ohmi*, K. Hirosawa, H. Ikeda, H. Koiso, Y. Ohnishi, M. Tobiyama,
 KEK/Soken-dai, Tsukuba, Japan,
 D. E. Khechen, CERN, Geneva, Switzerland

Abstract

Coherent beam-beam instability in head-tail mode has been predicted in collision with a large crossing angle. The instability is serious for design of future e^+e^- colliders based on the large crossing angle collision. It is possible to observe the instability in SuperKEKB commissioning. Horizontal beam size blow-up of both beams has been seen depending on the tune operating point. We report the measurement results of the instability in SuperKEKB phase II commissioning.

INTRODUCTION

Coherent beam-beam instability in head-tail mode has been studied for Phase II commissioning of SuperKEKB. β_x^* is squeezed to ~ 3 cm in the SuperKEKB design. The instability was seen in $\beta_x^* \sim 24$ cm ($8\times$ of the design) but not in 12 cm ($4\times$) at the design bunch population N_{\pm} [1] in strong-strong beam-beam simulation. The instability is serious for large β_x^* , because two beams correlate proportional to β_x^* .

β_x^*/β_y^* were squeezed step-by-step in Phase II commissioning. During the squeezing β^* , we had the chance to measure the instability. Table 1 shows the parameters of SuperKEKB. Beam-beam collision was established with the expected β^* in Phase II. The bunch population was 50-60% of the design, and the beam-beam parameter is limited for electron beam $\xi_y = 0.02$ [2]: that is, positron beam enlarges in vertical, increasing the bunch currents. Tune operating point is $(\nu_x, \nu_y) = (44.569, 46.609)$ and $(45.541, 43.608)$ for LER and HER, respectively. Any instability signal has not been seen in this operating point, but by changing the horizontal tune of one beam, the horizontal beam sizes of the both beams increase simultaneously. We present the experimental results and the beam-beam simulations in this paper.

Table 1: Parameters for SuperKEKB

parameter	design		Phase-II	
	LER	HER	LER	HER
$N_{\pm} (10^{10})$	9	6.5	4.8	4.0
$\varepsilon_{x/y} \text{ (nm/pm)}$	3.2/8.64	4.6/13	2.1/21	4.6/30
$\beta_{x/y}^* \text{ (mm)}$	32/0.27	25/0.3	200/3	100/3
ν_z	0.0247	0.028	0.022	0.026
ξ_x	0.0028	0.0012	0.0073	0.0025
$\sigma_z \theta_c / \sigma_x$	24.7	19.4	10	10

* ohmi@post.kek.jp

STUDY USING STRONG-STRONG BEAM-BEAM SIMULATION

Figure 1 shows the instability simulation for SuperKEKB commissioning before starting Phase II. Two cases of $\beta_{x,y}^*$ with $(8\times, 8\times)$ and $(4\times, 8\times)$ of the design were examined. The instability was seen in $(8\times, 8\times)$, but not in $(4\times, 8\times)$. Horizontal and synchrotron tunes are $\nu_x = 0.53$ and $\nu_z = 0.025$ for both rings.

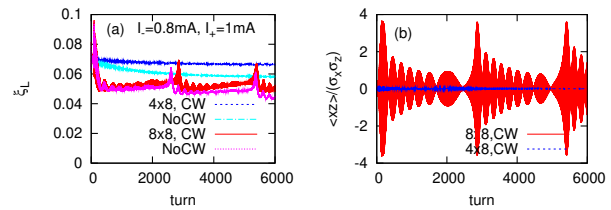


Figure 1: Strong-strong simulation results for SuperKEKB [1]. (a) and (b) show the beam-beam parameter and head-tail motion $\langle xz \rangle$, respectively, at the commissioning stage with IP beta, $(8\times, 8\times)$, and $(4\times, 8\times)$.

In reality, synchrotron tunes of two beams are different, $\nu_z^{(+)} = 0.0247$ and $\nu_z^{(-)} = 0.028$ for LER and HER respectively. Complex head-tail mode coupling between two beams can occur with combination of head-tail modes of two beams [3]. Figure 2 presents variation of tune and growth rate of beam-beam head-tail mode, where the horizontal tune is $\nu_x^{(\pm)} = 0.53$ for both beams. The threshold of the instability is very low ($0.05\times$ of the design bunch population). Mode coupling between $\nu_x^{(+)} + \nu_z^{(+)}$ and $\nu_x^{(-)} - 3\nu_z^{(-)}$ is seen in the right plot of Fig. 2.

Strong-strong simulations using the code (BBSS) have been performed for collision with different synchrotron tunes. Figure 3 presents the evolution of luminosity, dipole moment $\langle x \rangle$, beam size σ_x and correlation of $\langle xz \rangle$, where the horizontal tune is 0.53 for both beams. The horizontal beta function of IP is 4 times of the design, $\beta_x^* = 128/100$ mm. Instability was not seen for equal synchrotron tune ($\nu_z = 0.025$) as shown in Fig. 1. Oscillation in $\langle xz \rangle$ was seen in 1000 turns, but disappeared after that. Horizontal beam size of two beams increased about two times. Small coherent motion in $\langle x \rangle$ remained after 10,000 turns.

Table 2 summarizes simulation results for several horizontal tunes. The horizontal beam size is normalized by the design value. The width (range) of the luminosity and beam size represents lower and upper value; namely presence of a coherent oscillation. Even without coherent oscillation, the

BEAM-BEAM EFFECTS AT HIGH ENERGY e^+e^- COLLIDERS*

D. Shatilov[†], Budker Institute of Nuclear Physics, 630090 Novosibirsk, Russia

Abstract

One of the main requirements for future e^+e^- colliders is high luminosity. If the energy per beam does not exceed 200 GeV, the optimal choice will be a circular collider with “crab waist” collision scheme. Here, to achieve maximum luminosity, the beams should have a very high density at the IP. For this reason, radiation in the field of a counter bunch (BS – beamstrahlung) becomes an appreciable factor affecting the dynamics of particles. In particular, in the simulations for Further Circular Collider (FCC), new phenomena were discovered: 3D flip-flop and coherent X-Z instability. The first is directly related to BS. The second can manifest itself at low energy (where BS is negligible), but at high energies BS substantially changes the picture. In the example of FCC-ee, we will consider the features of beam-beam interaction at high-energy crab waist colliders, and optimization of parameters for high luminosity.

INTRODUCTION

FCC-ee is a double-ring e^+e^- collider to be built at CERN and operate in the wide energy range from Z-pole (45.6 GeV) to $t\bar{t}$ (up to 185 GeV). At such energies, beam-beam effects can get an extra dimension due to BS [1, 2]. FCC-ee apparently will be the first collider where BS plays a significant role in the beam dynamics. For this to happen, two conditions must be fulfilled: high energy and high charge density in the bunch. For example, the energy in LEP was large enough, but the charge density too small, so the effect was negligible. BS increases the energy spread (and hence the bunch length) and creates long non-Gaussian tails in the energy distribution, which can limit the beam lifetime due to a possible escape of particles beyond the energy acceptance.

The collider has a two-fold symmetry and two Interaction Points (IP) with a horizontal crossing angle and “crab waist” collision scheme [3, 4]. The luminosity per IP for flat beams ($\sigma_y \ll \sigma_x$) can be written as:

$$L = \frac{\gamma}{2e r_e} \cdot \frac{I_{tot} \xi_y}{\beta_y^*} \cdot R_H, \quad (1)$$

where I_{tot} is the total beam current which is determined by the synchrotron radiation power 50 MW. Therefore L can be increased only by making ξ_y larger and β_y^* smaller while keeping R_H reasonably large. We assume that ξ_y can be easily controlled by N_p (number of particles per

bunch), that implies adjusting the number of bunches to keep I_{tot} unchanged. The hour-glass factor R_H depends on L_i/β_y^* ratio, where L_i is the length of interaction area which in turn depends on σ_z and Piwinski angle ϕ :

$$\phi = \frac{\sigma_z}{\sigma_x} \operatorname{tg} \left(\frac{\theta}{2} \right), \quad (2)$$

$$L_i = \frac{\sigma_z}{\sqrt{1 + \phi^2}} \Rightarrow \frac{2\sigma_x}{\theta}. \quad (3)$$

Here θ is the full crossing angle, and expressions after \Rightarrow correspond to $\phi \gg 1$ and $\theta \ll 1$, see Fig. 1.

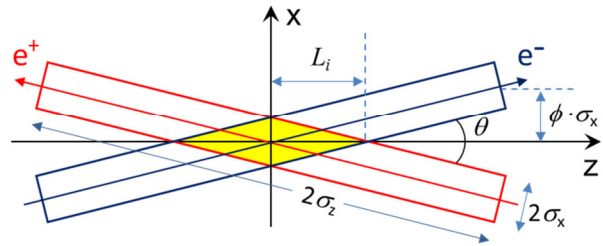


Figure 1: Sketch of collision with large Piwinski angle.

The beam-beam parameters for $\sigma_y \ll \sigma_x$ and $\theta \neq 0$ become [5]:

$$\xi_x = \frac{N_p r_e}{2\pi\gamma} \cdot \frac{\beta_x^*}{\sigma_x^2 (1 + \phi^2)} \Rightarrow \frac{N_p r_e}{\pi\gamma} \cdot \frac{2\beta_x^*}{(\sigma_z \theta)^2} \quad (4)$$

$$\xi_y = \frac{N_p r_e}{2\pi\gamma} \cdot \frac{\beta_y^*}{\sigma_x \sigma_y \sqrt{1 + \phi^2}} \Rightarrow \frac{N_p r_e}{\pi\gamma} \cdot \frac{1}{\sigma_z \theta} \sqrt{\frac{\beta_y^*}{\epsilon_y}}$$

In particular, $\xi_x \propto 1/\epsilon_x$ (in head-on collision) transforms to $\xi_x \propto \beta_x^*/\sigma_z^2$ when $\phi \gg 1$, and ξ_y dependence on σ_x vanishes. Further, because of the symmetry, we consider a model with one IP (that is a half ring of FCC-ee).

HIGH ENERGY

At very high energies (e.g. $t\bar{t}$ production, 175÷185 GeV) the beam lifetime is mainly determined by single BS photons [2], which imposes another limitation on the luminosity. An example is shown in Fig. 2. The black curve corresponds to the Gaussian distribution with σ_8 increased by 30% due to BS. As is seen, within 3-4 sigma the real distribution agrees well with it, but at large amplitudes there are long non-Gaussian tails. Their asymmetry is related to the fact that the damping time is comparable

* Work supported by Russian Science Foundation, N 14-50-00080.

[†] email: shatilov@inp.nsk.su

BEAM-BEAM BLOWUP IN THE PRESENCE OF X-Y COUPLING SOURCES AT FCC-EE

D. El Khechen*, K. Oide¹, F. Zimmermann, CERN, Geneva, Switzerland
¹ also at High Energy Accelerator Research Organisation, Tsukuba, Ibaraki, Japan

Abstract

FCC-ee, the lepton version of the Future Circular Collider (FCC), is a 100 Km future machine under study to be built at CERN. It acquires two experiments with a highest beam energy of 182.5 GeV. FCC-ee aims to operate at four different energies, with different luminosities to fulfill physics requirements. Beam-beam effects at such a high energy/luminosity machine are very challenging and require a deep understanding, especially in the presence of x-y coupling sources. Beam-beam effects include the beamstrahlung process, which limits the beam lifetime at high energies, as well as dynamic effects at the Interaction point (IP) which include changes in the beta functions and emittances. In this report, we will define the beam-beam effects and their behaviours in the FCC-ee highest energy lattice after introducing x-y coupling in the ring.

INTRODUCTION

Beam-beam effects including beamstrahlung have been studied for FCC-ee. Dynamic effects including dynamic β functions and dynamic emittances were simulated in the presence of vertical misalignments of the sextupoles. Tracking was performed in SAD [1] with a beam-beam element present at both IPs of the FCC-ee highest energy lattices (175 and 182.5 GeV). The beam-beam is represented by a weak-strong beam beam simulation (BBWS) [2] which is implemented in SAD. Beam blowup was observed by tracking in the presence of beam-beam and without beam beam. We will report on the different simulations and discuss the results.

DYNAMIC β FUNCTIONS AND EMITTANCES

Dynamic effects are the change of the Twiss parameters (β functions and emittances) at the IP due beam beam quadrupolar focusing. These dynamic effects are enhanced by running at half integer or integer resonance tunes and thus affecting the luminosity.

Analytical Estimations

Dynamic beta functions can be easily calculated by the half turn matrix as given in Eq. (1), where β , β_0 , μ , μ_0 are the dynamic β , the design β , the shifted betatron tune after beam beam and the design betatron tunes respectively and $\frac{1}{f}$ being the beam beam strength. Solving Eq. (1), we can obtain the dynamic beta function given in Eq. (2) where

$\xi_{x,y}$ is the so-called beam beam parameter and expressed in terms of β function and beam-beam force as given in Eq. (3)

$$\begin{pmatrix} \cos \mu & \beta \sin \mu \\ -\frac{1}{\beta} \sin \mu & \cos \mu \end{pmatrix} = \begin{pmatrix} 1 & 1 \\ -\frac{1}{2f} & 0 \end{pmatrix} \begin{pmatrix} \cos \mu_0 & \beta_0 \sin \mu_0 \\ -\frac{1}{\beta_0} \sin \mu_0 & \cos \mu_0 \end{pmatrix} \begin{pmatrix} 1 & 1 \\ -\frac{1}{2f} & 0 \end{pmatrix} \quad (1)$$

$$\beta = \frac{\beta_{x,y}}{\sqrt{1 - (2\pi\xi_{x,y})^2 + 4\pi\xi_{x,y} \cot(\mu_{0x,y})}} \quad (2)$$

$$\xi_{x,y} = \frac{\beta_{0x,y}}{4\pi f_{x,y}} \quad (3)$$

Analytical estimations of dynamic emittance require longer calculations. One way to calculate the dynamic horizontal emittance is given in [3]. The calculation of the dynamic vertical emittance is not straight forward since it requires the knowledge of the errors and corrections of the lattice.

Simulations of Dynamic Effects

The dynamic β functions and emittance were also simulated by an insertion of a thin quadrupole at both IPs representing the linear beam-beam. The thin quadrupole gives a kick as given in Eq. (4).

$$KL = \frac{4\pi f_{x,y}}{\beta_{0x,y}} \quad (4)$$

The beam beam parameters in this case are given to be (0.095,0.157) in the horizontal and vertical plane respectively. It is important to mention that the vertical emittance in the lattice is generated by vertically misaligned sextupoles to achieve an xy coupling of 0.2%. Furthermore, the values of the betatron tunes for the given lattice are $(\nu_x, \nu_y) = (0.553, 0.59)$. The new values of β functions and emittance, after the insertion of the thin quadrupole, are then extracted. The results of the simulations for the dynamic β perfectly match with the analytical estimations and the results of the dynamic effects are summarized in the Table. 1. It is important here to highlight that the values of the dynamic emittance depend essentially on the way the xy coupling is introduced in the lattice.

TRACKING AND BLOWUP

Tracking with Beam Beam

Tracking was also considered to study the beam beam dynamic effects. This was performed by inserting two beam

* dima.el.khechen@cern.ch

SOME ISSUES ON BEAM-BEAM INTERACTION AT CEPC*

Y. Zhang^{†1}, N. Wang, J. Wu¹, Y. Wang, D. Wang, C. Yu¹

Institute of High Energy Physics, CAS, 100049 Beijing, China

¹also at University of Chinese Academy of Sciences, 100049 Beijing, China

Abstract

In this paper, the beam-beam study in CEPC CDR is briefly introduced. Some issues related with beam-beam interaction will be emphasized. The bunch lengthening caused by impedance and beamstrahlung is simulated in a more self-consistent method. The initial result shows that the stable collision bunch current is lower considering the longitudinal wake field. During the courses of dynamic aperture optimization, it is found that there exist some disagreement between dynamic aperture and beam lifetime. We try to define the so-called diffusion map analysis to explain the difference between different lattices. Some initial result for different lattice solution is shown.

INTRODUCTION

The circular Electron Positron Collider(CEPC) is a large international scientific project initiated and housed by China. It was presented for the first time to the international community at the ICFA Workshop “Accelerators for a Higgs Factory: Linear vs. Circular”(HF2012) in November 2012 at Fermilab. The Conceptual Design Report (CDR, the Blue Report) was published in September 2018 [1]. The CEPC is a circular e^+e^- collider located in a 100-km circumference underground tunnel. The CEPC center-of-mass energy is 240 GeV, and at that collision energy will server as a Higgs factory, generating more than one million Higgs particles. The design also allows operation at 91 GeV for a Z factory and at 160 GeV for a W factory. The number of Z particles will be close to one trillion, and W^+W^- pairs about 15 million. Theses unprecedented large number of particles make the CEPC a powerful instrument not only for precision measurments on these important particles, but also in the search for new physics.

Beam-beam interactions are one of the most important limitation to luminosity. Beamstrahlung is synchrotron radiation excited by the beam-beam force, which is a new phenomenon in such high energy storage ring based e^+e^- collider. It will increase the energy spread, lengthen the bunch and may reduce the beam lifetime due to the long tail of photon spectrum [2, 3]. In this paper, we’ll first briefly show some simulation result in CEPC CDR. And then some initial result with self-consistent longitudinal wake field and beam-beam interaction is shown. In the end, we’ll discuss some disagreement between dynamic aperture and beam lifetime. We also did some attempt to define the so-called

diffusion map analysis to explain the cause of more halo particles in some lattice.

BEAM-BEAM STATUS IN CDR

The main parameters of CEPC CDR is shown in Table 1. There are two options for Z, where the detector solenoid strength is 3T or 2T. The 3T options is ignored in Table 1.

Table 1: Main Parameters (CDR)

	Higgs	W	Z(2T)
C_0 (km)		100	
IP		2	
E (GeV)	120	80	45.5
U0/turn (GeV)	1.73	0.34	0.036
θ (mrad)		16.5×2	
Piwinski Angle	3.48	7.0	23.8
N_p (10^{10})	15	12	8
Bunch Number	242	1524	12000
SR Power (MW)	30	30	16.5
β_x^*/β_y^* (m/mm)	0.36/1.5	0.36/1.5	0.2/1.0
ϵ_x/ϵ_y (nm/pm)	1.21/2.4	0.54/1.6	0.18/1.6
ξ_x/ξ_y	0.018/0.109	0.013/0.123	0.004/0.079
RF Voltage (GV)	2.17	0.47	0.1
f_{RF} (MHz)		650	
σ_{z0} (mm)	2.72	2.98	2.42
σ_z (mm)	4.4	5.9	8.5
ν_s	0.065	0.04	0.028
σ_p (10^{-4})	13.4	9.8	8
L ($10^{34} \text{cm}^{-2} \text{s}^{-1}$)	3	10	32

According to the LEP2 experience, the achieved maximum beam-beam parameter strongly depends on the SR damping decrement. Figure. 1 shows the beam-beam performance of CEPC and LEP2. The design beam-beam parameter is nearly 2-3 times higher that of LEP2 experience, which is the contribution of crab-waist scheme [4]. The crab-waist scheme helps to suppress the nonlinear betatron resonance with large Piwinski angle collision and crab-waist transformation. It has been tested in DAΦNE with new detector SIDDHARTA, where the peak luminosity increases with a factor of about 3. In a more complicated physics running with detector KLOE2, the peak luminosity increase about 50% [5].

Higgs

Figure. 2 shows the luminosity versus horizontal tune. There exist strong instability near the resonance $\nu_x - m\nu_s = n/2$, where the new found coherent X-Z instability causes xz moment oscillation and horizontal beam size blow up [6].

* Work supported by National Key Programme for S&T Research and Development (Grant NO. 2016YFA0400400) and NSFC Project 11775238.

[†] zhangy@ihep.ac.cn

KEKB INJECTION DEVELOPMENTS

K. Furukawa*, Injector Linac group

High Energy Accelerator Research Organization (KEK), Tsukuba, 305-0801, Japan
 SOKENDAI (The Graduate University for Advanced Studies), Tsukuba, 305-0801, Japan

Abstract

The e^-/e^+ SuperKEKB collider is now under commissioning. As e^-/e^+ beam injection for SuperKEKB greatly depends on the efforts during the previous KEKB project, the injection developments during KEKB are outlined as well as the improvements towards SuperKEKB. When KEKB was commissioned, approximately ten experimental runs per day were performed with e^-/e^+ injections in between. As another collider PEP-II had a powerful injector SLAC, the KEKB injector had to make a few improvements seriously, such as injection of two bunches in a pulse, continuous injection scheme, eventual simultaneous top-up injections, as well as many operational optimizations. The design of SuperKEKB further required the beam quality improvements especially in the lower beam emittance for the nano-beam scheme, as well as in the beam current for the higher ring stored current and the shorter lifetime.

INTRODUCTION

The energy-asymmetric electron-positron collider, KEKB B-Factory, had been operated successfully for 11 years from 1999 to 2010. It had contributed to the intensity frontier of particle physics by achieving the world highest luminosity at the time. During that period the operation of the collider became much advanced compared with the previous project TRISTAN [1].

In order to meet the beam injection requirements to the collider the injector went through a major reconstruction. The goal was essentially a higher injection rate with a full-energy injection and was mainly achieved by increasing the electron injection energy from 2.5 GeV up to 8 GeV. As the injection aperture became rather small down to 30 ps, the ring RF frequency was modified to have an integer relation between the injector and the ring [2]. The injector accomplished substantial progress during the KEKB period as well. Challenges from many different viewpoints were made to improve the machine. While many of them did not immediately provide meaningful contributions, accumulation of those trials brought significant difference in the performance of injector operation [3].

The collider has been upgraded for the SuperKEKB project since 2010 and is expected to be able to further elucidate the flavor physics of elementary particles with 40-fold improved luminosity, by doubling the stored beam current and also by the nano-beam scheme to shrink the beam size down to a twentieth at the interaction point [4, 5].

The upgrade for SuperKEKB was again a major challenge at the injector. The nano-beam scheme demands fairly small

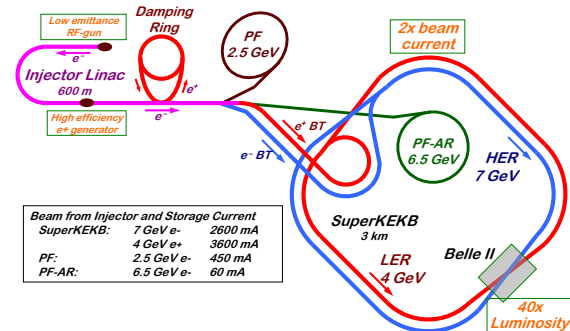


Figure 1: Layout of electron/positron accelerator complex with beam properties from the injector linac into four storage rings of SuperKEKB-HER, LER, PF and PF-AR.

transverse and longitudinal phase space as well as several times higher beam charge of the injection beams. The electron beam would be realized employing a newly designed RF gun [6]. The positron beam would be achieved with combination of a newly installed flux concentrator and a damping ring [7, 8].

Figure 1 shows the accelerator complex configuration at KEK. The injector linac delivers the beams not only to the SuperKEKB high-energy ring (HER) and low-energy ring (LER) but also to light sources of photon factory (PF) and photon factory advanced ring (PF-AR). Even during the SuperKEKB upgrade construction the injector was required to inject the beam into two light source storage rings [9].

Those injection developments during KEKB operation and SuperKEKB upgrade are described in this paper.

KEKB OPERATION

Two B factories of PEP-II and KEKB were operational at the same time [10]. While the SLAC injector to PEP-II was powerful enough, every endeavor at injector was made to satisfy the stable injection into KEKB.

For example, as the beam fluctuation was large in the early stage of the KEKB project, many stabilization loops were installed for beam properties like energies and orbits [11]. For energy stabilization a simple PI (proportional-integral) loop was applied between BPMs (beam position monitors) and RF systems as in Fig.2. Many of those loops were dependent on the beam modes where the beams were injected. Thus, a feedback loop management tool was constructed to supervise those many closed loops as in Fig. 3.

The construction of beam dumps at the middle of the both electron and positron beam transports to HER and LER have assisted the beam quality measurement without injection. It was extremely useful and used everyday.

* kazuro.furukawa@kek.jp

LOW EMITTANCE BEAM TRANSPORT FOR e^-/e^+ LINAC

Y. Seimiya*, N. Iida, M. Kikuchi, T. Mori, KEK, Tsukuba, Japan

Abstract

Design luminosity of SuperKEKB is $8 \times 10^{35} \text{cm}^{-2}\text{s}^{-1}$, which is 40 times higher than that of KEKB achieved. To achieve the design luminosity, the beam have to be transported to the SuperKEKB main ring with the high bunch charge (4 nC) and low emittance: 40/20 μm for horizontal/vertical electron beam emittance and 100/15 μm for positron beam emittance in Phase 3 final. In the LINAC and the beam transport line, the emittance growth is mainly induced by residual dispersion, beam phase space jitter, wake-field in acceleration structure, and radiation excitation. In the Phase 2 operation, we have evaluated and, if possible, corrected these effects on the emittance. Results of the emittance measurement is described.

INTRODUCTION

SuperKEKB is e^-/e^+ collider for high energy particle physics in KEK. The design luminosity of SuperKEKB is 40 times higher than that of KEKB achieved [1]. This high luminosity can be realized by both doubling the current and making the beam size a one-twentieth compared with that of KEKB. The Phase 2 commissioning was finished in July 2018. The LINAC was developed for SuperKEKB [2]. During the operation in Phase 2, collimator tuning to reduce background of Belle-II detector, β squeezing for small beam size at the collision point, collision tuning to maximize the high luminosity, and so on have been done [3]. The physics run is scheduled to start in March 2019 as the Phase 3. Required beam-parameters for Phase 2 and Phase 3 (final) are shown in Fig. 1. In Phase 3 final, requirement to the beam charge is 4 nC for both beams. Required horizontal/vertical emittance is 100/15 μm for positron beam and 40/20 μm for electron beam. We have to convey this high-quality beam to the main ring without emittance degradation as far as possible. Otherwise, the injection rate would be worse and the luminosity would not be able to reach the target value.

A footprint of the LINAC and the beam transport line (BT) is shown in Fig. 2. The LINAC is composed of Sector A, B, J-ARC, C, and 1-5. The LINAC has two kinds of electron gun; a thermionic gun to obtain high-current beam used for positron production and a photocathode RF gun for low emittance electron beam. The large emittance of the positron beam emittance for LER is reduced by a damping ring (DR), which is placed beside the end of Sector 2. The beam is extracted from the end of Sector 2 to the LTR line at 1.1 GeV and injected to the DR. After two cycles of the LINAC pulse, the damped beam is, through the RTL line, resumed to the start of Sector 3 in the LINAC. Positron beam is accelerated up to 4 GeV and transported through the positron BT line and finally reaches the low energy ring

* seimiya@post.kek.jp

Stage	Phase 2 (Mar. – Jul. 2018)		Phase 3 (Mar. 2019 –)	
	e+	e-	e+	e-
Beam	e+	e-	e+	e-
Bunch charge (nC)	1.5	1	4	4
Norm. Emit. ($\gamma\beta\epsilon$) (μm)	200/40 (Hor./Ver.)	150	100/15 (Hor./Ver.)	40/20 (Hor./Ver.)
Energy spread	0.16%	0.1%	0.16%	0.07%

Figure 1: Required beam-parameters for SuperKEKB injector LINAC and the beam transport line.

(LER). Low emittance electron beam is accelerated up to 7 GeV and transported through the electron BT line and finally reaches the high energy ring (HER). To maintain the low emittance, fine tuning is necessary in every place of the system.

SOURCES OF EMITTANCE GROWTH

We have evaluated several conceivable kinds of sources of the emittance growth.

Residual Dispersion

Through the residual dispersion, the energy spread converts to the beam size. First, an example of the dispersion correction at J-ARC section in the LINAC are shown in Fig. 3. where the horizontal axis shows path length along the beam line, blue and red lines show horizontal and vertical dispersion function, respectively. Before correction, large residual dispersion had emerged after the J-ARC as shown in the left inset of Fig. 3. By tuning the strength of quadrupole magnets, horizontal/vertical residual dispersion became small from 0.429/0.092 m to 0.024/0.017 m as shown in the right inset of Fig. 3.

In the same manner, we corrected dispersion in the RTL. In the RTL, there are two ARCs. For example, Fig. 4 shows before and after the dispersion correction in first ARC. The bottom figure in Fig. 4 shows residual dispersion. Blue and red lines show horizontal and vertical residual dispersion, respectively. After the dispersion correction, residual dispersion became smaller. Figure 5 shows values of residual dispersion before and after correction. In both ARCs, residual dispersion became smaller after the dispersion correction. But, the residual dispersion in the first ARC is still not small enough. We need more studies in detail on this issue.

Figure 6 shows improvement of the emittance due to dispersion correction. The emittance was measured with wire scanner (WS). First, we corrected the dispersion in the second ARC. By the correction, emittance was improved from

OVERALL INJECTION STRATEGY FOR FCC-ee

S. Ogur ^{*†}, F. Antoniou, T. K. Charles [‡], O. Etisken [§], B. Harer, B. Holzer, K. Oide [¶],
 T. Tydecks, Y. Papaphilippou, L. Rinolfi, F. Zimmermann, CERN, Geneva, Switzerland,
 A. Barnyakov, A. Levichev, P. Martyshkin, D. Nikiforov, BINP SB RAS, Novosibirsk, Russia,
 E. V. Ozcan, Bogazici University, Bebek, Istanbul, Turkey,
 K. Furukawa, N. Iida, T. Kamitani, F. Miyahara, KEK, Tsukuba, Ibaraki, Japan,
 I. Chaikovska, R. Chehab, LAL, Orsay, Paris, France,
 S. M. Polozov MEPhI, Moscow, Russia, M. Aiba, PSI, Zurich, Switzerland.

Abstract

The Future Circular electron-positron Collider (FCC-ee) requires fast cycling injectors with very low extraction emittances to provide and maintain extreme luminosities at center of mass energy varying between 91.2-385 GeV in the collider. For this reason, the whole injector complex table is prepared by putting into consideration the minimum fill time from scratch, bootstrapping, transmission efficiency as well as store time of the beams in synchrotrons to approach equilibrium emittances. The current injector baseline contains 6 GeV S-band linac, a damping ring at 1.54 GeV, a pre-booster to accelerate from 6 to 20 GeV, which is followed by 98-km top up booster accelerating up to final collision energies. Acceleration from 6 GeV to 20 GeV can be provided either by Super Proton Synchrotron (SPS) of CERN or a new synchrotron or C-Band linac, distinctively, which all options are retained. In this paper, the current status of the whole FCC-ee injector complex and injection strategies are discussed.

INTRODUCTION

The Future Circular electron-positron Collider (FCC-ee) is designed to provide precision study of Z , W , H bosons and top quark, as a potential first step to the global FCC project of CERN. In 98 km collider, these 4 particles will be studied in 4 different operational modes within the distinct time intervals (i.e. upgrades) of the collider [1].

The injector complex consists of a linac, damping ring, pre-booster and top-up booster, as presented in Fig. 1. Inevitably, this chain requires scheduling of bunches in order to fill the collider within minimum time meanwhile allocating enough time to the beams to approach to the equilibrium emittances of the circular accelerator for their stabilisation before the energy ramp up. On the other hand, the injector complex will have the one tenth of the bucket charge in the collider on average, therefore while topping up into the same collider bucket, we have needed to investigate the fluctuations of the bunch length as well as transverse emittances due to beamstrahlung, also known as boothstrapping [2]. The injection into the proceeding synchrotron (for example

from SPS to top-up booster) is also an important limiting parameter to the synchrotrons determining the required dynamic aperture as well as to the spacing between the bunches or the trains. In Table 1, the injection types have been tabulated. All in all, the FCC-ee injector complex will provide the necessary beams with the same accelerators yet distinct cycles as discussed in details in Table 2.

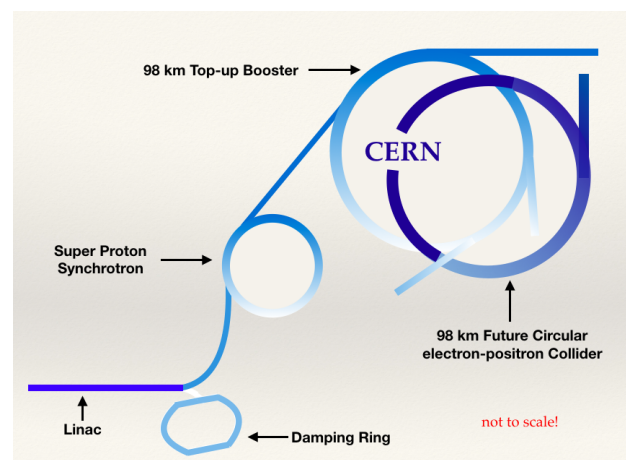


Figure 1: Layout of the FCC-ee.

Table 1: Injection types into the circular accelerators

accelerator	injection type
damping ring	on axis
pre-booster	off-axis
top-up booster	on-axis
collider	off-axis

ELECTRON AND POSITRON PRODUCTION

A low emittance RF-gun has been considered in order to preserve beam transmission and prevent emittance dilution due to wakefields throughout the injector complex. The novel RF-Gun operating at 2856 MHz frequency has been designed to provide 6.5 nC charge in a bunch with

* salim.ogur@cern.ch

† also Bogazici University, Bebek, Istanbul, Turkey

‡ also School of Physics, University of Melbourne, 3010, Victoria, Australia

§ also Ankara University, Ankara, Turkey

¶ also KEK, Tsukuba, Ibaraki, Japan

OVERALL DESIGN OF THE CEPC INJECTOR LINAC*

J. R. Zhang[†], Y. L. Chi, J. Gao, X. P. Li, C. Meng, G. X. Pei¹, S. L. Pei, D. Wang, C. H. Yu¹
 Institute of High Energy Physics, 100049 Beijing, China
¹also at University of Chinese Academy of Science, 100049 Beijing, China

Abstract

The CEPC injector consists of linac and booster. To meet the requirement of the booster, the linac should provide 10 GeV electron and positron beam at a repetition frequency of 100 Hz. In this paper, the overall design of the linac has introduced. For the linac one-bunch-per-pulse is adopted and bunch charge should be larger than 3 nC in the design. A 1.1 GeV damping ring with 75.4 m circumference has adopted to reduce the transverse emittance of positron beam to suitably small value.

INTRODUCTION

Circular Electron-Positron Collider (CEPC) [1] is a 100 km ring e^+e^- collider for a Higgs factory. It has proposed by the Institute of High Energy Physics (IHEP) of the Chinese Academy of Sciences (CAS) in collaboration with a number of institutions from various countries. The CEPC accelerator is composed of linac, booster, collider and the transports lines. The energy of the collider is 120 GeV. The CEPC booster provides 120 GeV electron and positron beams to the CEPC collider and is in the same tunnel as the collider. The energy of the linac is 10 GeV. The layout of CEPC accelerator shows in Fig. 1.

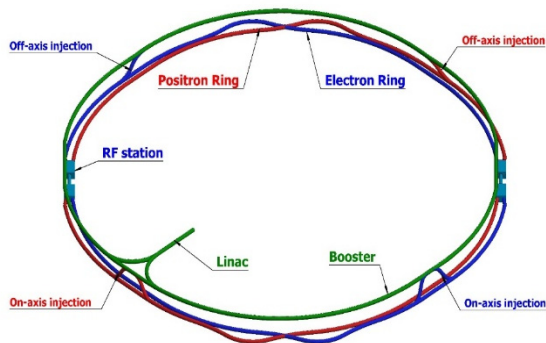


Figure 1: Layout of CEPC accelerator.

OVERVIEW OF THE LINAC

The linac is a normal conducting S-band linac with frequency in 2860 MHz and provide electron and positron beams at an energy up to 10 GeV. The main requirements of the booster to Linac shows in Table 1. Single bunch mode has adopted and the repetition frequency is 100 Hz.

Simplicity and high availability are the design principles. The layout baseline design is the linear scheme and there are 15% backups of the klystrons and accelerating structures. Considering the potential to meet higher requirements and the ability to update in the future, the bunch charge is designed to larger than 3 nC, which is important for positron source design.

Table 1: The requirements of the Booster to the Linac

Parameters	Value	Unit
e^-/e^+ beam energy	10	GeV
Repetition rate	100	Hz
e^-/e^+ bunch population	>1.5	nC
Energy spread (e^-/e^+)	$<2 \times 10^{-3}$	-
Emittance (e^-/e^+)	<120	nm

The linear scheme of linac layout as the baseline design shows in Fig. 2. The linac is composed of electron source and bunching system (ESBS), the first accelerating section (FAS) where electron beam is accelerated to 4 GeV, positron source and pre-accelerating section (PSPAS) where positron beam is accelerated to larger than 200 MeV, the second accelerating section (SAS) where positron beam is accelerated to 4 GeV and the third accelerating section (TAS) where electron and positron beam are accelerated to 10 GeV. Electron bypass transport line (EBTL) scheme has considered for bypass electron beam in electron mode. A 1.1 GeV damping ring at SAS is introduced to reduce the positron beam emittance. The short-range wakefields have considered in the simulation of beam dynamics.

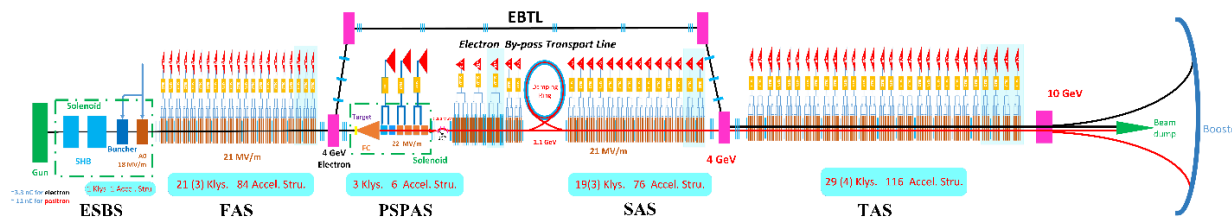


Figure 2: Layout of CEPC Linac.

* Work supported by NSFC (11705214)

[†] zhangjr@ihep.ac.cn

AN ON-AXIS INJECTION DESIGN FOR CEPC

X. Cui[†], C. Yu, Y. Zhang, J. Zhai, IHEP, Beijing 100049, China

Abstract

Considering the requirement on the dynamic aperture in the main collider, an on-axis injection method is needed for the Higgs energy at CEPC. A swap-out on-axis injection scheme using the booster as an accumulation ring is given in this paper. Some dynamical problems concerning the effectiveness of this injection scheme is also discussed.

INTRODUCTION

The CEPC is a circular e^+e^- collider with a 100-km circumference [1]. Its center-of-mass energy is 240 GeV, and it will serve as a Higgs factory at that collision energy. The design also allows operation at 160 GeV as a W factory and 91 GeV as a Z factory. The CEPC accelerator complex consists of a double-ring collider, a booster, a linac and several transport lines. The collider and booster are located in the same underground tunnel, while the linac is built at ground level. Electrons and positrons are generated and accelerated to 10 GeV in the collider, and then are injected into the booster ring. The beams are then accelerated to full-energy and injected into the collider. The geometry of the CEPC complex is shown in Fig. 1, and some key parameters of the booster and collider are shown in Table. 1.

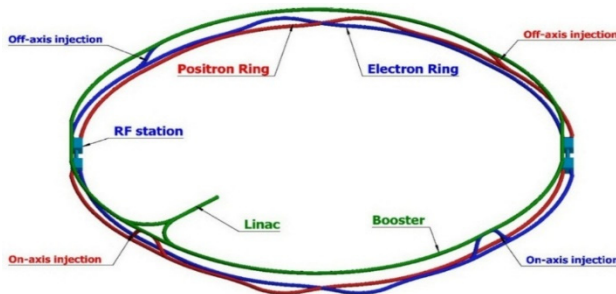


Figure 1: The geometry of the CEPC complex.

For the simplicity and robustness of the injection system, a conventional horizontal off-axis injection is chosen as the baseline design for Higgs, W, and Z mode. However, in the Higgs energy, when the errors and beam-beam effects are considered, the dynamic aperture in the collider may be not enough for an off-axis injection. To relax the requirements on dynamic aperture, an on-axis injection scheme, which is similar to the swap-out injection in HEPS [2], is proposed.

ON-AXIS INJECTION PROCESS

The idea of this on-axis injection is to use the booster as an accumulator ring, and inject the large bunch in the collider into the booster, not the other way around. Thus

off-axis injection and bunch merge are performed in the booster, whose dynamic aperture is large enough. A diagrammatic sketch of this injection process is shown in Fig. 2. In the injection, first fill the booster with small bunches whose bunch charge are 3% of the bunch charge in the collider. Ramp the booster up to 120 GeV, then several circulating bunches of the collider are injected back into the booster ring. After 4 damping times, the injected bunches will merge with the small bunches in the booster with the help of synchrotron radiation damping. Then the merged bunches will be injected back into the same buckets left empty from the last injection. This bunch exchange between the booster and collider ring can repeat until the booster is empty.

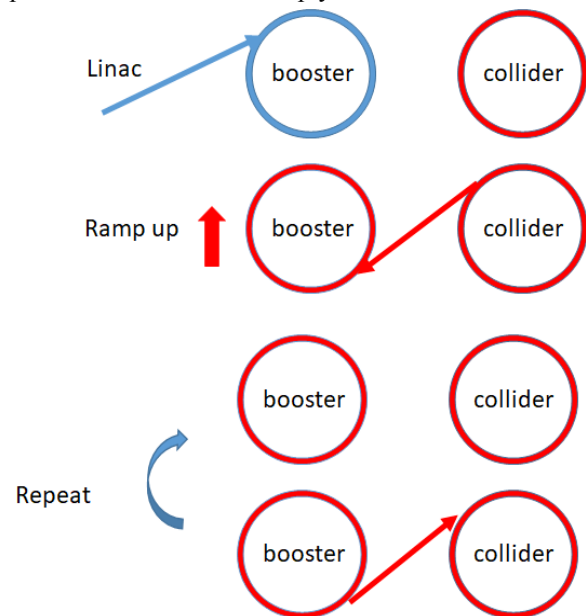


Figure 2: A sketch of the on-axis injection process.

With this on-axis injection scheme, the required horizontal dynamic aperture in the collider is reduced from $13\sigma_x$ to $8\sigma_x$. The number of exchanged bunches between the collider and booster every time is limited by the total current in the booster. With a 1mA booster current threshold, the time structure of the booster is shown in Fig 3. It is shown that the time needed for every on-axis injection is about 35s, which is less than the 47s required by the beam lifetime in the collider [1].

[†] cuihx@ihep.ac.cn

DESIGN AND BEAM DYNAMICS OF THE CEPC BOOSTER*

D. Wang[†], C. Yu¹, X. Cui, D. Ji, J. Zhai, Y. Liu, Y. Zhang¹, C. Meng, N. Wang, J. Gao,
 IHEP, 100049 Beijing, China

¹also at University of Chinese Academy of Sciences, 100049 Beijing, China

Abstract

The CEPC booster needs to provide electron and positron beams to the collider at different energy with required injection speed. A 10 GeV linac is adopted as the injector for CDR. Then the beam energy is accelerated to specific energy according to three modes of CEPC collider ring (H, W and Z). The geometry of booster is designed carefully in order to share the same tunnel with collider. The design status of booster including parameters, optics and dynamic aperture is discussed in this paper.

INTRODUCTION

The CEPC baseline design for CDR is a 100km double ring scheme with a same size booster whose energy starts from 10 GeV [1]. The booster provides electron and positron beams to the collider at different energies. Both the injection from zero current and the top-up injection should be fulfilled. Figure 1 shows the overall layout of CEPC injection chain. The booster is in the same tunnel as the collider, placed above the collider ring except in the interaction region where there are bypasses to avoid the two detectors on collider ring.

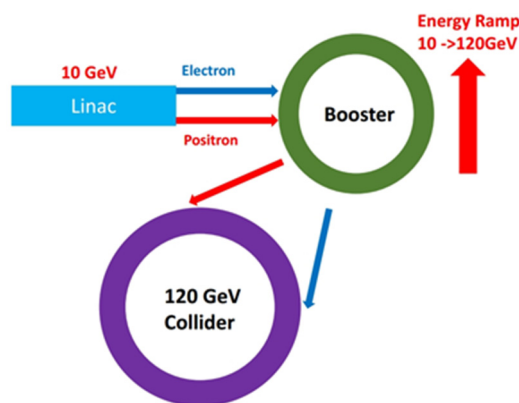


Figure 1: Overall layout of the CEPC injection chain.

BOOSTER PARAMETERS

Booster Design Requirements

The beam quality requirements in the booster are determined by the collider ring and the total beam current in the booster is limited by the RF power which is 1.0mA for Higgs, 4.0 mA for W and 10mA for Z. The energy acceptance of booster should be larger than 1% at four ener-

gy modes and the booster emittance at 120GeV should be lower than 3.6 nm in order to fulfill the requirement of injection to collider ring. The coupling of booster should be controlled under 0.5% which is defined by the requirement of Higgs on-axis injection scheme [1]. We assume 3% current decay for top up injection and the total efficiency of CEPC injection chain is 90%. With the limit for total beam current and the assumption of current decay in collider ring, the top up injection for Higgs mode and W mode needs only one cycle, and needs two cycles for Z mode. The top up injection time structures for the three energy modes are shown in Fig. 2. Furthermore, the dynamic aperture should be large enough for both injection and extraction to guarantee the required transfer efficiency which will be discussed in the last chapter.

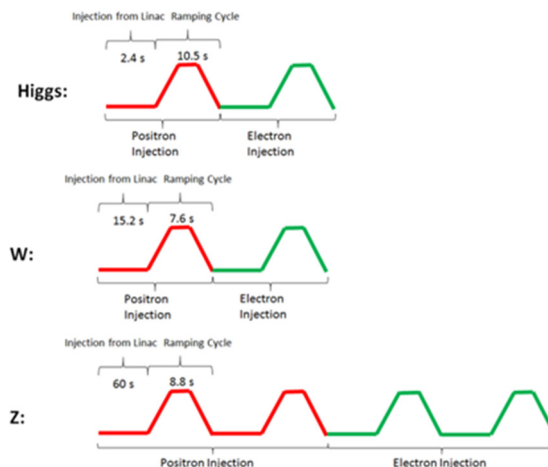


Figure 2: Top up injection time structure for Higgs, W and Z modes.

Beam Parameters at Different Energy

The main booster parameters at injection and extraction energies are listed in Table 1 and Table 2. The beam is injected from linac to booster by on-axis scheme and then injected from booster to collider at three different energies by off-axis scheme. Also the on axis injection from booster to collider for Higgs has been designed in case the dynamic aperture of collider ring at Higgs energy is not good enough for the off-axis injection.

After energy ramping, the booster emittance for Higgs and W approaches the value small enough to inject into the collider. The beam emittance for Z mode after energy ramping still cannot fulfil the collider injection requirement and further damping (5s) is needed before extraction from the booster. The emittance evolution in the booster for three energy modes is show in Fig. 3.

The top up injection time is 25.8 seconds for Higgs off-axis mode, 35.4 seconds for Higgs on-axis mode, 45.8

* Work supported by the National Key Programme for S&T Research and Development (Grant NO. 2016YFA0400400) and the National Natural Science Foundation of China (11505198 and 11575218).

[†] wangd93@ihep.ac.cn

COMMISSIONING OF POSITRON DAMPING RING AND THE BEAM TRANSPORT FOR SuperKEKB

N. Iida*, Y. Funakoshi, H. Ikeda, T. Ishibashi, H. Kaji, T. Kamitani,
 M. Kikuchi, T. Kobayashi, H. Koiso, F. Miyahara, T. Mori, Y. Ohnishi,
 Y. Seimiya, H. Sugimoto, H. Sugimura, R. Ueki, Y. Yano, D. Zhou,

High Energy Accelerator Research Organization (KEK), Tsukuba, Ibaraki 305-0801, Japan

Abstract

The Positron Damping Ring (DR) for SuperKEKB successfully started its operation in February 2018, and the commissioning was continued until the end of SuperKEKB Phase 2 in July without serious troubles. This paper describes achievements of the beam commissioning of injection and extraction lines (LTR and RTL) between the LINAC and DR. In the LTR commissioning, the positron beam with high emittance, wide energy spread, and high charge were transported and injected into the DR. In the RTL commissioning, special cares were necessary to preserve the low emittance. The observed emittance growth in the RTL was not a problem for Phase 2, but it should be resolved in the coming Phase 3. In this paper, brief results of the commissioning of the DR is also reported.

INTRODUCTION

SuperKEKB [1] is a double-ring asymmetric collider of 7-GeV electron ring (HER) and 4-GeV positron ring (LER) with the Belle II detector installed in the interaction region. The KEKB accelerator [2], the predecessor had been in operation from 1998 to 2010, with the then world's highest luminosity of $2.1 \times 10^{34} \text{ cm}^{-2} \text{ s}^{-1}$. To increase the luminosity by 40 times of KEKB, a new collision scheme called "Nano beam scheme" are adopted as well as two times high stored current is required. Since the stored beam has low emittance and high current, the lifetime is short, and the charge of the injection beam must also be high. We adopted an RF gun [3, 4] for generating the low-emittance electron beam. For positrons a flux concentrator [5](FC) as well as a damping ring had been adopted. The FC is a pulsed solenoid installed in right after the positron target to collect positrons generated at the target with high efficiency. The longitudinal phase distribution of the positron is huge, requiring some schemes for efficiently transporting the beam to DR as written in [6].

SuperKEKB is divided in three phases in its operation. In February 2016, we succeeded in operation of Phase 1 [7, 8] for about 5 months without Belle II detector, without collision. Completing construction of super-conducting final quadrupoles in a year and a half further, commissioning of DR and the collider with Belle II (Phase 2 [9]), in which a part of innermost detectors were unmounted, have commenced on January and March 2018 respectively. The required parameters for the positron injection beam of

SuperKEKB-LER are shown in Table 1. It should be noted that these values are defined as "ultimate" parameters in each stage that should be realized in harmony with a development of collision performance.

As shown in Fig. 1, the DR, a 1.1-GeV storage ring with a circumference of about 135.5 m has been constructed at 120 m downstream the positron target of the LINAC [10]. The positron beam is extracted from the end of Sector 2 of the LINAC whose energy is 1.1 GeV, and injected into the DR. Since the enormous energy spread from FC exceeds the energy acceptance of the DR, an energy compression system (ECS) is installed utilizing the first arc of the LTR. The damped beam from the DR is returned to the entrance of Sector 3 of the LINAC. The acceleration frequency of the DR is about 508.9 MHz, which is same as that of SuperKEKB, the resulting bunch length is too long to be accepted to the LINAC with acceleration frequency 2856 MHz (S-band). Thus a bunch compression system (BCS) in the second arc of RTL was installed. Figure 2 shows the particle distribution before and after the DR in the longitudinal phase space simulated with the parameters on Table 2. The parameters from the DR are modified from the initial design [11] to match the changes in the RF voltage from the design value of 1.4 to 1.0 MV, with the emittance accordingly changed from $89 \mu\text{m}$ to $64.3 \mu\text{m}$. As shown in Fig. 2, since positrons from

Table 1: Required parameters of injection beam for SuperKEKB-LER Phase 2 and 3

	DR Extraction	Phase2	Phase3-
$\gamma\epsilon_x [\mu\text{m}]$	64.3	< 200	< 100
$\gamma\epsilon_y [\mu\text{m}]$	3.2	< 40	< 15
$\sigma_\delta [\%]$	0.055	0.16	0.10
Charge [nC]	1.5	1.5	4.0

Table 2: Design Parameters of the Injection and Extraction Beam for DR (* shows a full width.)

Parameters	ECSin	ECSout	BCSin	BCSout
		=DRin	=DRout	
$\gamma\epsilon_x [\mu\text{m}]$		2800	64.3	
$\gamma\epsilon_y [\mu\text{m}]$		2600	3.2	
$\sigma_z [\text{mm}]$	$\pm 8^*$	$\pm 30^*$	6.6	1.3
$\sigma_\delta [\%]$	$\pm 5^*$	$\pm 1.5^*$	0.055	0.8
$R_{56} [\text{m}]$	-0.61			-1.05
$V_c [\text{MV}]$	41			21.5

* naoko.iida@kek.jp

PERFORMANCE OF THE FCC-ee POLARIMETER

N. Y. Muchnoi*,

Budker Institute of Nuclear Physics, 630090 Novosibirsk, Russian Federation
also at the Novosibirsk State University, 630090 Novosibirsk, Russian Federation

Abstract

Inverse Compton scattering is the classical way to measure the electron beam polarization. Eligibility of the approach at high energy domain has been demonstrated by LEP [1, 2], HERA [3] and SLD [4] experiments. Fast measurement of beam polarization allows to apply the resonant depolarization technique for precise beam energy determination [5, 6]. The distinctive feature of the FCC-ee polarimeter is the registration of scattered electrons along with scattered photons. Polarimeter is designed to measure the transverse polarization of the non-colliding pilot bunch with 1% accuracy every second. Furthermore the same apparatus allows to measure the beam energy, longitudinal beam polarization (if any) and transverse beam positions/sizes at the place of installation.

INTRODUCTION

The illustration for the process of Inverse Compton Scattering (ICS) is presented in Fig. 1.

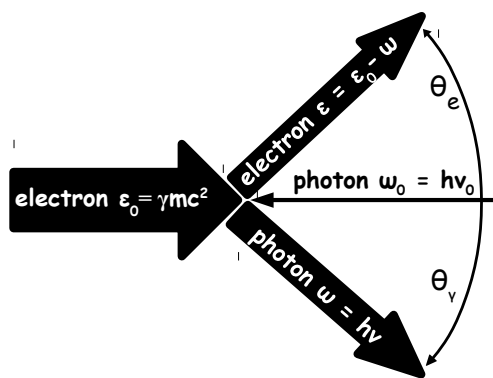


Figure 1: Inverse Compton scattering: the thickness of every arrow qualitatively reflects the energy of each particle. ω_0, ε_0 and ω, ε are the energies of the photon and electron in their initial and final states correspondingly, while θ_y and θ_e are the scattering angles of photon and electron.

Considering an ultra-relativistic case ($\varepsilon_0, \varepsilon, \omega \gg \omega_0$) we introduce the universal scattering parameter

$$u = \frac{\omega}{\varepsilon} = \frac{\theta_e}{\theta_y} = \frac{\omega}{\varepsilon_0 - \omega} = \frac{\varepsilon_0 - \varepsilon}{\varepsilon}, \quad (1)$$

bearing in mind the energy and transverse momenta conservation laws while neglecting the corresponding impacts of initial photon. Parameter u lies within the range $u \in [0, \kappa]$

and is limited from above by the longitudinal momenta conservation: κ is twice the initial energy of the photon in the rest frame of the electron, expressed in units of the electron rest energy:

$$\kappa = 4 \frac{\omega_0 \varepsilon_0}{(mc^2)^2} = 2 \times 2\gamma \frac{\omega_0}{mc^2}. \quad (2)$$

If the electron-photon interaction is not head on, the angle of interaction $\alpha \neq \pi$ affects the initial photon energy seen by the electron, and κ parameter becomes¹

$$\kappa(\alpha) = 4 \frac{\omega_0 \varepsilon_0}{(mc^2)^2} \sin^2 \left(\frac{\alpha}{2} \right). \quad (3)$$

Almost any experimental application of the backscattering of laser radiation on the electron beam for any reason implies the use of the scheme shown in Fig. 2. Laser radiation is inserted into the machine vacuum chamber, directed and focused to the interaction point where scattering occurs. The dipole is used to separate scattered photons (and electrons) from the electron beam, propagating in the machine's vacuum chamber. x -axis and z -axis define the coordinate system in the interaction point, the plane of the figure is the plane of machine, the vertical y -axis is perpendicular to the plane of figure. After the dipole, the coordinate system (x', z') is rotated by the beam bending angle θ_0 .

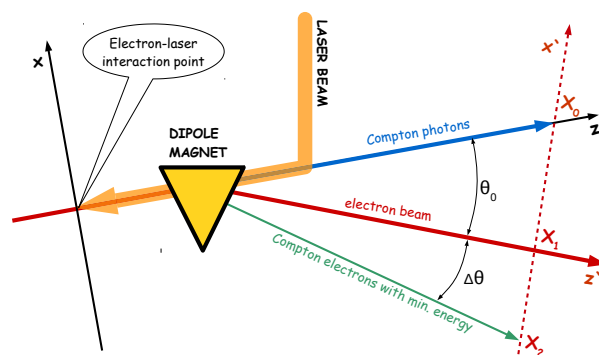


Figure 2: Regular layout of ICS experiments realization.

For the FCC-ee polarimeter we assume the interaction of laser radiation with electrons in the electron energy range $\varepsilon_0 \in [45 : 185]$ GeV. The energy of the laser photon ω_0 is coupled with the radiation wavelength in vacuum λ_0 : $\omega_0 = hc/\lambda_0$, where $hc = 1.239\,841\,93 \text{ eV} \cdot \mu\text{m}$. In particular when $\lambda_0 = 1 \mu\text{m}$, $\varepsilon_0 = 100 \text{ GeV}$ and $\alpha = \pi$ one obtains the "typical" value of κ parameter for the FCC-ee case, $\kappa \approx 1.9$. Maximum energy of backscattered photon ω_{max} obviously

¹ this is correct when $\tan(\alpha/2) \gg 1/\gamma$.

* N.Yu.Muchnoi@inp.nsk.su

RESONANT DEPOLARIZATION AT Z AND W AT FCC-EE

I. A. Koop[†]

Budker Institute of Nuclear Physics,
 also at Novosibirsk State University,

Novosibirsk State Technical University, [630090] Novosibirsk, Russia,

Abstract

Both future 100 km in circumference electron-positron colliders CEPC and FCC-ee need know beams energies with the extreme precision of 1–2 ppm. This can be done only with the help of Resonant Depolarization (RD) technique. Still, some beam parameters of these machines, like energy spread and damping decrements, are so high near 80 GeV per beam, that it is required special consideration and tricks to overcome the difficulties.

The author has written simple spin tracking code, which simulates main features of the RD process in presence of continuous energy diffusion due to synchrotron radiation fluctuations.

It was shown by this study, that the applicability of the RD method is limited by the effect of widening of the central and side band peaks of the spin precession spectrum when the synchrotron tune Q_s is chosen too low, say below $Q_s=0.05$. In this case spin precession lost its resonant nature due to overlap of the wide central spectrum peak with the nearby synchrotron side bands.

Dependencies of the spectrum peaks width from various beam parameters and a new RD-procedure recipe are presented.

INTRODUCTION

Beam emittances in FCCee are so small, that all spin resonances with the betatron motion frequencies are suppressed and their influence on the spin motion is negligible. Truly, at 80 GeV beam energy (spin tune $\nu_0 = \gamma a = 181.5$) the horizontal and the vertical beam emittances are expected to be $\varepsilon_x = 0.84$ nm and $\varepsilon_y = 1.7$ pm, respectively [1]. At Z ($\nu_0 = 103.5$) these emittances are of the same order, but optics for Z is slightly different [2].

The code ASPIRRIN [3, 4] provides reliable estimation of the strengths of the so-called “intrinsic” resonances $\nu_0 = \nu_{\pm k} = Q_j \pm k$. In Fig.1 are presented the modules of few resonance harmonics in the vicinity of Z-peak, while same plot for the W energy range is shown in Fig.2.

One can see that the maximal spin perturbation value does not exceed $w_k = 8 \cdot 10^{-5}$. This is much below of the critical level $(w_k)_{crit} = 0.01$ - a value which may shift the fractional part of the spin tune by $\delta\nu \approx (w_k)_{crit}^2 = 0.0001$ —the wanted accuracy of the fractional part of the tune measurement ($\Delta\nu = \nu_0 \cdot \Delta E/E = (100 \div 180) \cdot 10^{-6} \approx 10^{-4}$).

Taking all this into account, we concentrate now our attention on a study of integer resonances and their

synchrotron side band satellites. These resonances are driven by the closed orbit distortions or by the longitudinal magnetic field. The last is just the case in the detector region.

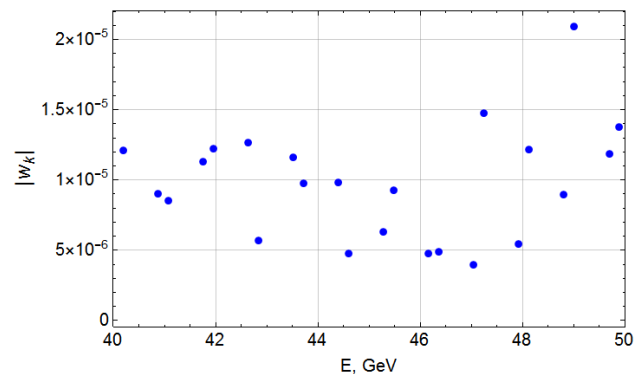


Figure 1: The strengths of few intrinsic resonances in vicinity of Z-peak beam energy.

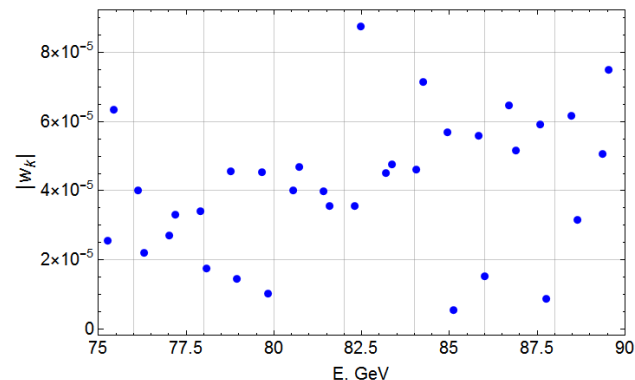


Figure 2: The strengths of few intrinsic resonances near the W-threshold beam energy.

CLOSED ORBIT DISTORTIONS

Sensitivity to misalignment of quads is very high in future electron-positron colliders. This can be expressed via the so-called spin-orbit response function $F_3(\theta)$, which defines the strength of the integer spin resonance $\nu_0 = k$ via the convolution of $F_3(\theta)$ with the dimensionless vertical orbit curvature $\Delta K_x(\theta)$ [3, 4]:

$$w_k = \frac{1}{2\pi} \int_0^{2\pi} F_3(\theta) \cdot \Delta K_x(\theta) d\theta.$$

In Fig.3 as example is plotted the module of $F_3(\theta)$ function for FCC-ee at 45.6 GeV calculated by the code ASPIRRIN. Its average value in arcs is about 250 and

[†] koop@inp.nsk.su

BEAM INSTRUMENTATION AT SUPERKEKB

G. Mitsuka*, M. Arinaga, J. W. Flanagan, H. Fukuma, H. Ikeda, H. Ishii,
 S. Iwabuchi, K. Mori, E. Mulyani, M. Tejima, and M. Tobiyama,
 KEK Accelerator Laboratory, 1-1 Oho, Tsukuba 305-0801, Japan

also at Graduate School for Advanced Study (SOKENDAI), 1-1 Oho, Tsukuba 305-0801, Japan
 G. S. Varner, U. Hawaii, Dept. Physics and Astronomy, 2505 Correa Rd., Honolulu HI 96822, USA
 G. Bonvicini, Wayne State U., 135 Physics Bldg., Detroit MI 48201, USA

Abstract

Phase 2 commissioning of the SuperKEKB electron-positron collider has been performed with final focus optics from February 8 to July 17, 2018. The main aims of Phase 2 commissioning were to verify the novel nano-beam collision scheme and achieve the machine luminosity $O(10^{34} \text{ cm}^{-2}\text{s}^{-1})$. The beam instruments including the bunch-by-bunch feedback and orbit feedback systems, which are central to the beam diagnostics at SuperKEKB, were successfully operated throughout Phase 2. In this talk, we will present the commissioning results focusing on beam diagnostics and show prospects for the final phase of commissioning from next spring.

INTRODUCTION

The SuperKEKB collider (2016–) is a major upgrade to the KEKB collider (1998–2010) at KEK. Colliding 7 GeV electrons in the high energy ring (HER) and 4 GeV positrons in the low energy ring (LER), with a factor of two higher beam currents and the novel nano-beam scheme [1], will provide 40 times larger luminosity than KEKB.

Commissioning of SuperKEKB has been proceeded along the following three periods. *Phase 1* from February 1 to June 28, 2016 aimed to perform scrubbing run for new vacuum chambers and low emittance tuning for new arc lattice. After closing Phase 1, the superconducting final quadrupoles (QCS) and the Belle II detector except for the inner silicon-based VXD tracking system were installed. *Phase 2* started on February 8, 2018 with commissioning of the positron damping ring (DR) and was followed by commissioning of the HER and LER from March 19 to July 17, 2018. The main parameters of the HER, LER, and DR at Phase 2 are summarized in Table 1. *Phase 3* physics operation is scheduled from March 2019 with the complete Belle II detector.

Main tasks of Phase 2 are first to achieve electron-positron collisions, second to verify the nano-beam collision scheme, and finally to establish control of beam-induced backgrounds resulting from low beta functions at the interaction point (IP).

Beam instruments at SuperKEKB are designed for beam diagnostics, e.g. establishing the circulating orbit, finding the beam-beam kick, accumulating large beam currents, etc. In the rest of this paper, we present the performance of beam instrumentation at Phase 2 and prospects for Phase 3.

* gaku.mitsuka@kek.jp

BEAM INSTRUMENTATION AT DR

Beam Position Monitor

There are totally 83 beam position monitors (BPMs) in the DR [2]. A BPM consists of four button electrodes with a diameter of 6 mm, where two electrodes are attached each other in one flange (see Fig. 1). We use the detection circuit VME 18K11 L/R that employs a log-ratio amplifier.

Figure 2 shows a schematic diagram of the BPM timing system. First, the main frequency divider generates bunch revolution timing that is synchronized with the injection bunch timing. Second, the 32 channel digital delay unit inserted between the main frequency divider and 18K11 further adjusts the timing offset. The second timing adjustment is needed for the timing differences $\sim 200 \text{ ns}$ owing to the BPM locations relative to the injection point and sizable cable lengths.

Table 1: Main parameters of the SuperKEKB HER, LER, and DR at Phase 2

	HER	LER	DR
Energy (GeV)	7	4	1.1
Circumference (m)		3016	135
Max. current (mA)	800	860	12
Bunch length (mm)	5	6	6.6
RF frequency (MHz)		508.877	
Harmonic number		5120	230
Betatron tune (H/V)	44.54/ 46.56	45.54/ 43.56	8.24/ 7.17
Synchrotron tune	0.02	0.018	0.025
T. rad. damp time (ms)	58	43	12
x-y coupling (%)	0.27	0.28	10
Emittance (nm)	3.2	4.6	29
Peak luminosity ($\text{cm}^{-2}\text{s}^{-1}$)		5.5×10^{33}	
Beam position monitor	486	444	83
Turn-by-turn monitor	69	70	83
Trans. FB system	2	2	1
Visible SR monitor	1	1	1
X-ray size monitor	1	1	0
Betatron tune monitor	1	1	1
DCCT	1	1	1
Bunch current monitor	1	1	1
Beam loss monitor	105 (IC) and 101 (PIN)		34

FAST LUMINOSITY MONITORING OR THE SUPERKEKB COLLIDER (LUMIBELLE2 PROJECT)

P. Bambade, S. Di Carlo, D. Jehanno, V. Kubytskyi, C.-G. Pang, Y Peinaud,
 LAL, Univ. Paris-Sud, CNRS/IN2P3, Université Paris-Saclay, 91400 Orsay, France
 Y. Funakoshi, S. Uehara, KEK, 305-0801 Tsukuba, Japan

Abstract

LumiBelle2 is a fast luminosity monitoring system prepared for SuperKEKB. It uses sCVD diamond detectors placed in both the electron and positron rings to measure the Bhabha scattering process at vanishing photon scattering angle. Two types of online luminosity signals are provided, Train-Integrated-Luminosity signals at 1 kHz as input to the dithering feedback system used to maintain optimum overlap between the colliding beams in horizontal plane, and Bunch-Integrated-Luminosity signals at about 1 Hz to check for variations along the bunch trains. Vertical beam sizes and offsets can also be determined from collision scanning. This paper will describe the design of *LumiBelle2* and report on its performance during the Phase-2 commissioning of SuperKEKB.

INTRODUCTION

SuperKEKB uses the so-called *nano-beam scheme* to reach a very high instantaneous luminosity of $8 \times 10^{35} \text{ cm}^2 \text{ s}^{-1}$ [1]. It consists of using a large crossing angle at the interaction point (IP) to enable colliding 2500 ultra-low emittance bunches with very small beam sizes (design value $\sigma_y \sim 50 \text{ nm}$). The luminosity is very sensitive to beam-beam offsets, e.g. caused by vibration of mechanical supports induced by ground motion. In order to maintain the optimum beam collision condition, orbit feedback systems are essential at the IP [2]. At SuperKEKB, the beam-beam deflection method is used for orbit feedback in the vertical plane, while in the horizontal plane, a dithering orbit feedback system using the luminosity as input, similar to that operated in the past at PEP-II, has been adopted [3,4].

For this purpose, a fast luminosity monitor based on sCVD diamond detectors, named *LumiBelle2*, was developed and tested during the Phase-2 commissioning of SuperKEKB. By measuring the rate of Bhabha events on each side of the IP at vanishing photon scattering angle, *LumiBelle2* can provide both Train-Integrated-Luminosity (TIL) signals and Bunch-Integrated-luminosity (BIL) signals simultaneously, over a large range of luminosities. The TIL signals are needed by the dithering orbit feedback system at 1 kHz, with relative precisions better than 1% [5]. BIL signals are important to probe potential luminosity differences between the numerous bunches along the trains. Another luminosity monitoring system named ZDLM (Zero Degree Luminosity Monitor) is also installed in the immediate vicinity. It uses Cherenkov and scintillator detectors [6], providing important complementary measurements. In addition, the ECL-LOM (Electro-

magnetic Calorimeter Luminosity On-line Measurement) is operated in the backward and forward end-caps of the Belle II detector, measuring the coincidence rates of back-to-back Bhabha events in the opposite sectors, with the ability to provide absolute values of the luminosity after proper internal calibration [7].

In this paper, we describe the design of *LumiBelle2*, including results of detector tests with a ^{90}Sr electron isotope source, the experimental set-up and the DAQ based on a FPGA, and then report on obtained luminosity monitoring performances, based on simulation and measurements pursued during the Phase-2 commissioning period, both with colliding beams, and with single beams, for background evaluations.

DESIGN AND LAYOUT

The placement of the *LumiBelle2* detectors was carefully studied to ensure sufficient signal rates while limiting the background contamination, taking also into account space constraints on the beam line. This resulted in choosing locations 10 and 29 m downstream of the IP in the Low Energy Ring (LER) and High Energy Ring (HER), to measure, respectively, Bhabha scattered positrons and photons [8]. To increase the rate of extracted positrons, a custom made beam pipe section with a depression of 15 mm and 45° inclined windows is used in the LER, see Fig. 1. A Tungsten radiator with an effective thickness of 4 Radiation Lengths (1 RL = 3.5 mm) was added to enhance the electromagnetic showers and boost the detection efficiency [9].

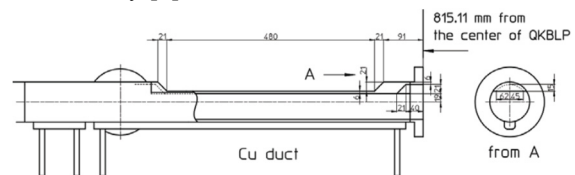


Figure 1: *LumiBelle2* LER window shaped beam pipe.

The RF of SuperKEKB is about 500 MHz, with bunches stored nominally almost every other bucket (so-called quasi 2-bucket fill pattern), which implies collisions every 4 ns. For BIL monitoring at high counting rate, signals from neighbouring bunches must be separated. A new diamond detector with a thickness of $140 \mu\text{m}$, coupled with a broadband 2 GHz 40 dB current amplifier from CIVIDEC [10] at the front-end, are used for this purpose. Low attenuation half-inch HELIAX coaxial cables are used to avoid signal broadening during the transfer to the data acquisition system in the Belle II Electronics Hut located about 100 m away.

HIGH PRECISION EXPERIMENTS IN THE J/ψ , $\psi(2S)$ AND τ SECTOR

I. B. Nikolaev* on behalf of the KEDR Collaboration
Budker Institute of Nuclear Physics, 630090, Novosibirsk, Russia
Novosibirsk State University, 630090 Novosibirsk, Russia

Abstract

High precision experiments in charmonium sector require beam energy calibration. VEPP-4M [1] storage ring with energy measurement by resonant depolarization (RD) method provided high precision mass measurement of J/ψ - and $\psi(2S)$ - mesons with KEDR detector with accuracy 2×10^{-6} [2]. This narrow resonances can be used for calibration of energy scale of other accelerators such as BEPC-II or future Super Charm-Tau Factories equipped with Compton backscattering (CBS) energy measurement system.

BEAM ENERGY MEASUREMENT

Resonant Depolarization Method

The resonant depolarization (RD) method [3] is the most accurate technique of beam energy measurement. The accuracy achieved is about 10^{-6} . The method was successfully applied in the high precision measurements of the mass of elementary particles from ϕ -meson to Z -boson.

The method is based on the measurement of the spin precession frequency Ω , which depends on the beam Lorentz factor γ and well-known normal μ_0 and anomalous μ' parts of the electron magnetic moment:

$$\Omega = \omega_r \left(1 + \gamma \frac{\mu'}{\mu_0} \right), \quad (1)$$

where ω_r is the beam revolution frequency in the storage ring. The spin precession frequency is determined by the moment of resonant destruction ($\Omega = n\omega_r \pm \omega_d$, where $n \in \mathbb{Z}$) of the beam polarization in an external electromagnetic field with a frequency ω_d .

The beam polarization could be measured in several ways: using intensity of intra-beam scattering (Touschek effect) [4]; intensity of synchrotron light [5]; asymmetry of Compton backscattering [6]; scattering asymmetry on internal target [7]. At the VEPP-4M beam polarization is determined by intra-beam scattering [8]. The beam is depolarized by a TEM wave which is created by two matched striplines. They are connected to a high frequency generator with tunable frequency, which is computer controlled. The generator frequency ω_d and the VEPP-4M revolution frequency ω_r are stabilized by a rubidium atomic clock with an accuracy 10^{-10} . A polarized beam is prepared in the VEPP-3 booster with polarization time 1.3 hours at $E=1.55$ GeV or 0.6 hours at $E=1.85$ GeV then injected into VEPP-4M. In order to suppress beam size and orbit instabilities a relative count rate difference $\Delta = \dot{N}_{pol}/\dot{N}_{unpol} - 1$ of the polarized and unpolarized bunch is under observation.

* I.B.Nikolaev@inp.nsk.su

The depolarization frequency is measured with an accuracy better than 10^{-6} . Double energy calibrations with opposite directions are performed in order to suppress dangerous side 50 Hz resonances. The determination of center of mass energy at the interaction point (IP) requires taking into account following effects: vertical orbit distortions and spin precession frequency width; solenoid field of the detector; coherent energy loss asymmetry; electron and positron energy difference and beam separation in parasitic IP; β -function chromaticity and beam potential [9, 10]. Corrections and errors are about few keV. Between calibrations VEPP-4M energy is reconstructed [11] by using some parameters of VEPP-4M storage ring: field of bending magnet measured by nuclear magnetic resonance method; environment and storage ring temperatures; beam orbits.

Compton Backscattering

The RD method meets problem with beam polarization near τ -lepton production threshold ($E = 1777$ MeV) due to close vicinity to $\Omega_s/\omega_r - 1 = 4$ spin resonance [12]. An additional method of energy monitor for τ mass measurement experiment is required. The process of Compton backscattering (CBS) allows one to determine beam energy by measuring maximum energy of scattering photon:

$$E = \frac{\omega_{max}}{2} \left(1 + \sqrt{1 + \frac{m_e^2}{\omega_0 \omega_{max}}} \right), \quad (2)$$

ω_0 is the initial energy of laser photon; m_e is the electron mass. For the first time this method was realized in [13] and firstly applied in particle experiments for tau mass measurement at VEPP-4M [14]. The scattered photons are registered by high purity germanium detector (HPGe). The detector is calibrated by number of well known γ -sources. The achieved accuracy of the method in beam energy range $E = 1.7 - 1.9$ is about 60 keV. Absolute calibration of the CBS method was done via comparison with RD. The experience of system exploitation at VEPP-4M helped with same systems at BEPC-II [15] and at VEPP-2000 [16] colliders.

HIGH PRECISION EXPERIMENTS AT VEPP-4M WITH KEDR DETECTOR

The data analysis of J/ψ and $\psi(2S)$ mass measurement is based on three J/ψ scans with integrated luminosity 0.7 pb^{-1} and on four $\psi(2S)$ scans with integrated luminosity 1.0 pb^{-1} [2]. Each scan has several points with different energies which cover resonance shape. The beam energy is calibrated before and after data acquisition in each scan point. The resonance masses were determined by fitting

POLARIZATION ISSUES AT CEPC

Sergei Nikitin*, BINP SB RAS, Novosibirsk

Abstract

We study a possibility of obtaining transversely polarized electron/positron beams at the CEPC collider. At the beam energy of 45 GeV, this requires the use of the special wigglers to speed up the radiative self-polarization process. A numerical estimation of the depolarizing effect of the collider field errors is made, taking into account the modulation of the spin precession frequency by synchrotron oscillations. In addition, we consider an alternative possibility of obtaining polarization by accelerating the polarized particles in the booster and then injecting them into the main ring. This option saves time spent on the polarization process, and can also be crucial for obtaining longitudinal polarization.

INTRODUCTION

This work is devoted to obtaining transverse and longitudinal polarizations within the framework of the CEPC Collider project and is based on materials presented by the author in [1, 2].

Particle transverse polarization at least of 10% is needed to apply the resonant depolarization technique [3] in the experiment on precise Z-pole mass measurement. Because of too long time of radiative polarization in the basic version of the magnetic structure of CEPC, it becomes necessary to use strong non-uniform wiggler magnets to speed up the polarization process. Such wigglers can cause a significant increase in the spread of the spin precession frequency. In turn, this leads to an intensification of the depolarizing effect of quantum fluctuations in the presence of the guiding field imperfections. The calculations of this effect should take into account the synchrotron modulation of the spin tune. We consider the main obstacles to obtaining the radiative self-polarization at CEPC with 45 and 80 GeV. It is necessary to determine the critical level of errors in the CEPC magnet alignment by calculating their response in the spin motion.

In addition, we are trying to imagine an alternative way of obtaining polarization at CEPC. The rate is made for acceleration of polarized electrons in the booster using the Partial Siberian Snake technique [4] for crossing spin resonances. Injection into the collider can provide for two modes - with transverse and longitudinal polarizations. The kinematic scheme of longitudinal polarization can include the restoration of vertical polarization in the arcs and two spin rotators at the ends of the section with IP.

SPEEDING UP POLARIZATION PROCESS

The well-known Sokolov-Ternov mechanism of radiation self-polarization of particles in an ideal storage ring is characterized by the time τ_p of polarization build-up to the extent

$$P_0 = 0.92 [5]:$$

$$\frac{1}{\tau_p} = \frac{5\sqrt{3}}{8} \frac{r_e \Lambda_e c \gamma^5}{R^3} \langle K^3 \rangle, \quad (1)$$

where r_e , Λ_e , γ are the electron radius, Compton wave length and relativistic factor respectively; K is the orbit curvature in units of the inverse machine radius R ; $\langle \dots \rangle$ is averaging over the storage ring azimuth (ϑ). The design time of the radiative polarization in the 100 km CEPC is huge: 260 hrs at 45 GeV! At 80 GeV, this time falls as $(45/80)^5$ to 16 hrs. To speed up the polarization process, it is possible to apply the long-known method [5] based on the use of N_w special wiggler magnets (the so-called shifters) with such a distribution of the vertical field along the orbit that $\int B_w ds = 0$ and $\int B_w^3 ds \neq 0$. Let every shifter consist of three bending magnets. The field of edge magnets (B_-) is much smaller in magnitude than the field of the central one (B_+) and opposite in sign to it. The field of the latter is directed like the bending field in the arcs. Since $|B_+|^3 \gg |B_-|^3$, the equilibrium degree of polarization in the ideal case is close to the maximum (P_0). The shifters decrease the polarization time in accordance with the equation (L_- and L_+ are the corresponding magnet lengths):

$$\tau_p^w = \tau_p \left[1 + N_w \frac{B_+^3 L_+ + 2|B_-|^3 L_-}{2\pi R < B_0 > B_0^2} \right]^{-1}. \quad (2)$$

The fraction of radiation energy loss enhancement is

$$u = N_w \frac{B_+^2 L_+ + 2B_-^2 L_-}{2\pi R < B_0 > B_0}. \quad (3)$$

The harmful effect of the shifters is an increase in the beam energy spread:

$$\frac{\Delta E_w}{\Delta E} = \left[\frac{\tau_p}{\tau_p^w} \cdot \frac{1}{1+u} \right]^{1/2}. \quad (4)$$

The effectiveness of the described system as applied to CEPC can be judged by its parameters in Table 1. The Eqs. (2-4) are written in the isomagnetic approximation (the characteristic field in the CEPC magnets is $B_0 \approx 0.013$ T at 45.6 GeV, the averaged-over-azimuth field $\langle B_0 \rangle \approx 0.01$ T). At the same time, the calculated data presented in the table refer to the detailed design structure.

The reduction of τ_p by an order, down to $30 \div 20$ hours, means that it becomes possible to polarize the beams up to 10% in a few hours. This degree of polarization is quite sufficient for its observation by a laser polarimeter under the conditions of application of the resonant depolarization technique for determining the energy of the particles [6]. As the analysis below shows, a further increase in the field of wigglers and their number leads to an undesirable increase of depolarizing effects due to the large energy spread.

* nikitins@inp.nsk.su

Content from this work may be used under the terms of the CC BY 3.0 licence (© 2018). Any distribution of this work must maintain attribution to the author(s), title of the work, publisher, and DOI.

IDEAS FOR LONGITUDINAL POLARIZATION AT THE Z/W/H/TOP FACTORY

I. A. Koop^{†,2}, A. V. Otboev, Yu. M. Shatunov¹,

Budker Institute of Nuclear Physics, [630090] Novosibirsk, Russia

¹also at Novosibirsk State University, [630090] Novosibirsk, Russia

²also at Novosibirsk State Technical University, [630090] Novosibirsk, Russia

Abstract

Different schemes for getting the longitudinal polarization at FCC-ee are considered. Depolarization rates for rings with spin rotators are evaluated and methods of acceleration of polarized beams in a booster synchrotron are proposed.

INTRODUCTION

First ideas on how the stable longitudinal polarization of colliding electrons and positrons can be achieved were proposed in 70-th [1–4]. In this paper we analyse the possibilities to use 90° spin rotators which are installed at proper bending angle relative to the Interaction Point (IP) of the FCC-ee collider [5].

The crab-waist collision scheme assumes an operation with extremely small vertical beam emittance. Therefore only the solenoid type spin rotators with a compensated x - y coupling can be used for spin manipulations in a ring. Also due to strong Synchrotron Radiation (SR) and associated with that fast energy diffusion the schemes which utilises the idea of Siberian Snake can't be used. Restoration of the vertical spin direction in main arcs of FCC-ee is mandatory. Only then the spin-orbit coupling effects and the depolarization rates are minimised to the acceptable level.

LONGITUDINAL POLARIZATION

Near the Z-peak (beam energy around 45.6 GeV) the spin tune $\nu_0 = \gamma a$ is equal to $\nu_0 = 103.5$. Here γ is the Lorentz factor and $a = g'/q_0 = 0.0016$ states for the anomalous magnetic moment of an electron. Hence, if spin is directed longitudinally at IP, it shall be rotated two times by 90° —first by a bend in the horizontal plane and then by a solenoid around the longitudinal axis, see Fig. 1.

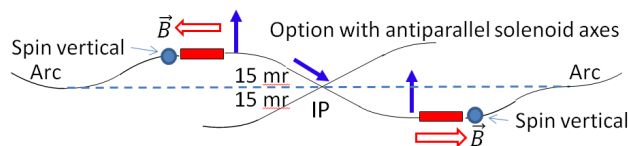


Figure 1: The proposed spin and velocity rotation sequences for achieving the longitudinal polarization at Z.

The corresponding velocity vector bending angle is $\phi = 0.5\pi/\nu_0 \approx 0.015$, while the needed longitudinal field integral is $BL = 0.5\pi BR/(1+a) \approx \pm 235$ T·m per rotator.

Remind, that due to antisymmetric layout of all spin rotations in this scheme, the net spin rotation is zero. There-

[†]koop@inp.nsk.su
 WEXAA04

fore the equilibrium spin direction in main arcs is the same as without spin rotators and, moreover, it is independent on the particle's energy. This is very important, because guaranties the cancelation of spin-orbit coupling in arc's dipole magnets. Spin direction is chromatic only in the chicane magnets, which rotate spin in the horizontal plane. But their contribution to radiative depolarization by quantum fluctuations of SR is negligible. Another remark: the global spin precession frequency is not affected by such an insertion and can be used for beam energy determination applying the Resonant Depolarization (RD) method.

Unfortunately, the accumulated bending angle distribution in FCC-ee experimental straight section is not fully antisymmetric relative to IP—at the left side bends with negative curvature are much weaker compared to bends on the right side from IP, see Fig. 2.

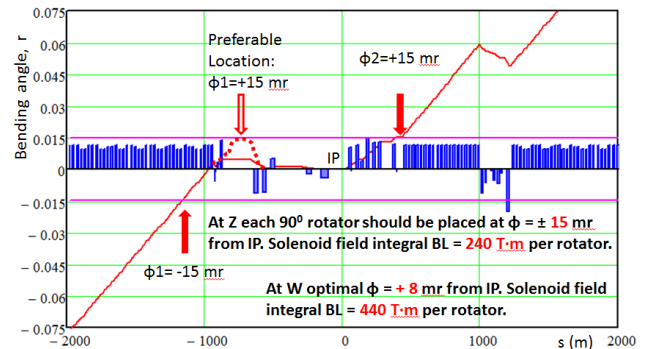


Figure 2: The accumulated bending angle distribution in FCC-ee experimental straight section (red solid curve). The dotted curve shows the desirable bending angle dependence optimal for the operation with longitudinal polarization at Z. The alternative place for inserting of the left side spin rotator is $\phi_1 = -15$ mr—seems easier for realization.

Therefore, for realization of the discussed above the ideal spin rotation scheme shown in Fig. 1, the geometry of bends on the left side of the straight section should be changed so, as to provide empty drifts at $\phi = +15$ mr from IP. This is schematically shown in Fig. 2 by the dotted red line. The alternative place for inserting the left side spin rotator, shown at Fig. 2 by the red arrow, is $\phi = -15$ mr. This option, probably, is easier for realization, because all changes in the ring layout should be done at much larger distance from IP, thus not affecting the background problems from SR near detector. In this option the angle between axis of the left and the right rota-

IR DESIGN ISSUES FOR HIGH LUMINOSITY AND LOW BACKGROUNDS*

M. K. Sullivan[†], SLAC National Accelerator Laboratory, 94025 Menlo Park, CA, USA

Abstract

New e^+e^- accelerator designs aim for factory-like performance with high-current beams and high luminosities. These new machines will push interaction region designs to new levels and require a careful evaluation of all previous background sources as well as introduce possibly new background sources. I present here a summary of standard background sources and also suggest a new possible background source for Synchrotron Radiation (SR) namely, specular reflection. In addition, one will have to pay closer attention to the beam tail particle distribution as this may become a significant source of SR background from the high-current and high-energy beams of these new designs.

INTRODUCTION

The Interaction Region (IR) of a colliding beam e^+e^- accelerator is always one of the more challenging aspects of the collider design. In order to obtain a high luminosity, usually done by having many beam bunches, nearly all designs now have a separate storage ring for each beam. This in turn means that the collision has a crossing angle (only the PEP-II B-factory had separate storage rings and a head-on collision through the use of strong bending magnets close to the Interaction Point (IP)). Crossing angles for new or recently completed designs range from ± 15 mrad (FCCee [1,2]) to ± 41.5 mrad (superKEKB [3]). The demand for high-luminosity ($\sim 10^{34}$ - 10^{36} $\text{cm}^{-2}\text{s}^{-1}$) requires the final focus magnets to be close to the IP (~ 1 m) in order to get the necessary small spot size at the collision point. I will first discuss some of the standard layout issues for a collision point and how these affect the background studies. Then I will concentrate on the various background issues related to SR and, in particular, discuss the potential for specular reflection to become a possible new SR background source. I will then look more closely at the issue of the beam tail particle distribution and how this distribution can become an important source of SR backgrounds. Finally, I will mention the standard beam particle backgrounds that must always be studied along with some of the other accelerator related issues that must be evaluated before an IR design can be accepted.

THE IR DESIGN

Final Focus Quadrupoles

As mentioned above, modern factory designs have a

* Work supported by the U.S. Department of Energy, Office of Science, Office of Basic Energy Sciences, under Contract No. DE-AC02-76SF00515 and HEP

[†] sullivan@slac.stanford.edu

crossing angle between the beams at the collision point. The crossing angle is imposed by the requirement that the focusing elements in each beam are independent (i.e. there are no shared magnets – no quadrupoles that have both beams). In addition, the Final Focus (FF) magnets are placed close to the IP. The short L^* values (~ 1 - 2 m) in these designs mean that these FF quadrupoles are quite strong and that the beta functions in these quads tend to be large. This makes the FF magnets an important source of SR production. This is especially true of the high-energy (FCCee and CEPC) designs. Here the FF magnets are focusing a very high-energy beam and the SR energy spectrum from these magnets is well into the MeV range. The photons from this higher energy spectrum need to be masked and the high energy of these photons make this more difficult. Figures 1a and 1b illustrate the masking issues for SR that comes from the FF magnets.

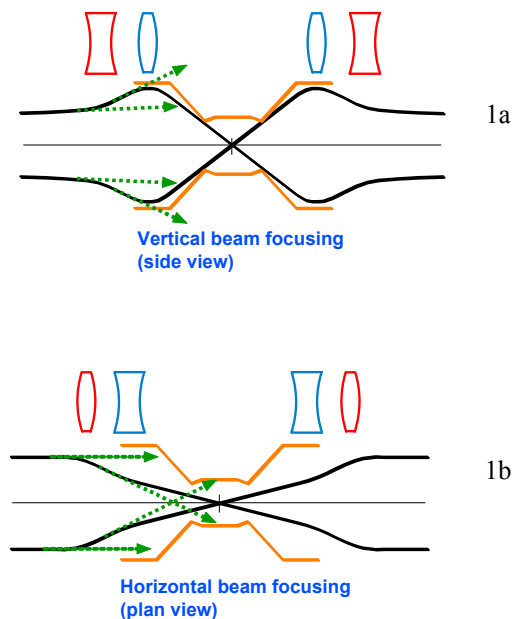


Figure 1: Illustration of the primary issues in shielding a central beam pipe from the SR coming from final focus magnets. 1a: Vertical view of the FF magnets and IP. The SR generated in the vertical comes from the beam when it is defocused in X-focusing magnet (red outline) which is usually before the Y-focusing magnet (blue outline) the last magnet before the IP. The X-focusing magnet generates fans of SR that are between the two green dashed arrows in the drawing. There is another fan from the Y-focusing magnet that is between the outside green dashed arrows and the beam envelope that hits the IP. This radiation is easier to shield than the radiation shown in 1b. 1b: Plan view showing the horizontal radiation fans generated by the beam in the X-focusing magnet which is before the Y-focusing magnet. This radiation is more difficult to shield.

Content from this work may be used under the terms of the CC BY 3.0 licence (© 2018). Any distribution of this work must maintain attribution to the author(s), title of the work, publisher, and DOI.

MACHINE DETECTOR INTERFACE FOR THE e^+e^- FUTURE CIRCULAR COLLIDER

M. Boscolo*, O.R. Blanco-Garcia, INFN/LNF, Frascati, Italy
 N. Bacchetta¹, E. Belli², M. Benedikt, H. Burkhardt, M. Gil Costa, K. Elsener,
 E. Leogrande, P. Janot, H. Ten Kate, D. El Khechen, A. Kolano, R. Kersevan,
 M. Lueckhof, K. Oide, E. Perez, N.A. Teherani, O. Viazlo, Y. Voutsinas and
 F. Zimmermann, CERN, Geneva, Switzerland
 M. Dam, Niels Bohr Institute, Copenhagen, Denmark
 A. Blondel, M. Koratzinos, DPNC/Geneva University, Geneva, Switzerland
 A. Novokhatski, M. Sullivan, SLAC, Menlo Park, California, USA
 A. V. Bogomyagkov, E. B. Levichev, S. Sinyatkin, BINP SB RAS, Novosibirsk, Russia
 F. Collamati, INFN-Rome1, Rome, Italy
¹also INFN-Padova, Padova, Italy
²also at University of Rome Sapienza and INFN-Roma1, Rome, Italy

Abstract

The international Future Circular Collider (FCC) study [1] aims at a design of p-p, e^+e^- , e-p colliders to be built in a new 100 km tunnel in the Geneva region. The e^+e^- collider (FCC-ee) has a centre of mass energy range between 90 (Z-pole) and 375 GeV ($t\bar{t}$). To reach such unprecedented energies and luminosities, the design of the interaction region is crucial. The crab-waist collision scheme [2] has been chosen for the design and it will be compatible with all beam energies. In this paper we will describe the machine detector interface layout including the solenoid compensation scheme. We will describe how this layout fulfills all the requirements set by the parameters table and by the physical constraints. We will summarize the studies of the impact of the synchrotron radiation, the analysis of trapped modes and of the backgrounds induced by single beam and luminosity effects giving an estimate of the losses in the interaction region and in the detector.

LAYOUT AND DESIGN CRITERIA

The FCC-ee collider with 100 km circumference and a wide range of beam energies, from 45.6 to 182.5 GeV, aims at unprecedented levels of energies and luminosities. The requirements at the collision point for the accelerator and detector make the interaction region (IR) one of the most challenging parts of the overall design, this region is named machine detector interface (MDI). Table 1 summarizes the most relevant beam parameters for the MDI design.

To reach the target luminosity of $2.3 \times 10^{36} \text{cm}^{-2}\text{s}^{-1}$ at the Z-pole the crab-waist collision scheme is a necessary ingredient together with pushing the beam current to the limit, obtainable with double rings. The baseline optics for the FCC-ee double-ring collider is described in Ref. [3]. The main characteristics of the optics design are two interaction points (IPs) per ring, horizontal crossing angle of

Table 1: FCC-ee beam parameters most relevant for the IR design

Parameter	Z	W ⁻ W ⁺	ZH	$t\bar{t}$
E_{beam} (GeV)	45.6	80	120	182.5
Luminosity ($10^{34} \text{cm}^{-2}\text{s}^{-1}$)	230	28	8.5	1.55
Beam current (mA)	1390	147	29	5.4
Particles/bunch (10^{11})	1.7	1.5	1.8	2.3
Horiz. emittance (nm)	0.27	0.84	0.63	1.46
Vert. emittance (pm)	1.0	1.7	1.3	2.9
β_x^* (m)	0.15	0.2	0.3	1.0
β_y^* (mm)	0.8	1.0	1.0	1.6
σ_x^* (μm)	6.4	13	13.7	38.2
σ_y^* (nm)	28	41	36	68
SR bunch length (mm)	3.5	3	3.15	1.97
total bunch length (mm)	12.1	6	5.3	2.54
RF Acceptance (%)	1.9	2.3	2.3	3.36
DA energy accept. (%)	1.3	1.3	1.7	-2.8/+2.4
Rad. Bhabha Lifetime (min)	68	59	38	40
Beamstr. Lifetime (min)	> 200	> 200	18	18

30 mrad at the IP and the crab-waist scheme with local chromatic correction system. A so-called tapering of the magnets scales all the magnetic fields with the local beam energy as determined by the SR. This optics is being improved and modified, for instance one of the most relevant modification for the IR design is the reduction of β_x^* to 15 cm at the Z to mitigate the coherent beam-beam instability [4]. Nominal emittances are very small and especially in the vertical plane the target value of $\epsilon_y = 1 \text{ pm}$ at the Z-pole poses stringent requirements on misalignment tolerances as well as on coupling correction. The design restricts the total synchrotron radiation (SR) power at 100 MW, thus the stored current per beam varies from 1.4 A at Z to 5.4 mA at $t\bar{t}$. Following the LEP2 experience where the highest local critical energy was 72 keV for photons emitted 260 m from the IP [5] the FCC-ee optics design maintains critical energies from bending

* manuela.boscolo@lnf.infn.it

BEAM BLOWUP DUE TO SYNCHRO-BETA RESONANCE WITH/WITHOUT BEAM-BEAM EFFECTS*

K. Oide[†], KEK, Tsukuba, Japan
 D. El Khechen, CERN, Geneva, Switzerland

Abstract

A blowup of vertical emittance has been observed in particle tracking simulations with beam-beam and lattice misalignments [1]. It was somewhat unexpected, since estimation without lattice errors did not predict such a blowup unless a residual vertical dispersion at the interaction point (IP) is larger than a certain amount. Later such a blowup has been seen in a tracking of lattices without beam-beam effect.

A possible explanation of the blowup is given by a Vlasov model for an equilibrium of quadratic transverse moments in the synchrotron phase space. This model predicts such a blowup as a synchro-beta resonance mainly near the first synchrotron sideband of the main x - y coupling resonance line.

INTRODUCTION

Beam-beam simulations with lattice, with misalignments or x - y coupling sources such as skew quadrupoles are important to estimate the beam lifetime and luminosity evolution under more realistic situation. Such simulations have been tried for FCC-ee collider rings at τ energy, 182.5 GeV. As a result, significant blowups are seen, and the magnitudes depend on the random number for the misalignments of sextupoles to generate the vertical emittance. Figure 1 shows an example of such a blowup for two seeds of random numbers of misalignments of arc sextupoles. Note that the residual dispersion at the IP for seed 3 is smaller than the previous criteria given in Table 1, while giving even larger blowup than another seed 19, which has larger dispersions at the IP.

Table 1: Tolerances for residual dispersions at the IP for each energy of FCC-ee, obtained by quasi strong-weak model without lattice given by D. Shatilov [2]. The tolerance $\Delta\eta_y^*$ corresponds to 5% increase of vertical beam size σ_y^* at the IP with beamstrahlung.

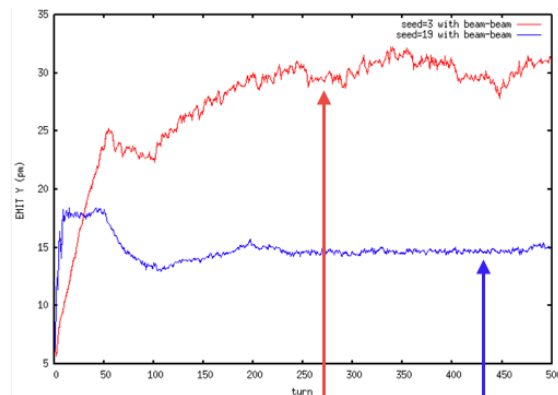
Beam energy [GeV]	45.6	80	120	175
Design σ_y^* [nm]	28	41	35	66
Energy spread ^a [%]	0.13	0.13	0.165	0.185
$\Delta\eta_y^*$ [μm]	1	5	4	6

^a with beamstrahlung

Such a blowup was somewhat unexpected, since the residual dispersion at the interaction point (IP) was not very large

* Work supported by JSPS KAKENHI Grant Number 17K05475. Also supported by the European Commission under Capacities 7th Framework Programme project EuCARD-2, grant agreement 312453, and under the Horizon 2020 Programme project CREMLIN, grant agreement 654166.

[†] katsunobu.oide@cern.ch



Coupling (%)	0.2	0.2
RMS of sext. Offset (°)	11	15
Seed	3	19
η_y @ (IP.1, IP.2) (°)	(-5.3, 4.24)	(-8.9, 8)
$\eta_{py} \times \beta_y^*$ @ (IP.1, IP.2) (°)	(6.8, 1.04)	(35.4, 23)
R2 parameter	(1.8×10^{-3} , 1.8×10^{-3})	(-5.1×10^{-5} , -1.8×10^{-4})

Figure 1: Blowup of vertical emittance measured at the IP by a particle tracking with beam-beam, beamstrahlung, and lattice. The arc sextupoles are vertically misaligned randomly to produce the vertical emittance of the design ratio $\varepsilon_y/\varepsilon_x = 0.2\%$. Two examples for different seeds are shown, corresponding residual vertical dispersions at the IP in the table.

compared to the criteria given by beam-beam simulations without lattice. As well, simulations of beam-beam with lattice but without misalignments or skew quads, did not show such blowups [3].

METHOD AND SETUP

First let us describe the method to examine the effect in this paper:

- Lattice: FCCee_t_217_nosol_2.sad, 182.5 GeV, half ring is simulated assuming a perfect period 2 periodicity. Machine parameters are listed in Ref. [2].
- The vertical emittance around the closed orbit is generated by skew quadrupole added on each sextupole in the arc. Their magnitudes on a pair of sextupoles with the $-I$ transformation between them are parametrized as

$$(k_1 + sk_2, k_2 + sk_1), \quad (1)$$

where $k_{1,2}$ are two random numbers and s is a parameter to represent the symmetry. Then $s = +1/-1$

EARLY COMMISSIONING OF THE LUMINOSITY DITHER SYSTEM FOR SUPERKEKB*

Y. Funakoshi[†], T. Kawamoto, M. Masuzawa, S. Nakamura, T. Oki, M. Tobiyama, S. Uehara,
R. Ueki, KEK 305-0801 Tsukuba, Japan
A. S. Fisher, M. K. Sullivan, D. Brown, SLAC, 94025 Menlo Park, U.S.A.
U. Wienands, ANL 60439 Argonne, U.S.A.
P. Bambade, S. Di Carlo, D. Jehanno, C. Pang, LAL, 91898, Orsay, France
D. El Khechen, CERN, CH-1211, Geneva, Switzerland

Abstract

SuperKEKB is an electron-positron double ring collider at KEK which aims at a peak luminosity of $8 \times 10^{35} \text{cm}^{-2} \text{s}^{-1}$ by using what is known as the “nano-beam” scheme. A luminosity dither system is employed for collision orbit feedback in the horizontal plane. This paper reports a system layout of the dither system and algorithm tests during the SuperKEKB Phase 2 commissioning.

INTRODUCTION

The SuperKEKB collider [1] employs a luminosity dither system that was used at SLAC for PEP-II [2] [3] for maintaining the horizontal offset of the two beams at the IP and maximizing luminosity. For this purpose, a collision orbital feedback based on the beam-beam deflection was used in both vertical and horizontal planes at KEKB. With the “nano-beam” scheme, however, the horizontal beam-beam parameters are much smaller than those at KEKB, and detecting a horizontal orbit offset at IP using the beam-beam deflection is not effective at SuperKEKB. Therefore, a dithering method was introduced for SuperKEKB. A good collision condition is sought for by dithering the positron beam (LER, Low Energy Ring), and once a good collision condition is found, it is maintained by an active orbital feedback, which moves the electron beam (HER, High Energy Ring) relative to the LER by creating a local bump at the IP. The algorithm of the system is described elsewhere [4]. The dither system was tested with colliding beams in the SuperKEKB Phase 2 commissioning.

DITHERING SYSTEM

System Layout

The block diagram of the dither system is shown in Fig. 1. The system consists of fast luminosity monitors, a lock-in amplifier, coils for dithering, a programmable amplifier whose functions are gain and phase adjustments for each power supply, actuators (a bump system called “iBump system” which is also used for the fast vertical feedback), a controller for the iBump system, a dither control system (the actual feedback algorithm will be run in an IOC on a PLC) and power supplies of the dithering coils. Those devices are distributed

three different locations, *i.e.* a beam line in the SuperKEKB tunnel, Tsukuba B4 control room which is located near the beam line and Belle 2 Electronics Hut where the Belle 2 data acquisition electronics are assembled. PLC and the iBump system are connected through the EPICS control network and the whole dither system is control by the EPICS system. The system is also connected to the SuperKEKB center control room through the network and can be monitored and controlled therefrom.

Dither Coils

Eight sets of Helmholtz coils for the dithering system were designed and fabricated and their magnetic properties were measured at SLAC [5]. The coils were installed in the SuperKEKB tunnel in June 2015. Each set consists of a pair of coils to provide a horizontal kick and/or another pair of coils to provide vertical kick to the positron beam. The coils are designed to be mounted on the vacuum pipes directly. The coils are installed at 8 locations in the LER, 4 on the right side of the IP (ZD1RP, ZD2RP, ZD3RP and ZD4RP) and another 4 on the left side (ZD1LP, ZD2LP, ZD3LP and ZD4LP), as is shown in Fig. 2. Three types of coils are needed to be designed as the cross sections of the beam pipes vary by location. Two types (ZD1L/RP, ZD2L/RP) are symmetric in shape and have both horizontal and vertical coils while the third type (ZD3L/RP and ZD4L/RP) is asymmetric as this type is mounted on the vacuum pipe ante-chamber and have coils for the vertical kick. Field harmonics were evaluated by a rotating coil system, shown in Fig. 3. The required field uniformity of 0.1% is achieved over a range of ± 10 mm, even with the asymmetric type coil. The LER beam is kicked sinusoidally by the coils in the horizontal direction around the IP at a frequency of 79 Hz. The coils for vertical kick are prepared in order to correct the x-y coupling in the IP bump region.

Luminosity Monitor

Two types of fast luminosity monitors are used for studying dither. They both detect photons, re-coiled electrons, or positrons from radiative Bhabha scattering in the very forward (“zero degree”) direction. One monitoring system is called zero degree luminosity monitor (ZDLM) and is based on Cherenkov and scintillation counters [6]. The other system is developed by LAL, which uses diamond sensors and is called “LumiBelle2” [7]. Required accuracy of the

* Work supported by U.S.-Japan Science and Technology Cooperation Program in High Energy Physics.

[†] yoshihiro.funakoshi@kek.jp

MACHINE DETECTOR INTERFACE FOR CEPC*

S. Bai^{#1}, C. H. Yu^{1,2}, Y. W. Wang¹, Y. Zhang^{1,2}, D. Wang¹, H. P. Geng¹, Y. S. Zhu¹, J. Gao¹,
 Z. H. Liu³, Qi Yang³

¹Institute of High Energy Physics, [100049] Beijing, China

²University of Chinese Academy of Sciences, [100049] Beijing, China

³Huiyu vacuum technology company, [110000] Shenyang, China

Abstract

The Circular Electron Positron Collider (CEPC) is a proposed Higgs factory with center of mass energy of 240 GeV to measure the properties of Higgs boson and test the standard model accurately. Machine Detector Interface (MDI) is the key research area in electron-positron colliders, especially in CEPC, it is one of the criteria to measure the accelerator and detector design performance. In this paper, we will introduce the CEPC superconducting magnets design, solenoid compensation, synchrotron radiation and mask design, detector background, collimator, mechanics assembly etc on, which are the most critical physics problem.

INTRODUCTION

With the discovery of a Higgs boson at about 125 GeV, the world high-energy physics community is investigating the feasibility of a Higgs Factory, a complement to the LHC for studying the Higgs [1]. There are two ideas now in the world to design a future higgs factory, a linear 125×125 GeV e^+e^- collider and a circular 125 GeV e^+e^- collider. From the accelerator point of view, the circular 125 GeV e^+e^- collider, due to its low budget and mature technology, is becoming the preferred choice to the accelerator group in China. MDI is one of the most challenging field in CEPC design, it almost covered all the common problems in accelerator and detector. Background is an important issue in MDI study. Every kinds of background source will increase the initial particles into detector, producing energy deposition in detector, which will make bad influence on the life of detector. Particles which hit the inner wall of beam pipe or collimators may interact with materials, producing lots of secondary particles into detector. These secondary particles will disturb the experiment and make damage to each layers. So it is necessary to reduce lost particles into detector.

The central field strength of CEPC detector solenoid is about 3T, it will introduce strong coupling of horizontal and vertical betatron motion, increasing the vertical emittance and also the vertical orbit. If it is not compensated, the IP beam size will increase, and degrade the luminosity.

In this paper, we will introduce the critical issues of CEPC MDI, including the superconducting magnets design,

solenoid compensation, detector background, collimator design and mechanics assembly etc on.

MDI LAYOUT AND IR DESIGN

The machine-detector interface is about ± 7 m in length in the IR as can be seen in Fig. 1, where many elements need to be installed, including the detector solenoid, luminosity calorimeter, interaction region beam pipe, beryllium pipe, cryostat and bellows. The cryostat includes the final doublet superconducting magnets and anti-solenoid. The CEPC detector consists of a cylindrical drift chamber surrounded by an electromagnetic calorimeter, which is immersed in a 3T superconducting solenoid of length 7.6 m. The accelerator components inside the detector should not interfere with the devices of the detector. The smaller the conical space occupied by accelerator components, the better will be the geometrical acceptance of the detector. From the requirement of detector, the conical space with an opening angle should not larger than 8.11 degrees. After optimization, the accelerator components inside the detector without shielding are within a conical space with an opening angle of 6.78 degrees. The crossing angle between electron and positron beams is 33 mrad in horizontal plane. The final focusing quadrupole is 2.2 m from the IP [2]. The luminosity calorimeter will be installed in a longitudinal location 0.95~1.11 m, with an inner radius of 28.5 mm and outer radius 100 mm. Primary results are got from the assembly, interfaces with the detector hardware, cooling channels, vibration control of the cryostats, supports and so on.

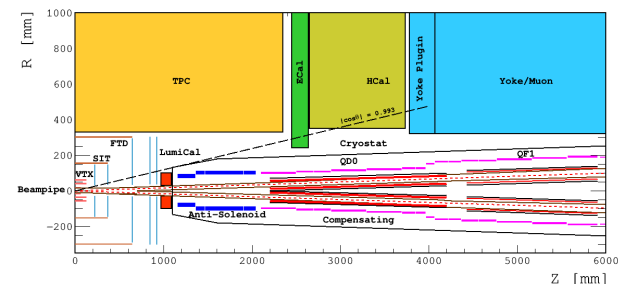


Figure 1: CPEC IR layout.

BEAM PIPE

To reduce the detector background and radiation dose from beam loss, the vacuum chamber has to accommodate the large beam stay clear region. In order to keep precise shaping, all these chambers will be manufactured with

* Work supported by National Key Programme for S&T Research and Development (Grant NO. 2016YFA0400400), and National Natural Science Foundation of China (NSFC, Project 11605210)
 # baisha@ihep.ac.cn

BEAM BACKGROUND AT SUPERKEKB DURING PHASE 2 OPERATIONS

A. Paladino* on behalf of the BEAST group, KEK - IPNS, Tsukuba, Japan

Abstract

The SuperKEKB accelerator, the upgrade of the KEKB machine, will operate at an unprecedented instantaneous luminosity of $8 \times 10^{35} \text{cm}^{-2}\text{s}^{-1}$, providing the Belle II experiment an expected integrated luminosity of about 50ab^{-1} in ten years of operation. With the increased luminosity, the beam background is expected to grow significantly with respect to KEKB, leading, among other effects, to possible damage of detector components and suppression of signal events. We present studies done during the Phase 2 operation of SuperKEKB to evaluate the contribution of each background source, including the Touschek effect, beam-gas scattering, synchrotron radiation, and injection background. We also present studies performed on collimators and other solutions adopted to mitigate beam backgrounds in the interaction region.

INTRODUCTION

The SuperKEKB [1] asymmetric e⁺e⁻ collider is an upgrade of the KEKB machine that will provide the Belle II experiment [2] an unprecedented instantaneous luminosity of $8 \times 10^{35} \text{cm}^{-2}\text{s}^{-1}$, with an expected integrated luminosity of about 50ab^{-1} in ten years of operation. The upgrade is based on the so called "nano-beam scheme", proposed for the first time by P. Raimondi for the SuperB project [3]. The idea behind the nano-beam scheme is to squeeze as much as possible the vertical beta function of the beams at the IP, maximizing the luminosity, which is given by the following formula, assuming flat beams and equal horizontal and vertical beam sizes for the two beams:

$$L = \frac{\gamma_{\pm}}{2er_e} \frac{I_{\pm}\xi_{y\pm}}{\beta_{y\pm}^*} \frac{R_L}{R_{\xi_y}} \quad (1)$$

where γ is the Lorentz factor, e the elementary electric charge, r_e the electron classical radius, I_{\pm} the beam current, $\xi_{y\pm}$ the beam-beam parameter, $\beta_{y\pm}^*$ the vertical beta function at the IP, R_L the luminosity reduction factor, R_{ξ_y} the beam-beam reduction factor. + and - indices refer to positron and electron beams respectively. Squeezing the beta-function by a factor 20 with respect to KEKB and doubling the beam currents, a 40 times higher luminosity can be achieved. SuperKEKB basic parameters are summarized in Table 1.

The Belle II detector, an upgraded version of the Belle detector, is placed around the IP. Its vertex reconstruction performance will be improved thanks to the new Vertex Detector (VXD), whose readout electronics can tolerate the 10 Mrad dose expected for the whole period of operation. The purpose of the Phase 2 operation, together with the

commissioning of SuperKEKB in its final configuration, is to verify that the level of backgrounds in the interaction region are compatible with the expectations.

Table 1: Basic parameters for SuperKEKB Phase 2 and Phase 3 operations. The former number refers to the Low Energy Ring (LER), the latter to the High Energy Ring (HER).

	Phase 2	Phase 3
Energy [GeV]	4.0/7.007	4.0/7.007
Beam current [A]	0.327/0.279	3.6/2.6
Number of bunches	789	2500
ϵ_x [nm]	1.7/4.6	3.2/4.6
$\xi_{y\pm}$	0.028/0.019	0.088/0.081
$\sigma_{y\pm}^*$ [nm]	692/486	48/62
$\beta_{y\pm}^*$ [mm]	3.0/3.0	0.27/0.30
$\beta_{x\pm}^*$ [mm]	200/100	32/25
Luminosity [$\text{cm}^{-2}\text{s}^{-1}$]	2.62×10^{33}	8×10^{35}

BELLE II AND BEAST DETECTORS

For Phase 2, the Belle II detector was used in its final configuration, except for the Vertex Detector (VXD), where only one slice of the final silicon vertex tracker was used, as shown in Fig 1. The remaining volume was occupied by some of the BEAST II detectors:

- FANGS: hybrid silicon pixel detectors.
- CLAWS: plastic scintillators with SiPM readout.
- PLUME: double sided CMOS pixel sensors.

Outside of the VXD volume, other BEAST II detectors were used:

- Diamond sensors for ionizing radiation dose monitoring in the interaction region.
- PIN diodes for ionizing radiation dose monitoring around QCS magnets.
- ³He detectors for thermal neutron flux measurements.
- TPC detectors for fast neutron flux and direction measurements.

BACKGROUND SOURCES

In this section, the most relevant beam background sources in SuperKEKB are described.

* antonio.paladino@pi.infn.it

COMMISSIONING STATUS OF SuperKEKB VACUUM SYSTEM

K. Shibata[†], Y. Suetsugu, T. Ishibashi, K. Kanazawa, M. Shirai, S. Terui, and H. Hisamatsu
High Energy Accelerator Research Organization (KEK), 305-0817 Tsukuba, Ibaraki, Japan

Abstract

In the upgrade from the KEKB B-factory (KEKB) to the SuperKEKB, approximately 90% and 20% of the beam pipes and vacuum components of the positron ring and the electron ring, respectively, were replaced with new ones. In the Phase-1 commissioning in 2016, vacuum scrubbing and confirmation of the stabilities of new vacuum components at approximately 1 A were carried out, and some problems, such as pressure bursts accompanied with beam losses, were revealed. During the subsequent shutdown, the countermeasures against the problems were taken, and new beam pipes and components, such as beam pipes for the interaction point, and beam collimators were installed. The Phase-2 commissioning, where beam collision tuning was mainly performed, was carried out from March to July 2018. The collimators suppressed the background noise of the particle detector for high-energy physics (Belle II detector) very well, and the frequency of the pressure burst drastically decreased though typical beam currents were lower than those in Phase-1. So far, the vacuum system of the SuperKEKB has been working generally well, and no serious problems have been observed.

INTRODUCTION

The SuperKEKB [1], which is an upgrade of the KEKB, is a high-luminosity electron–positron collider. The main ring (MR) of the SuperKEKB with a circumference of 3016 m is composed of two rings, i.e., the high-energy ring (HER) for 7.0 GeV electrons and the low-energy ring (LER) for 4.0 GeV positrons. Over a period of 10 years, the SuperKEKB project is expected to achieve a 50-fold increase in the integrated luminosity over the original KEKB. The design luminosity is $8.0 \times 10^{35} \text{ cm}^{-2}\cdot\text{s}^{-1}$, which is approximately 40 times the KEKB's record. In the SuperKEKB, the luminosity will be increased by increasing the beam current to 2.6 A (electrons) and 3.6 A (positrons), which are twice as much as in the KEKB, and adopting a novel “nanobeam” collision scheme, which requires a much smaller emittance beam than the KEKB. In order to achieve this challenging goal, many upgrades are required, among which the upgrade of the vacuum system [2-4] is a crucial requirement.

After more than five years of upgradation work on the KEKB, the commissioning of the SuperKEKB commenced in 2016, and two of three commissioning phases have been completed so far. The first commissioning (Phase-1), which was dedicated to accelerator tuning without the Belle II detector [5], was carried out from February to June 2016 [6]. During the subsequent shut-

down period, the remained upgradation works including the “roll-in” of the Belle II detector [5] to the collision point were performed. The second commissioning (Phase-2), where beam collision tuning was mainly performed, was carried out from March to July 2018.

VACUUM SYSTEM UPGRADATION

Outline of Upgradation

For the LER, in order to realize small beam emittance, the beam optics was drastically changed compared to that of the KEKB, and a large number of magnets need to be rearranged, replaced, and added. Consequently, approximately 93% of the beam pipes and vacuum components were replaced with new ones. On the other hand, in the HER, the wiggler section was newly made to reduce the emittance, but in the arc sections, no replacement of the magnet was performed. Furthermore, because the beam energy of the HER is reduced from 8.0 GeV to 7.0 GeV, the power of the synchrotron radiation (SR) decreases to the tolerance level of a conventional copper beam pipe, in spite of doubling the beam current. Therefore, approximately 80% of the components in the HER can be reused. Only in the interaction region and the new wiggler section, the beam pipes and components were replaced with new ones. Figure 1 shows the location where the vacuum components were replaced in both rings. The reused components of the HER were left undisturbed in the tunnel during the upgradation work keeping vacuum inside although all vacuum pumps were tuned off. However, these components were sometimes exposed to air temporarily when broken components were replaced with new ones.

The target vacuum pressure in the MR is on the order of 10^{-7} Pa at the designed beam current. In the LER, because of the higher beam currents, the SR power and the photon density are consequently higher, and the resultant heat and gas loads are also larger than those of the KEKB. As a solution to this issue, an effectively distributed pumping scheme using a strip-type NEG (ST707, SAES GETTERS Co. Ltd.) was adopted as the main pump for the arc sections of the LER. The expected effective linear pumping speed is approximately $0.14 \text{ m}^3\cdot\text{s}^{-1}\cdot\text{m}^{-1}$ for CO just after the NEG activation. In order to achieve the required pressures, a linear pumping speed of approximately $0.1 \text{ m}^3\cdot\text{s}^{-1}\cdot\text{m}^{-1}$ is required if we assume a photo-desorption coefficient of $1 \times 10^{-6} \text{ molecules}\cdot\text{photon}^{-1}$, which was obtained at a beam dose of $3 \times 10^3 \text{ A}\cdot\text{h}$ in the KEKB and will be accrued after approximately 1 year beam operation at the designed beam current in the case of the SuperKEKB. To evacuate non-active gases and to enable more efficient evacuation in relatively high-pressure regimes, noble-type sputter ion pumps with a nominal pumping speed of $0.4 \text{ m}^3\cdot\text{s}^{-1}$ are provided as an

[†] kyo.shibata@kek.jp

SINGLE BUNCH INSTABILITIES AND NEG COATING FOR FCC-ee

E. Belli*, P. Costa Pinto, G. Rumolo, A. Sapountzis, T. Sinkovits, M. Taborelli,
 CERN, Geneva, Switzerland

G. Castorina, M. Migliorati, University of Rome La Sapienza and INFN Sez. Roma1, Rome, Italy
 B. Spataro, M. Zobov, INFN/LNF, Frascati (Rome)

Abstract

The high luminosity electron-positron collider FCC-ee is part of the Future Circular Collider (FCC) study at CERN and it has been designed to cover the beam energy range from 45.6 GeV to 182.5 GeV to study the properties of the Higgs boson and other particles. Electron cloud build up simulations on the Z resonance revealed the necessity of minimising the Secondary Electron Yield (SEY) of the pipe walls by applying a Ti-Zr-V Non-Evaporable Getter (NEG) coating in the entire ring. Beam dynamics simulations at 45.6 GeV pointed out that minimising the thickness of this layer is mandatory to reduce the resistive wall (RW) impedance, thus increasing the single bunch instability thresholds and ensuring beam stability during operation. However, reducing the coating thickness can affect the performance of the material and therefore the SEY. For this reason, an extensive measurement campaign was performed at CERN to characterise NEG thin films with thicknesses below 250 nm in terms of activation performance and SEY measurements. This paper also presents the FCC-ee longitudinal impedance model which includes all the current machine components.

INTRODUCTION

In 2014, CERN launched the Future Circular Collider (FCC) study [1] for the design of different circular colliders for the post-LHC era. This study is investigating a high energy proton-proton machine (FCC-hh) to reach a centre-of-mass energy of 100 TeV and a high luminosity electron-positron collider (FCC-ee) as a potential first step to cover a beam energy range from 45.6 GeV to 182.5 GeV, thus allowing to study the properties of the Higgs, W and Z bosons and top quark pair production thresholds with unprecedented precision. Table 1 summarizes the main beam parameters on the Z resonance which represents the most challenging scenario from the beam stability point of view.

Due to the beam parameters and pipe dimensions, electron cloud (EC) and collective effects due to the electromagnetic fields generated by the interaction of the beam with the vacuum chamber can be very critical aspects for the machine by producing instabilities that can limit its operation and performance.

This paper will present an estimation of the EC build up in the main magnets of the positron ring, the contributions of specific vacuum chamber components to the total impedance budget and their effects on single bunch beam dynamics. Special attention has been given to the resistive wall (RW) impedance, whose value is increased by a layer of

Table 1: FCC-ee baseline beam parameters at Z running. SR and BS stand for synchrotron radiation and beamstrahlung.

Beam energy [GeV]	45.6
Circumference C [km]	97.75
Number of bunches/beam	16640
Bunch population N_p [10^{11}]	1.7
Beam current I [A]	1.39
RF frequency f_{RF} [MHz]	400
RF voltage V_{RF} [MV]	100
Energy loss per turn [GeV]	0.036
Momentum compaction α_c [10^{-5}]	1.48
Bunch length $\sigma_{z,SR}/\sigma_{z,BS}$ [mm]	3.5/12.1
Energy spread $\sigma_{dp,SR}/\sigma_{dp,BS}$ [%]	0.038/0.132
Horizontal tune Q_x	269.138
Vertical tune Q_y	269.22
Synchrotron tune Q_s	0.025
Horizontal emittance ϵ_x [nm]	0.27
Vertical emittance ϵ_y [pm]	1.0

Non-Evaporable Getter (NEG) coating which is required to reduce the Secondary Electron Yield (SEY) of the pipe walls for electron cloud mitigation [2, 3]. The studies presented in this paper will show that for the proposed lepton collider at 45.6 GeV the single bunch instability thresholds can be increased by decreasing the coating thickness. For this reason, in parallel to these numerical studies, an extensive measurement campaign was performed at CERN to investigate NEG thin films with thicknesses below 250 nm in terms of activation performance and SEY measurements, with the final purpose of finding the minimum effective thickness satisfying impedance, vacuum and electron cloud requirements.

Besides the RW, other impedance sources have been analyzed and the longitudinal impedance model thus obtained has been used to study the microwave instability and to predict its effects on the stability of the beam.

ELECTRON CLOUD STUDIES

This section presents EC build up studies in the positron ring of the lepton collider at 45.6 GeV. Build up simulations have been performed in the drift space and in all the magnets of the machine (dipoles and quadrupoles in the arcs and final focusing quadrupoles in the interaction region) by using the PyECLOUD [4, 5] code.

The bunch parameters used for simulations are listed in Table 1 while Table 2 summarizes the magnetic parameters of each element. For the beam optics in the arcs and around the interaction point, one can refer to [6]. In the arcs, the

* eleonora.belli@cern.ch

CEPC SUPERCONDUCTING MAGNETS*

Y. S. Zhu[†], X. C. Yang, M. Yang, F. S. Chen, W. Kang

Key Laboratory of Particle Acceleration Physics and Technology, Institute of High Energy Physics, Chinese Academy of Sciences, Beijing 100049, China

Abstract

A Circular Electron Positron Collider (CEPC) with a circumference about 100 km, a beam energy up to 120 GeV is proposed to be constructed in China. CEPC will be a double ring collider with two interaction points. Most magnets for CEPC accelerator are conventional magnets, but some superconducting magnets are required in the interaction region. Final focus superconducting high gradient quadrupoles are inside the solenoid field of Detector magnet, so superconducting anti-solenoid is need to minimize the effect of the solenoid field on the beam. In addition, high strength superconducting sextupole magnets are also required. In this paper, the layout and conceptual design of CEPC interaction region superconducting magnets are described, and the R&D plan is presented.

INTRODUCTION

A Circular Electron Positron Collider (CEPC) with a circumference about 100 km is proposed to be constructed in China. It is an important part of the world plan for high-energy physics research. The CEPC center-of-mass energy is 240 GeV, and at that collision energy it will serve as a Higgs factory. The design also allows operation at lower beam energy to be a Z or W factory. The accelerator complex of CEPC consists of a linear accelerator (Linac), a damping ring (DR), the Booster, the Collider and several transport lines [1]. The heart of the CEPC is a double-ring collider with two interaction points.

There are a large number of magnets in the CEPC collider ring, and the magnets occupy over 80% of the circumference. Most magnets for CEPC accelerator are conventional magnets, except some superconducting magnets are needed in the interaction region of CEPC collider ring. Compact high gradient superconducting quadrupole doublet magnets are usually required on both sides of the interaction point (IP) to final focus the beam to achieve high luminosity [2-4]. The CEPC final focus superconducting quadrupoles are inside the solenoid field of Detector magnet, so superconducting anti-solenoid is need to minimize the effect of the solenoid field on the beam. In addition, high strength superconducting sextupole magnets are also required in the CEPC interaction region.

SUPERCONDUCTING MAGNET SYSTEM

The requirements of the final focus quadrupole doublets QD0 and QF1 are based on the circumference 100 km of CEPC, L^* of 2.2 m, and a beam crossing angle of 33 mrad

in the CEPC interaction region. The requirements of the quadrupole magnets are listed in Table 1.

Table 1: Requirements of CEPC Interaction Region Quadrupole Magnets

Magnet	Field gradient (T/m)	Magnetic length (m)	Width of GFR (mm)
QD0	136	2.0	19.51
QF1	110	1.48	27

The crossing angle between the electron and positron beams is 33 mrad in horizontal plane. The final focusing quadrupole is 2.2 m from the IP, and the QD0 and QF1 magnets are designed to be twin aperture quadrupole magnets. They are operated fully inside the solenoid field of the Detector magnet with a central field of 3.0 T. To minimize the effect of the longitudinal detector solenoid field on the accelerator beam, anti-solenoids before QD0, outside QD0 and QF1 are needed. Their magnetic field direction is opposite to the detector solenoid, and the total integral longitudinal field generated by the detector solenoid and anti-solenoid coils is zero. It is also required that the total solenoid field inside the QD0 and QF1 magnet should be close to zero.

The CEPC Machine Detector Interface (MDI) layout at one side of the interaction point is shown in Fig. 1, where QD0, QF1 and Anti-solenoid are the accelerator magnets.

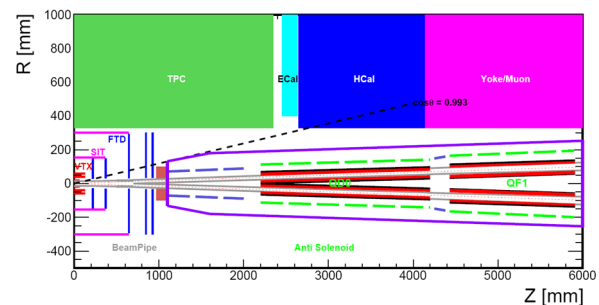


Figure 1: CEPC MDI layout.

According to the layout of the MDI, accelerator devices can only start after $z=1.1$ m along the longitudinal axis, so the available space for the anti-solenoid before QD0 is limited. In addition, the angle of the accelerator magnet seen from the IP point must be small and satisfy the requirement from the Detector. Taking into account the high field strength of twin aperture quadrupole magnet, high central field of anti-solenoid and the limited space, superconducting technology based on NbTi conductor will be used for these interaction region superconducting quadrupole magnets and anti-solenoids.

* Work supported in part by the Yifang Wang scientific Studio of the Ten Thousand Talents Project and in part by the National Natural Science Foundation of China under Grant 11875272.

[†] Email address: yszhu@ihep.ac.cn

CEPC COLLIDER AND BOOSTER MAGNETS*

Mei Yang[†], Fusan Chen, Wen Kang, Xianjing Sun, Yingshun Zhu

Key Laboratory of Particle Acceleration Physics and Technology, Institute of High Energy Physics, Chinese Academy of Sciences, Beijing 100049, China

Abstract

A Circular Electron Positron Collider (CEPC) with a circumference of about 100 km, a beam energy up to 120 GeV is proposed to be constructed in China. Most magnets for CEPC booster and collider ring are conventional magnets. The quantities of the magnets are large, so the cost and power consumption are two of the most important issues for the magnet design and manufacturing. The dual aperture dipole and quadrupole magnet with low current high voltage are used in the collider ring. Whereas in the booster the dipole magnet works at very low field, so a low packing factor dipole magnet or a coil type without iron design will be investigated and chosen. In this paper, the conceptual design of the CEPC main magnets are described in detailed and the R&D plan is presented.

INTRODUCTION

A Circular Electron Positron Collider (CEPC) is proposed to be constructed in China. It is an important part of the world plan for high-energy physics research. The CEPC will operated at different beam energy of Z, W and Higgs factory. The accelerator complex of CEPC consists of a linear accelerator (Linac), a damping ring (DR), the booster, the collider and several transport lines. The booster and the collider ring are in the same tunnel with a circumference of about 100 km [1].

There are about 9370 magnets in the collider ring and nearly 20000 magnets in the booster ring. Most magnets except some magnets in the interaction region operated at a relatively low field are designed as conventional magnets. A significant effort has been made in optimizing of the power consumption, manufacturing and operation cost of the magnets like that in the LEP and FCC-ee [2-3]. The synchrotron radiation damages to the conductor are considered with more space on the coil windings to place the radiation absorber. All the magnets have been designed using OPERA software [4].

COLLIDER MAGNET SYSTEM

The CEPC collider ring is a double ring collider and most of the dipoles and quadrupoles have similar strength and length. To reduce the cost and power consumption, 2384 dipoles and 2392 quadrupoles are designed as dual aperture magnets to provide magnetic field for both beams whose separation is 350 mm.

Besides the dual aperture magnet design, several special technologies are used to reduce the magnet cost, including

the core steel dilution for dipoles and aluminium conductors instead of copper. To reduce the magnet power consumption, the low current density and high voltage operation mode are used to cut down power consumption of the magnet power supply and the power cables. The main magnet requirements are listed in Table 1. The gap height of the dipoles is 70 mm and the aperture diameter of quadrupoles and sextupoles is 76 mm and 80 mm, respectively.

Table 1: Main Parameters of CEPC Collider Ring Magnets

Magnet	Field strength	Magnetic length	Width of GFR
Dipole	0.0373 T	28.7 m	13.5 mm
Quadrupole	8.42 T/m	2.1 m	12.2 mm
Sextupole	506.2 T/m ²	1.4 m	13.9 mm

Dual Aperture Dipole Magnet

The dipoles are kept as long as possible to limit the synchrotron radiation losses which have a length of 28.7 m. Its iron is divided into five segments for easily fabrication and transportation. The 'I' shape core magnet sharing one coil is chosen to save about 50% power consumption and provide two identical field in the twin apertures. In the first and last segments, the dipole-sextupole combined magnet profile are used to reduce the sextupole strength of the individual sextupoles.

Considering the beam energy saw tooth effect, the trim coils are used for both apertures to adjust the field by the order of $\pm 1.5\%$ independently. 2D field simulation results show that the field quality is sensitive to the position of the aluminium busbars and the trim coil in one aperture has no coupling effect in the other aperture. Figure 1 shows the cross section of the dual aperture dipole magnet with and without the sextupole component.

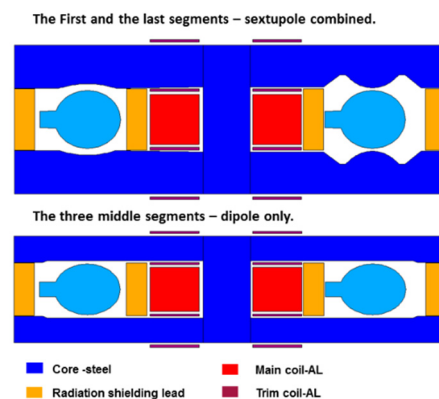


Figure 1: Cross section of the dual aperture dipole.

* Work supported in part by the Yifang Wang scientific Studio of the Ten Thousand Talents Project.

[†] Email address: yangmei@ihep.ac.cn

LARGE SCALE SUPERCONDUCTING RF PRODUCTION

Carlo Pagani, INFN-LASA and Università degli Studi di Milano, Milano, Italy

Abstract

The efficient plug to beam power conversion promised by the use of Superconducting RF to accelerate particle beams is still the driving force to pursue the development of this technology. Once the effective gain reached the level to pay for cryogenics, big physics laboratories started to believe on SRF, investing resources and proposing large challenging projects. Since then the cooperation with industry has been crucial to transform a few lab results into reliable SRF cavities and related ancillaries. This process started in the eighties and reached the actual paradigm with the realization of the European XFEL. All the new large scale projects in construction or proposed should start from the analysis of this experience and move forward from there.

INTRODUCTION

Superconducting radiofrequency (SRF) cavities have been in routine operation over the past 30 and more years in a variety of settings, from pushing frontier accelerators for particle physics to applications in nuclear physics and materials science. Used in a number of accelerator based projects, with different frequencies and shapes, they were instrumental in pushing CERN's LEP collider to new energy regimes, in getting high energy and in driving the newly inaugurated European X-ray Free Electron Laser. Nowadays, being the basic technology well understood, almost any type of accelerating structure can be successfully built taking advantage of the technological level that has been reached thanks to the investments done by the big projects in 1980s and 1990s.

At first, it was not clear that superconductivity had much value for RF technology. But it was soon realized that in the practical frequency range of RF accelerators, from hundred MHz to a few GHz, the use of SRF cavities would produce in any case a significant breakthrough due to the increase in the conversion efficiency from plug-to-beam-power, cryogenics included. It was simply a question of developing the technology, and that required investment and big projects.

The High-Energy Physics Lab at Stanford University in the US was a pioneer in applying SRF to accelerators, demonstrating the first acceleration of electrons with a lead-plated single-cell resonator in 1965. Also in Europe, in the late 1960s, SRF was considered for the design of proton and ion linacs at KFK in Karlsruhe, but to really compete with the well-established normal conducting technology the path was still long and tortuous. Following these forerunners since the early 1970s SRF has been introduced in the design of particle accelerators, but results were modest and a number of limiting factors had to be understood and handled. As usual for any new technology a lot of science supported industrial development was needed to reach the current status of the art. In par-

ticular lead and niobium used as superconductor were originally too dirty for SRF. In practice, the different orders of magnitude obtained theoretically with superconductivity in terms of surface resistance were strongly reduced by the normal conductive impurities coming from both the superconductors themselves and the TIG welding electrodes.

However, the pioneering results while not astonishing have been sufficient to convince scientists that was just a question of technology and, once the effective gain reached the level to pay for cryogenics, big physics laboratories started to believe on SRF investing resources and proposing challenging projects. Since then the cooperation with industry has been crucial to transform lab results into reliable items.

SRF TECHNOLOGY AND BIG PROJECTS

The first successful test of a complete SRF cavity at high gradient and with beam was performed at Cornell's CESR facility at the end of 1984, involving a pair of 1.5 GHz, five-cell bulk niobium cavities with a gradient of 4.5 MV/m. This cavity design was then used as the basis for the CEBAF facility to be built at Jefferson Lab in US and convinced KEK in Japan to ask industry to produce a large number of SRF cavities to upgrade the energy of their TRISTAN electron-positron collider.

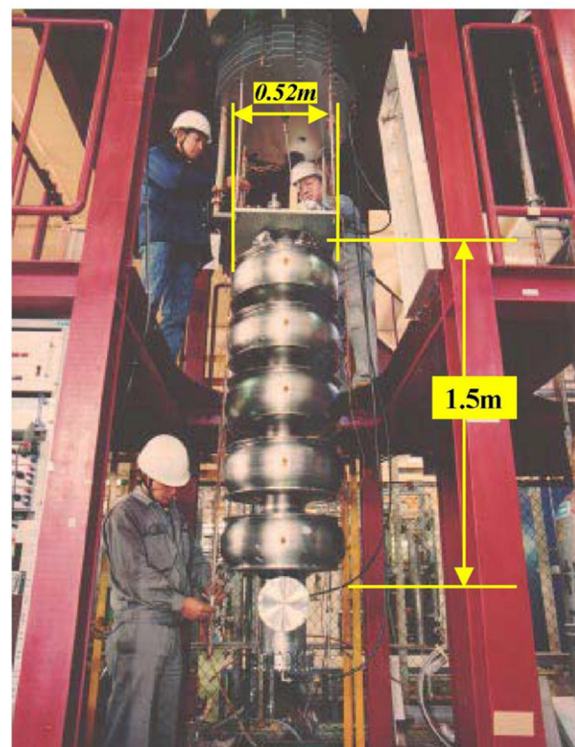


Figure 1: TRISTAN cavity prepared for test at KEK.

Content from this work may be used under the terms of the CC BY 3.0 licence (© 2018). Any distribution of this work must maintain attribution to the author(s), title of the work, publisher, and DOI.

SRF SYSTEMS FOR KEKB AND SuperKEKB

K. Nakanishi, M. Nishiwaki[#], T. Kobayashi, KEK, Tsukuba, Japan
 K. Hirosawa, SOKENDAI, Tsukuba, Japan

Abstract

Eight superconducting accelerating cavities were operated for more than ten years at the KEKB. Commissioning operation of SuperKEKB is ongoing and those cavities are also used to accelerate the electron beam of 2.6 A. There are some issues to address the large beam current and to realize stable operation. One issue is a large HOM power of 37 kW expected to be induced in each cavity module. In particular, the power emitted out to the downstream of the cavity is simulated to be large. To cope with the HOM power issue, we have installed an additional HOM damper to the downstream of the cavity module. Another issue is degradation of Q values of the cavities during the ten years operation. Cause of the degradation was particle contamination. To clean the cavity surface, high pressure rinsing (HPR) is an effective way. Therefore we have developed a horizontal HPR. In this method, a nozzle for water jet is inserted horizontally into the cavity module without disassembly of the cavity. We applied the horizontal HPR to our degraded cavities. The RF performances of those cavities have been successfully recovered. In this report, present status of our cavity will be presented. Additionally, low level RF control issues for SuperKEKB upgrade will be introduced.

Table 1: RF-related Operation Parameters in HER

Parameters	KEKB (operation)	SuperKEKB (design)
Energy [GeV]	8.0	7.0
Beam current [A]	1.4	2.6
Number of bunches	1585	2500
Bunch length [mm]	6~7	5
Total beam power [MW]	~5	8.0
Total RF voltage [MV]	15.0	15.8

OVERVIEW OF KEKB AND SUPERCONDUCTING CAVITY

KEKB accelerator was an electron-positron asymmetric energy ring collider for B-meson physics, consisting of high energy ring (HER) for the electrons and low energy ring (LER) for the positrons. The circumference was around 3 km. The beam energies of HER and LER were 8 and 3.5 GeV, respectively. The maximum beam currents were 1.4 A for HER and 2.0 A for LER. KEKB was operated until June 2010, with a world record luminosity of $2.1 \times 10^{34} / \text{cm}^2/\text{s}$ [1].

One serious concern for high-current storage rings is the coupled-bunch instability caused by the accelerating mode of the cavities. This issue arises from the large detuning of the resonant frequency of the cavities that is needed to compensate for the reactive component of the

beam loading. In order to mitigate this problem, two types of cavities were adopted in KEKB operation [2, 3]: one is a superconducting cavity (SCC) [4, 5], and the other is a normal conducting cavity called ARES [6, 7]. ARES, which is a unique cavity specialized for KEKB, consists of a three-cavity system operated in the $\pi/2$ mode: the accelerating (A-) cavity is coupled to a storage (S-) cavity via a coupling (C-) cavity. The A-cavity has higher-order-modes (HOM) damped structures.

In HER, RF systems consisted of hybrid system of eight superconducting cavities (SCC, Fig. 1) and 12 ARES cavities, while LER was operated with 20 ARES cavities without SCCs. Table 1 shows operation-related parameters of HER. The total beam power was 5 MW and the total RF voltage was 15 MV. The large beam power and RF voltage were shared with SCC and ARES cavities by giving an appropriate beam phase-offset between them so that each SCC delivered the power of 400 kW to the beam. The HOM load induced by the large beam current was absorbed by a set of ferrite HOM dampers located at the beam pipes of both ends of the cavity, called small beam pipe (SBP) and large beam pipe (LBP). The absorbed power in 1.4 A-operation reached 16 kW without any problems.

Operation statistics and maintenances of SCC in KEKB were summarized in Ref. [3] in detail. Many monitors were set over the ring to identify a cause of each trip. RF trips of the SCC were mainly caused by discharging in the cavity or a high power input coupler. The trip rate in eight cavities was 0.5 times/day at 1.4 A-operation. After adopting the crab crossing, the trip rate decreased to 0.1 times/day because the beam current was lowered to 1.1 A. In order to maintain stable operations, 1) warming up the system to room temperature was performed twice a year, 2) safety inspections due to high pressure safety regulations of cryogenics were carried out once a year, 3) the input coupler conditioning before cooling with bias voltage was performed and 4) regular conditioning every 2 or 3 weeks was carried out. As a result, SRF system of KEKB had been operated safely and stably.

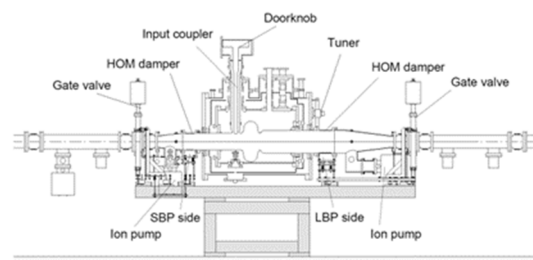


Figure 1: Cross-sectional drawing of the superconducting cavity module of KEKB.

[#]michiru.nishiwaki@kek.jp

CEPC CIVIL ENGINEERING DESIGN*

Yu Xiao[†], Yellow River Engineering Consulting Co., Ltd., 450003 Zhengzhou, China

Abstract

The CEPC is a circular e^+e^- collider located in a 100 km circumference underground tunnel. Preliminary site selection and the design of the CEPC civil engineering will be introduced in this paper.

INTRODUCTION

CEPC consists of a Collider, the injection system into the Collider whose main components are a Linac, a

Booster, and transport lines, and two large physics detectors. Civil construction houses all of the components of the CEPC and reserve space for SPPC, as illustrated in Fig. 1. The layout and construction of each part is determined by their geometric relationships, environmental conditions and safety considerations. Practicality, adaptability and operating efficiency are criteria to be carefully considered in the design of the civil construction.

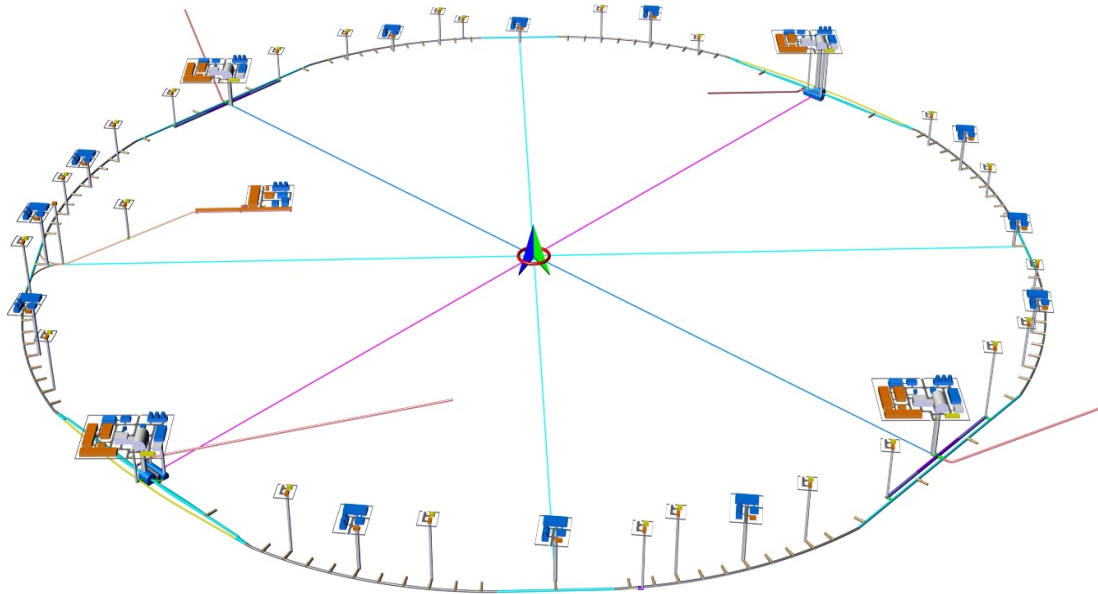


Figure 1: Layout of surface and underground CEPC structures.

The following defines the scope of work and the requirements to be met.

- The main tunnel to house the Collider and Booster synchrotrons, auxiliary tunnels for the Booster bypass and RF equipment, the Linac tunnel and equipment gallery and transport line tunnels. The main tunnel is 100 km in circumference and 100 m below ground.
- The experiment halls are 100 m below ground and span 30~40 m. There are additional chambers such as power source halls, cryogenics halls and spaces for the water cooling system, etc.
- There are accesses to the experiment halls, such as access tunnels, transport shafts, and emergency exits.
- There are ancillary structures at ground level, including structures near the shaft openings, structures to house substations and electric distribution, cryogenics rooms, and ventilation fan rooms.

- Space for staging the construction equipment and materials and dumping sites.
- Included in the project scope are related lifting equipment, conveyance, systems for electric supply, drainage, ventilation and air conditioning, communication, controls and monitoring, safety escape, and firefighting. The firefighting system includes fire alarms, hydrants, gas fire-extinguishing system, and a smoke exhaust system. Maintenance of these systems as well as their potential for future upgrades is fully considered in their design.

PRELIMINARY SITE SELECTION

Basic Principles of Site Selection

In the selection of the CEPC site, besides engineering

* Work supported by Yellow River Engineering Consulting Co., Ltd.
[†] email address: 328565909@qq.com

FCC-ee OPERATION MODEL, AVAILABILITY & PERFORMANCE*

Andrea Apollonio, Michael Benedikt, Olivier Brunner, Arto Niemi, Jörg Wenninger, Frank Zimmermann[†], CERN, Geneva, Switzerland; Stephen Myers, ADAM SA, Meyrin, Switzerland; Yoshihiro Funakoshi, Katsunobu Oide, KEK, Tsukuba, Japan; John Seeman, SLAC, Stanford, U.S.A.; Qing Qin, IHEP Beijing, P.R. China; Catia Milardi, INFN Frascati, Italy

Abstract

This document discusses the machine parameters and expected luminosity performance for the proposed future circular lepton collider FCC-ee. Particular emphasis is put on availability, physics run time, and efficiency. Key performance assumptions are compared with the operational experience of several past and present colliders including their injectors — LHC, LEP/LEP-2, PEP-II, KEKB, BEPCII, DAFNE, SLC and the SPS complex.

INTRODUCTION

In the following, we describe the goals and assumptions for the FCC-ee operation plan, and we confront our assumptions with the corresponding statistical information from several similar colliders, especially KEKB and PEP-II.

GOALS, MODES, PARAMETERS

The baseline FCC-ee features four modes of operation: (1) on the Z pole, (2) at the WW threshold, (3) at the HZ production peak, and (4) at the $t\bar{t}$ threshold. Running modes (1)–(3) are combined into a ‘phase 1’. Running mode (4) implies a major reconfiguration and is called ‘phase 2’.

The physics goals of FCC-ee require the following integrated luminosities for the different operation modes [1, 2], summed over two interaction points (IPs): 150 ab^{-1} at and around the Z pole (88, 91, 94 GeV centre-of-mass energy); 10 ab^{-1} at the W^+W^- threshold (~ 161 GeV with a \pm few GeV scan); 5 ab^{-1} at the HZ maximum (~ 240 GeV); 1.5 ab^{-1} at and above the $t\bar{t}$ threshold (a few 100 fb^{-1} with a scan from 340 to 350 GeV, and the remainder at 365 GeV).

FCC-ee machine parameters for all modes of operation are summarized in Table 1.

ESTIMATING ANNUAL PERFORMANCE

The annual luminosity estimates for FCC-ee at each mode of operation are derived from three parameters:

- Nominal luminosity L : taken to be 10–15% lower than the luminosity simulated for the baseline beam parameters. This nominal luminosity is considered from the third year onward in phase 1 (Z pole), and from the second year in phase 2 ($t\bar{t}$ threshold). The luminosity for the first and second year of phase 1 and for the first year of phase 2 are assumed to be smaller, on average, by

another factor or two, in order to account for a learning period during initial operation.

- It is assumed that 185 days per year are scheduled for physics. These 185 days are obtained by subtracting from one year (365 days), 17 weeks of extended winter shutdown (120 days), 30 days of annual commissioning, 20 days for machine development, and 11 days for technical stops.
- Nominal luminosity L and time for physics T are converted into integrated luminosity L_{int} via an ‘efficiency factor’ E , according to

$$L_{\text{int}} = ETL . \quad (1)$$

The efficiency factor E is an empirical factor, whose value can be extrapolated from other similar machines, or by simulations with average failure rate and average downtime. Thanks to the top-up mode of operation, it is expected that E will be about five percent lower than the availability of the collider complex. We assume an availability of at least 80% and, thereby, a corresponding efficiency $E \geq 75\%$.

The assumed 17 weeks of average winter shutdown are longer than the time required for the installation and RF commissioning of new cryomodules (see Table 2 below). Also the 20 days per year allocated for machine development (MD) are higher than the corresponding number for LEP (e.g. in the year 2000 only 5 days of LEP MDs were scheduled [3]).

CONFIGURATIONS AND SHUTDOWNS

The machine operation is expected to start with Z running, similar to LEP-1, as this requires the lowest RF voltage, implying the smallest amount of RF installation and the associated minimum beam impedance.

The changes in the machine configuration required between the Z, W and H running, can be implemented during the successive winter shutdowns.

The length of these FCC-ee winter shutdowns is likely to be dominated by the installation and RF commissioning of new cryomodules in preparing for, or during transition to, the next running modes. Considering only a single cryomodule transport per working day, the minimum total length of the winter shutdown is estimated as

$$n_{\text{working days}} = n_{\text{cryomodule}} + 10 + 10 + 25 , \quad (2)$$

where the first 10 days refer to the end of the installation, the second 10 days to the cool down, and the last 25 days to

* This work was supported by the European Commission under the HORIZON 2020 project ARIES no. 730871.

[†] frank.zimmermann@cern.ch

KEKB/SUPERKEKB CRYOGENICS OPERATION

K.Nakanishi*, K.Hara, T.Honma, K.Hosoyama, M.Kawai
Y.Kojima, Y.Morita, H.Nakai, N.Ohuchi, H.Shimizu

High Energy Accelerator Research Organization(KEK), 305-0801 Tsukuba, Japan
T.Endo, T.Kanekiyo, Hitachi Plant Mechanics Co.,Ltd., 744-0002 Kudamatsu, Japan

Abstract

At KEK, the operation of the superconducting cavities was started with TRISTAN accelerator in 1988 [1]. The superconducting cavities are continuously operated even after that. In this paper, the operation of the refrigerator for the superconducting cavities of KEKB/SuperKEKB is mainly introduced. In KEKB/SuperKEKB, the superconducting magnets are also used. They have their own refrigerator [2].

The refrigerator for the superconducting cavity for KEKB/SuperKEKB was constructed for the TRISTAN accelerator [3]. The capacity of the refrigeration is 8.1 kW at 4.4 K [4] [5]. Since the number of superconducting cavities used in KEKB / SuperKEKB is smaller than that of TRISTAN, there is a margin for the capacity of the refrigerator. In order to operate this old refrigerator, proper maintenance is necessary, and periodic inspection and equipment updating are carried out.

CRYOGENIC SYSTEM FOR SUPERCONDUCTING CAVITIES

Large-scale Helium Refrigerator

KEKB was built in the tunnel of the TRISTAN accelerator. The TRISTAN accelerator was operated from 1986 to 1995. The superconducting acceleration cavities were installed in 1988 to increase the beam energy. The cryogenic system for superconducting cavities was also established by Hitachi, Ltd. simultaneously. In 1989 superconducting acceleration cavities were added, and cryogenic systems were also enhanced. Its design capacity was increased from 4kW to 6.5kW. Schematic diagram of the refrigerator for superconducting cavities is shown in Fig. 1. By adding expansion turbines (T4 and T5), it became possible to operate the refrigerator without liquid nitrogen. By adopting the supercritical turbine expander (T3), the capacity of refrigerator was increased. And, two compressors (C5 and C6) were added. As a result, the practical refrigeration capacity was reached to 8.1kW at 4.4K.

KEKB took over many facilities from TRISTAN. The cryogenic system for superconducting cavities is one of them. This refrigerator is still used in SuperKEKB.

Superconducting Cavity

In TRISTAN, a cryostat for superconducting acceleration cavities had two of 5cell cavities (See Fig. 2). Finally, 16 cryostats were installed. An estimation of the heat loads are

shown in Table 1. The total heat load for TRISTAN cryogenic system at 4.4K is about 4 kW, which can be sufficiently cooled by the enhanced refrigerator.

KEKB accelerator operated from 1998 to 2010. In KEKB, a cryostat for superconducting acceleration cavities had a single-cell cavity (See Fig. 3). 8 cryostats were installed. The static heat load is about 30W/cryostat [6]. The RF loss is 100W/cavity. As can be seen from Table 1, the main component of the heat load is the RF loss of superconducting cavities. In KEKB, there is enough margin for refrigerating capacity, because the number of superconducting cavities is small. Since the RF loss of the cavity changes according to the acceleration voltage, The sum of the compensation heater power and the RF loss is controlled to be constant. The RF loss of the Table 1 includes the output power of the compensation heaters.

From 2007 to 2010, two superconducting crab cavities were adopted. The crab cavity have a superconducting device called coaxial coupler. To cool the coaxial coupler, a liquid helium of about 5g/s was required (See Fig. 4). As a result, the thermal load appeared to be about 100W larger than the superconducting acceleration cavity.

In SuperKEKB, the crab cavities are not used. They have been removed. The eight superconducting cavities are still in operation.

Transfer Line

A high-performance transfer line is required to supply liquid helium from the helium refrigerator installed on the ground to the underground cryostat. The cross-section of transfer line was shown in Fig. 5 The heat load is about 1W/m as shown in Table 1. In KEKB, an improved transfer line was developed, and the performance was tested. The cross-section of the improved transfer line was shown in Fig. 6. In multi-channel transfer line, the heat load was only 0.05W/m. The multi-channel transfer line was adopted to connect from refrigerator to D10 test stand as shown in Fig. 1. The single-channel transfer line was adopted to connect between the cryostats and existing multi-channel transfer line in KEKB.

Liquid Nitrogen Circulation System

The cryostat of the superconducting cavity and the transfer line have the radiation shield which called 80K shield. To cool the 80K shield, a nitrogen circulation system was adopted. A circulation system is very suitable for cooling the shield by pipe cooling. This is because cooling in a single pass can not sufficiently cool the downstream. In the case of using a circulation system, the refrigerant returns in two-phase flow, so that all passes are completely cooled. As

* kota.nakanishi@kek.jp

Content from this work may be used under the terms of the CC BY 3.0 licence (© 2018). Any distribution of this work must maintain attribution to the author(s), title of the work, publisher, and DOI.

CONCEPTIONAL DESIGN OF CEPC CRYOGENIC SYSTEM

Jianqin Zhang[†], Shaopeng Li, Ruixiong Han, IHEP, CAS [100049] Beijing, China

Abstract

The Circular Electron and Positron Collider (CEPC) has two rings, the booster ring and the collider ring. There are 336 superconducting cavities in total, which group into 68 cryomodules. In the booster ring, there are 96 1.3 GHz 9-cell superconducting cavities. In the collider ring, there are 240 650 MHz 2-cell cavities. There are 4 cryo-stations along the 100 km circular collider. Each cryo-station is supplied from a common cryogenic plant, with one refrigerator and one distribution box. The cooling capacity of each refrigerator is 18 kW @ 4.5 K.

INTRODUCTION

The Circumference of CEPC is 100 km with the booster ring and the collider ring. The collider ring is located in the tunnel, with the booster ring on the surface. There are 336 superconducting cavities in total. In the booster ring, there are 96 ILC type 1.3 GHz 9-cell superconducting cavities, eight of them will be packaged in one 12-m-long module. There are 12 such modules. In the collider ring, there are 240 650 MHz 2-cell cavities, six of them will be packaged in one 11-m long module. There are 56 of them.

All the cavities will be cooled in a liquid-helium bath at a temperature of 2 K to achieve a good cavity quality factor. The cooling benefits from helium II thermophysical properties of large effective thermal conductivity and heat capacity as well as low viscosity and is a technically safe and economically reasonable choice. There are 4 cryo-stations along the 100km circular collider, as shown in Fig. 1.

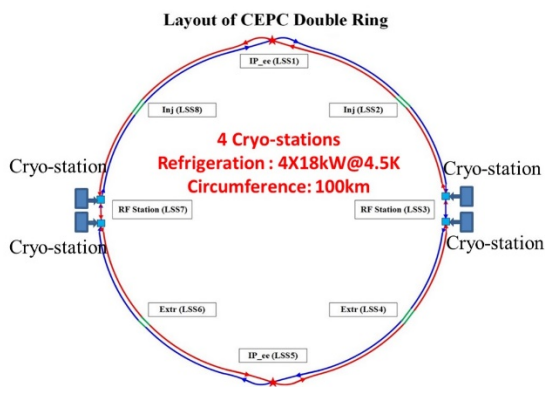


Figure 1: Layout of the CEPC cryogenic system.

CRYOGENIC DISTRIBUTION

General Layout

There are 4 cryo-stations. Each cryo-station includes

[†]jqzhang@ihep.ac.cn.

two strings; one string groups 3 modules from the Booster and the other groups 10 modules from the Collider. The temperature of the RF cavities is 2 K. In order to decrease the high thermodynamic cost of refrigeration at 2 K, the design of the cryogenic components aims at intercepting heat loads at higher temperatures. There are two shields intercept both radiation and conduction at two temperatures: 40 ~80 K and 5~8 K.

During operation, one-phase helium of 2.2 K and 1.2 bar is provided by the refrigerator to all cryomodules. Each cryomodule has one valve box with two valves. The JT-valve is used to expand helium to a liquid helium separator. A two-phase line connects each helium vessel and connects to the major gas return header once per module. A small diameter warm-up/cool-down line connects the bottom of the helium vessels at both ends. The cavities are immersed in baths of saturated superfluid helium, gravity filled from a 2 K two-phase header. Saturated superfluid helium flows along the two-phase header which is connected to the pumping return line and then to the refrigerator. Details of Booster and Collider cryogenic strings are in Figs. 2 and 3.

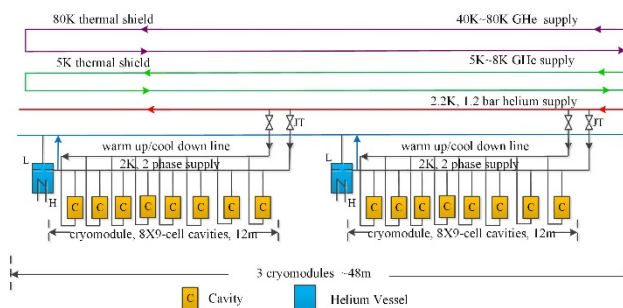


Figure 2: Booster cryogenic string.

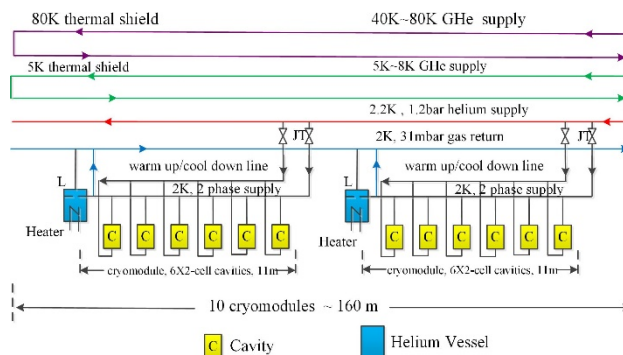


Figure 3: Collider cryogenic string.

OPERATION OF SUPERKEKB IN PHASE 2

Y. Funakoshi*, Y. Arimoto, H. Ikeda, T. Ishibashi, N. Ohuchi, S. Terui, X. Wang,
KEK 305-0801 Tsukuba, Japan

Abstract

The Phase 2 commissioning of SuperKEKB was performed from March to July 2018. In this report, the operation statistics and the QCS quench issue which we encountered during Phase 2 are described.

INTRODUCTION

The purpose of SuperKEKB is to search for a new physics beyond the standard model of the particle physics in the B meson regime. SuperKEKB consists of the injector Linac, a damping ring for the positron beam and two main rings; *i.e.* the low energy ring (LER) for positrons and the high energy ring (HER) for electrons and the physics detector named Belle-II. The beam energies of LER and HER are 4 GeV and 7 GeV, respectively. The design beam currents of LER and HER are 3.6 A and 2.6 A, respectively. The design luminosity is $8 \times 10^{35} \text{cm}^{-2}\text{s}^{-1}$. More detailed parameters of SuperKEKB is described elsewhere [1]. The Phase 1 beam commissioning of SuperKEKB was done from Feb. to June 2016 without the Belle-II detector and the IR magnets [2]. The Phase 2 commissioning was performed from March to July 2018. The highlights of the Phase 2 beam commissioning are written elsewhere [3]. In this report, the operation statistics and the QCS quench issue which we encountered during Phase 2 are described.

OPERATION STATISTICS

Figure 1 shows operation statistics of SuperKEKB Phase 2 commissioning from April to July. The Phase 2 main ring commissioning started in the middle of March. But the operation in March is not included in these statistics. During the Phase 2 commissioning, the commissioning of the Belle 2 detector was also done and it collected an integrated luminosity of $\sim 500 \text{pb}^{-1}$. Those are counted as "Luminosity Run". The "Machine Tuning" category includes vacuum scrubbing with beams and other hardware tuning without beams such as tuning of the beam size monitors and RF aging. The "Machine Study" category includes a dedicated machine study on the effects of the electron clouds, a collimator study, a radiation measurement and others. "Beam tuning" includes the optics tuning for squeezing IP (Interaction Point) beta functions, the beam injection or injector tuning, the detector beam background tuning, the beam collision tuning, the beam-based BPM tuning and others. A regular maintenance was done as a general rule every 2 weeks for about 8 hours. The "Troubles" category includes the QCS quench problem shown below. As a comparison, the operation statistics of KEKB for 8 years are also shown in Fig. 2. The beam tuning and machine tuning time are much longer than those in

KEKB, since SuperKEKB is still in an early stage in its life and the first beam collision was done in Phase 2.

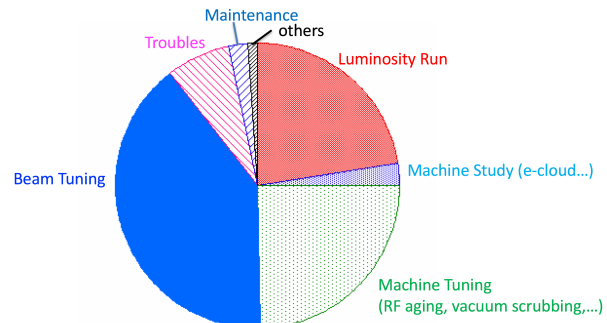


Figure 1: Operation statistics of SuperKEKB Phase 2 (April 2018 ~ July 2018).

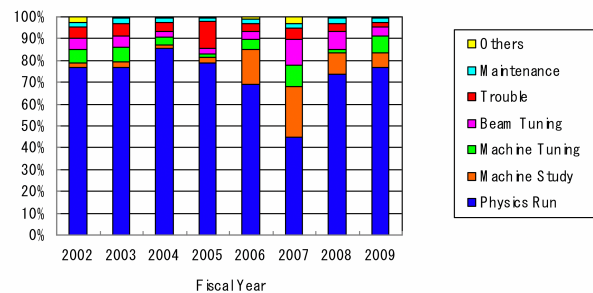


Figure 2: Operation statistics of KEKB for 8 years.

QCS QUENCH ISSUES

QCS is a generic name of the superconducting magnets near the IP at SuperKEKB which includes the final focus doublet named "QC1" and "QC2". The detailed design of the QCS magnets is described elsewhere [1]. Figure 3 shows a schematic view of the QCS magnet system. In addition to the final focus doublet quadrupoles, we need many kinds of corrector coils in order to cancel unwanted leakage fields, to correct effects of fabrication errors or alignment errors of the magnets and to widen dynamic aperture with the extremely small beta functions at the IP.

In the Phase 2 beam commissioning, we recognized that the QCS quench induced by beam hit is a serious issue for beam operation. Table 1 shows a list of the QCS quenches which occurred during the Phase 2 operation [4]. In the table, the injection kicker magnet system for the beam injection consists of two set of pulse magnets, K1 and K2. K1 and K2 make an orbit bump in the horizontal direction around the injection point for the stored beam. The quench on April 1st and 2nd was caused by unbalance of K1 and K2 due to timing errors of the pulse magnets and the orbit

* yoshihiro.funakoshi@kek.jp

SUMMARY ON ACCELERATOR INFRASTRUCTURES AND COMMISSIONING AND OPERATION

Y. Funakoshi*, KEK 305-0801 Tsukuba, Japan

Abstract

In this paper, summary of the working group on “Accelerator Infrastructures and Commissioning & Operation” is described.

LIST OF TALKS

The following talks were given in the working group #12 “Accelerator Infrastructures and Commissioning & Operation”.

- BEPCII Status: given by Qing Qing (IHEP)
- CEPC Civil Engineering design and Infrastructure: given by Yu Xiao (Yellow River Engineering Consulting Co., Ltd)
- Operation Model, Availability and Performance: given by Frank Zimmermann (CERN)
- CEPC Cryogenic System: given by Jianqin Zhang (IHEP)
- LHC Commissioning The good, the bad the ugly: given by Frank Zimmermann (CERN)
- KEKB/SuperKEKB Cryogenics Operation: given by Kota Nakanishi (KEK)
- Operation of SuperKEKB in Phase 2: given by Yoshihiro Funakoshi (KEK)
- A site-specific ILC-CFS design and the Green ILC: given by Masakazu Yoshioka (Iwate University)
- DAΦNE as Open Accelerator Test Facility: given by Catia Milardi (INFN)

The talks are categorized into 3 groups, *i.e.* civil engineering and infrastructure, cryogenic system and beam operation. In the following, a summary of each group is given.

SUMMARY OF CIVIL ENGINEERING AND INFRASTRUCTURE

Two talks were given for this topic. One was on ILC and the other was on CEPC. The talk on ILC covered the site investigation, conceptual designs of a surface access facility, underground facilities and interaction region facilities and reuse of waste heat from the facilities. Of the topics, the site investigation of ILC was very impressive. The unique ILC candidate site is “Kitakami highland”. This site has been decided considering the following aspects, *i.e.* geology, topography, availability of important social infrastructures

* yoshihiro.funakoshi@kek.jp

and small impact on the natural environment. As for geology, the site consists of a large and uniform granite area without active faults. Due to this feature, the risk for the underground construction is low and the ground motion or vibration is expected to be very small. In the Great East Japan earthquake on March 11th 2011, all fragile equipment and long glass tubes were not damaged at all at “Esashi earth tide observatory underground facility” which locates in the same granite zone as ILC. The reasons for this is that the earthquake ground motion in the granite zone is coherent and that the earthquake ground motion in the deep underground is 20 % of the ground surface. The Japanese government will make an decision on approval or disapproval of ILC within this year (2018).

The other talk is on CEPC. In the talk, the site investigation and the layout of the project, conceptual designs of the civil engineering system. The designs include tunnels, shafts, surface buildings, electrical engineering, the cooling water system, the ventilation and air-conditioning system, the fire protection system and the permanent transportation and lifting equipments. As for the the site investigation, 5 candidate sites were investigated. Qinhuangdao site is the best among the five candidate sites based on the terrain and geological conditions. But in general, all the sites are suitable for the underground construction of such a large scale. The main geological problems encountered can be solved by engineering measures. The CDR of the CEPC project was submitted on August 2018.

SUMMARY OF CRYOGENIC SYSTEM

Two talks were given on this subject. One talk was on the KEK cryogenic system. A cryogenic system for the superconducting cavity system was first constructed for TRISTAN in 1988 at KEK. Basically the same system has been used for 30 years also for KEKB and SuperKEKB, since the heat load for KEKB and SuperKEKB was less than that for TRISTAN. Although all of cryogenic system at KEK are very old, they are working very well. Experiences on the maintenance and troubles with the cryogenic system were given in the talk. The experiences should be referred in the future machines.

The other talk was on the cryogenic system for CEPC. Features of the CEPC cryogenic system is a 2K refrigerator using superfluidity He and a high heat load of 47.5 kW (4.5K equivalent heat load). Aggressive R&D works on the 2K JT heat exchanger and the cold compressor are under way. The cryogenic group at IHEP has manufactured 58 1.3GHz 9-cell cryomodules for EXFEL cooperated with domestic companies. This was very impressive. It will be a